CLONING AND CHARACTERIZATION OF NOVEL NOD LIKE RECEPTORS AS CYTOPLASMIC IMMUNE SENSORS

by

Yetiş Gültekin

B.S., Biology, Ankara University, 2007

Submitted to the Institute for Graduate Studies in
Science and Engineering in partial fulfillment of
the requirements for the degree of
Master of Science

Graduate Program in Molecular Biology and Genetics

Boğaziçi University

2011

ACKNOWLEDGEMENTS

To start with, I would like to express my appreciation and thanks to my thesis supervisor Assoc. Prof. Nesrin Özören for her endless support and guidance during my thesis. Hopefully, with her innovative and inexhaustible dynamism, this thesis will be a good initiator for the great future projects of the Apoptosis and Cancer Immunology Laboratory.

Many thanks go to Serkan Uğurlu M.D. for teaching and helping me with all the laboratory basics. In addition to that I would like to thank my project partner Duygu Demiröz for being at my side whenever I needed. Moreover, I would like to express my appreciation to Elif Eren M.Sc. to be one of the most helpful and thoughtful lab and project partners. Many thanks also go to my colleagues who are the members of AKİL: Şahru Yüksel Ph.D., Ali Can Sahillioğlu, Ulaş Özkurede, Chara Charsou M.Sc. and Mustafa Can Ayhan for their support, friendship and making AKİL very enjoyable and valuable for me.

I would like to express my thanks to Assist. Prof. Arzu Çelik and Assoc. Prof. Batu Erman for devoting their time to evaluate this thesis.

I would also like to thank Gamze Küser M.Sc., Duygu Dağlıkoca M.Sc., Tuncay Şeker M.Sc., İzzet Akiva M.Sc., Zeynep Özcan M.Sc., Ece Terzioğlu Kara M.Sc., Neslihan Zöhrap, Aslı Uğurlu, Mahmut Can Hız, Burçak Özeş, Yeliz Yılmaz Sert, Funda Ejder, Pınar Deniz, Gönenç Çobanoğlu, Selen Zülbahar, Yıldız Koca, Alperen Erdogan and all other friends from our department for their constant moral support.

For the generous supply of cells and plasmids, I am more than thankful to Prof. Gabriel Nunez at the University of Michigan Ann Arbor, Department of Pathology; Assoc. Prof. Maria Soengas at the Spanish National Cancer Research Center; Assoc. Prof. Batu Erman at Sabancı University, Department of Biological Sciences and Bioengineering; Prof. Ahmet Koman and Prof. Kuyaş Buğra at Boğaziçi University Department of Molecular Biology and Genetics; Assoc. Prof. Bünyamin Akyol at Izmir Institute of Technology Department of Molecular Biology and Genetics.

I also want to express my thanks to Assit. Prof. Stefan Fuss for confocal microscopy training. Without his support, we could not manage to take pretty beautiful photos.

I am also very grateful to my teachers, especially to Hülya Çaylaksevdi and Nursel Gürses, for being by my side whenever I needed them. In addition to that I would like to thank to Ali Mansur and Metin Mansur for their support during my thesis.

Last but not the least, I would like to express my special thanks to my close friends: Sinem Kocaoğlan, Kübra Karaman and Çağlar Gök.

This study was supported by EMBO-SDIG 1468 grant to Assoc. Prof. Nesrin Özören and TEV award to Yetiş Gültekin.

ABSTRACT

CLONING AND CHARACTERIZATION OF NOVEL NOD LIKE RECEPTORS AS CYTOPLASMIC IMMUNE SENSORS

NOD like receptors recognize infection and cellular damage. They are characterized by an N terminal protein interaction domain, central oligomerization domain, termed nucleotide binding domain and leucine rich repeat domain at the C-terminus. NLRC3 protein has the characteristic NBD-LRR configuration with a CARD domain. T lymphocytes have the highest expression level of NLRC3. It was suggested that it functions as a novel suppressor of T cell activation. NLRP13 shares the NBD-LRR configuration, but contains a PYRIN domain. Placenta is the only known tissue to express NLRP13. We found that both EGFP-NLRC3 and EGFP-NLRP13 fusion proteins are mainly localized in the cytoplasm but they can also be localized in mitochondria; therefore, they can be considered as cytoplasmic immune sensors. To determine the possible interactions of NLRC3 and NLRP13 with inflammasome components, co-immunoprecipitation experiments were performed. Co-IP results suggest that both NLRC3 and NLRP13 can interact with ASC and Caspase 1. The outcomes of Co-IP were verified with co-localization of ASC and Caspase 1 with NLRC3 and NLRP13 in HEK293FT cells via confocal microscopy. Under confocal microscopy, we detected for the first time that inflammasome like complexes assembled when Caspase 1 and ASC were co-transfected with NLRC3 or NLRP13 in HEK293FT cells. One of the Co-IP results suggests that NLRC3 can also interact with Caspase 5 and RFP NLRC3 co-localized with EGFP Caspase 5 in the HEK293FT cells. Dose and time dependent transfection of NLRC3 induces the speck formations of ASC in the stable EGFP ASC HEK293FT cells. However, NLRP13 does not cause speck formation as efficiently as NLRC3. To test the effects of NLRC3 and NLRP13 on NF-κB signaling, luciferase reporter gene assay has been performed. Overexpression of NLRC3 and NLRP13 proteins resulted in NF-κB downregulation.

ÖZET

SİTOPLAZMİK BAĞIŞIKLIK ALICILARI OLARAK YENİ NOD AİLESİ ALICILARIN KLONLANMASI VE KARAKTERİZASYONU

NOD benzeri alıcılar dokulardaki enfeksiyonu ve hücresel hasarı tespit ederler. Amino uçtaki protein etkileşim bölgesi, orta kısımda yer alan nükleotid bağlanma alanı olarak bilinen oligomerizasyon bölgesi ve karboksil uçta bulunan lösince zengin tekrarlı bölge NLR'ların kendilerine özgü yapısıdır. NLR protein ailesi üyelerinden NLRC3, CARD bölgesiyle birlikte bu proteinlere özgü olan NBD-LRR yapısına sahiptir. T lenfositlerinde yüksek oranda ifade edilen NLRC3 geni, T hücrelerinin aktivasyonunu baskılayan yeni bir protein olarak önerilmiştir. NLRP13 proteini NBD-LRR yapısını paylaşır fakat PYRIN bölgesini kapsar. NLRP13 geninin ifade edildiği yer olarak bilinen tek doku plasentadır. Hem EGFP NLRC3 hem de EGFP NLRP13 proteinleri başlıca sitoplazmada bulunduğu fakat mitokondride de bulunabildikleri gözlemledik. Bu nedenle NLRC3 ve NLRP13 proteinlerinden sitoplazmik bağışıklık alıcıları olarak söz edilebilir. NLRC3 veya NLRP13 proteinlerinin inflamazom bileşenleri ile olası etkileşimlerini belirlemek için eş-immünçöktürme deneyleri yapıldı. Bu deneyler sonucunda, hem NLRC3 hem de NLRP13 proteinlerinin ASC ve Kaspaz 1 proteinleri ile etkileşimde olduğunu ilk kez biz gösterdik. İmmünçöktürme sonuçları konfokal mikroskobu ile yapılan eş-yerleştirme deneyleriyle HEK293FT hücrelerinde doğrulandı. Konfokal mikroskobu altında ECFP Kaspaz 1 ve RFP ASC proteinleri, EGFP NLRC3 veya EGFP NLRP13 proteinleriyle birlikte HEK293FT hücrelerinde ifade edildiğinde inflamazom benzeri komplekslerin oluştuğu tespit edildi. İmmünçöktürme sonuçlarından biri NLRC3 proteinin Kazpaz 5 ile etkileşebiliceğini öne sürmektedir. RFP NLRC3 ile EGFP Kazpaz 5 proteinleri HEK293FT hücrelerinde eş yerleşmiştir. NLRC3 geninin devamlı EGFP ASC ifade eden HEK293FT hücrelerinde ifade edilmesi, ASC proteinin doza ve zamana bağlı olarak speck oluşumunu artırmaktadır. Ancak NLRP13 geninin doza ve zamana bağlı ifadesi ASC proteinin speck oluşturmasını NLRC3 kadar arttırmamıştır. NLRC3 ve NLRP13 proteinlerinin NF-κB sinyal yolağı üzerine olan etkisi luciferaz haberci gen

deneyi ile test edilmiş, hem NLRC3 hem de NLRP13 proteinlerinin NF-κB sinyalini düşürdüğü gözlenmiştir.

TABLE OF CONTENTS

LIST OF FIGURES

LIST OF TABLES

LIST OF ABBREVIATIONS

AD	Acidic Transactivation Domain
APS	Amonium Persulfate
ASC	Apoptosis-associated Speck Like Protein Containing CARD
BIR	Baculoviral Inhibitory Repeat Like Domain
BLS	Bare Lymphocyte Syndrome
BSA	Bovine Serum Albumine
BS	Behçet's Syndrome
CIITA	Class II transactivator
CAPS	Cryopyrinopathies
CARD	Caspase Recruitment Domain
CBB	Coommassie Brilliant Blue
cDNA	Complementary DNA
CGRP	Calcitonin Gene-Related Peptide
CLR	C-Type Lectin Like Receptor
CO_2	Carbondioxide
CFP	Cyan Fluorescent Protein
DAMPS	Damage Associated Molecular Pattern
DC	Dendritic Cell
DD	Death Domain
DMEM	Dulbecco's Modified Eagle Medium
DMSO	Dimethyl Sulfoxide
DNA	Deoxyribonucleic Acid
dsDNA	Double Stranded DNA
dsRNA	Double Stranded RNA
EDTA	Ethylenediaminetetraacetic Acid
E. coli	*Escherichia coli*
EGFP	Enhanced Green Fluorescent Protein
ER	Endoplasmic Reticulum
FBS	Fetal Bovine Serum
FDA	Food and Drug Administration

GFP	Green Fluorescent Protein
H_2O	Water
HBS	HEPES Balanced Salt
HEK	Human Embryonic Kidney
IgG	Immunoglobulin G
INF	Interferon
IL	Interleukin
IL1R	IL1 Receptor
IP	Immunoprecipitation
IRAK	IL1R Kinase
kb	Kilobase
kDa	Kilodalton
LB	Luria Bertani Broth
LPS	Lipopolysaccaride
LRR	Leucin Rich Repeat
mA	Miliamper
MDP	Muramyl Dipeptide
mg	Miligram
$MgCl_2$	Magnesium Chloride
min.	Minutes
miRNA	MicroRNA
ml	Mililiter
mm	Millimeter
mM	Milimolar
mRNA	Messanger RNA
MSH	Melanocyte Stimulating Hormone
mt	Mutant
NaCl	Sodium Chloride
NBD	Nucleotide Binding Domain
NEAA	Non-esential Amino acid
NF-κB	Nuclear Factor κ B
ng	Nanogram
NK	Natural Killer

NLR	NOD Like Receptor
NOD	Nucleotide Oligomerization Domain
OD	Optic Density
ORF	Open Reading Frame
PAMP	Pathogen Associated Molecular Patterns
PBS	Phosphate Buffered Saline
PCR	Polymerase Chain Reaction
Pen/Strep	Penicillin/Streptomycin
PGN	Peptidoglycan
PRR	Pattern Recognition Receptor
PYD	PYRIN Domain
RBC	Red Blood Cell
RFP	Red Fluorescent Protein
RIP	Receptor Interacting Protein
RLR	RIG I Like Receptors
RT-PCR	Reverse Transcriptase Polymerase Chain Reaction
rpm	Rotations per Minute
SDS	Sodium Dedocyl Sulfate
SDS-PAGE	SDS- Polyacrylamide Gel Electrophoresis
sec.	Seconds
shRNA	Short Hairpin RNA
siRNA	Small Interference RNA
TAE	Tris-Acetate-EDTA
TBS	Tris Buffered Saline
TBST	Tris Buffered Saline Tween
TEMED	Tetramethylethylenediamine
TGF	Transforming Growth Factor
TIR	Toll/IL1R Homology
TLR	Toll Like Receptor
TNF	Tumor Necrosis Factor
TRAF	TNF Receptor Associated Factor
TWEEN	Polysorbate
WB	Western Blot

WT	Wild-Type
x g	Times Gravity
V	Volt

LIST OF SYMBOLS

^{o}C	Centigrade degree
V	Volt
v	Volume
w	Weight
α	Alpha
β	Beta
γ	Gamma
µg	Microgram
µl	Microliter

1. INTRODUCTION

1.1 Innate Immunity

The relationships among organisms have evolved into four different outcomes. These are commensalism, mutualism, symbiosis as well as parasitism. Parasitism is a burden to the host organism which has to develop several strategies in order to detect and eliminate the parasites. Higher organisms are equipped with a basic defense mechanism called innate immunity. The innate immune system is the first line of defense against pathogens and is conserved from plants to animals (Wilmanski et al., 2008). It consists of three basic barriers which can be mentioned as physical, chemical and biological.

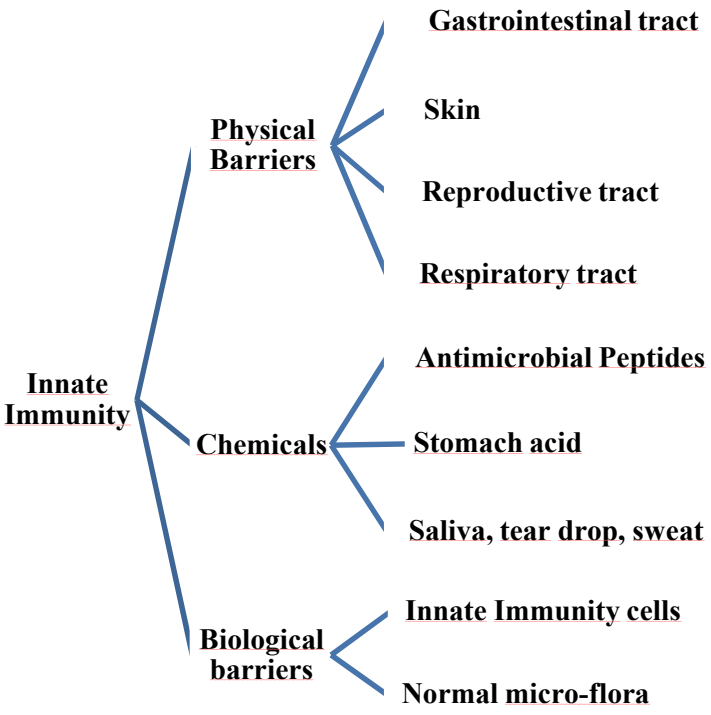

Figure 1.1. The Barriers of Innate Immunity.

Physical barriers are the common portals for the entry of microbes namely the gastrointestinal tract, the skin, the reproductive tract and the respiratory tract. Microbes can enter the host from the external environment through these interfaces by physical contact,

ingestion or breathing. However, these portals are protected by continuous epithelia that provide not only physical but also chemical barriers against infection. The internal epithelia secrete mucus. It includes many mucins. These surfaces prevent the microorganisms from adhering to the epithelia (Kim et al., 2010). In addition to physical barriers, chemical substances are microbicidal and important in inhibiting the microbial growth. To illustrate the point, lysozyme and phospholipase A are secreted in tears and saliva. They contain several histatins which have antimicrobial properties. The acidic pH of the stomach and the digestive enzymes like pepsin, bile salt, fatty acids and lysolipids found in the upper gastrointestinal tract create a substantial chemical barrier to infection. Further down the intestinal tract, antibacterial and antifungal peptides are expressed and secreted. Paneth cells produce cryptdins or alpha defensins (Ouellette et al., 2010). Antimicrobial peptides have a role in the immune defenses of many organisms from plants to the vertebrates. In short, antimicrobial peptides are an important part of the basic defense in all organisms.

Biological barriers can be stated as the final one in innate immunity. It includes normal micro-flora and innate immunity cells. Most epithelial surfaces are associated with a normal flora of nonpathogenic commensal bacteria. They compete with pathogenic microorganisms not only for nutrients but also for attachment sites on epithelial cells. This flora can also produce several antimicrobial substances. For instance, the vaginal lactobacilli produce lactic acid. Some strains of the lactobacilli genus also produce bacteriocins which have an impact on inhibiting the growth of closely related bacterial strains (Sánchez et al., 2010).

The cellular members of innate immunity are the final part of biological barriers. These are mast cells, eosinophils, basophiles, natural killer cells and the phagocytic cells such as the macrophages, neutrophils and dendritic cells (DCs). Their function within the immune system is to identify and eliminate pathogens that might cause infection. Under normal circumstances, they circulate the human body via the vascular and lymphatic systems. On the other hand, under the stress of infection, they are recruited to the sites of infection where they recognize and digest microbes for intracellular killing. Neutrophiles and monocytes can migrate to extra-vascular sites of infection by binding to epithelial adhesion molecules and fight against the pathogens.

1.2. Pattern Recognition Receptors

The cells of innate immunity recognize microbes via a limited number of germ line encoded proteins which are known as pattern recognition receptors (PRRs). In contrast to the large repertoire of rearranged receptors utilized by the acquired immunity, these receptors are not produced by somatic gene recombination. PRRs have several common characteristics. Firstly, PRRs are able to discriminate between non-infectious self and infectious non-self by sensing pathogen-associated molecular patters (PAMPs), which are expressed by pathogens and conserved among microorganisms. These PAMPs can include many different molecules ranging from lipopolisaccaride (LPS), peptidoglycan, lipoproteins, and proteins such as flagellin to microbial nucleic acids which may be ds-RNA, ss-RNA or unmethylated DNA (Franchi et al., 2009) (Akira S. et al., 2006). In short, PAMPs are essential for the survival of the microorganisms; therefore, it is difficult for microorganisms to alter these molecules. Secondly, PRRs are constitutively expressed in the host and detect the pathogens regardless of their life cycle stages. Thirdly, PRRs comprise an array of sensors present in the plasma, plasma membranes, and host cytosol (Franchi et al., 2009). Lastly, PRRs are germ line encoded, nonclonal, and independent of immunological memory (Akira et al., 2006). Acumulating evidence indicates that PRRs are also responsible for recognizing endogenous molecules released from damaged cells, termed damage associated molecular patterns (DAMPs) (Takeuchi et al., 2010).

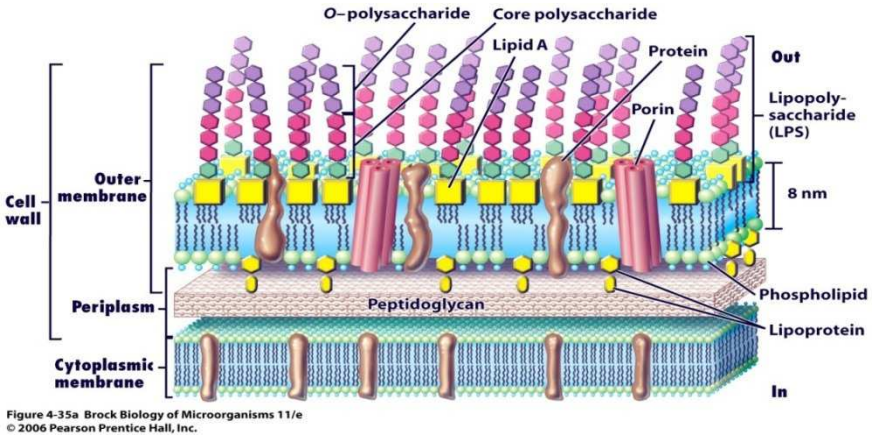

Figure 1.2. Pathogen-associated Molecular Patters

PPRs can be mainly classified into five different groups. These are Toll like receptors (TLRs) (Takeda et al., 2004), NOD like receptors (NLRs) (Inohara et al., 2003), RIG1 like receptors (RLRs) (Yaneyama et al., 2007), C-type lectin like receptors (CLRs) (Hashimoto et al., 1988) and cytosolic DNA sensors like AIM2 (Bryant C. et al., 2009). There are several cells which have an ability to phagocytize the infection agents. These PRRs can be expressed in these various nonprofessional immune cells. The intracellular signaling cascades triggered by these PRRs lead to transcriptional expression of inflammatory mediators that coordinate the elimination of pathogens and infected cells. Nonetheless, aberrant activation of this system causes immunodeficiency, septic shock, or induction of autoimmunity (Takeuchi et al., 2010).

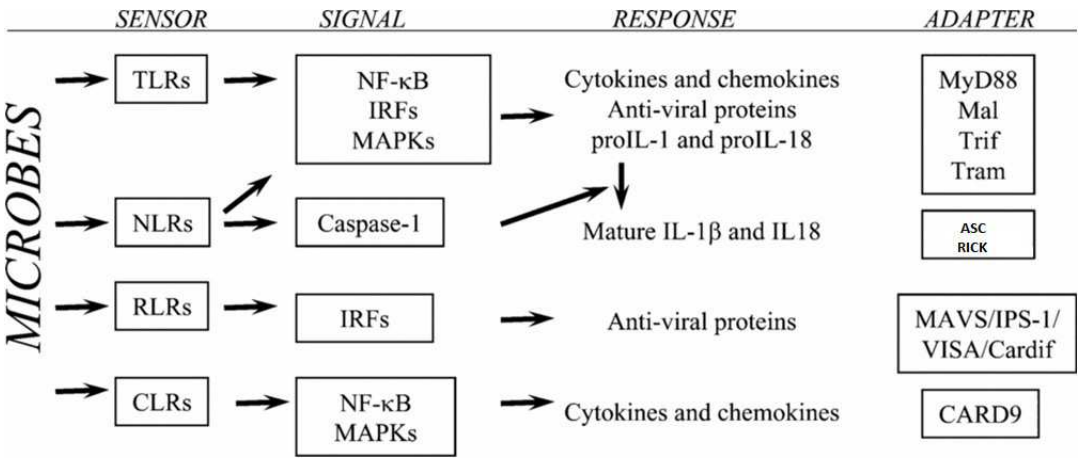

Figure 1.3. Main Classes of PRRs (modified from Palsson-McDermott et al., 2007).

1.2.1. Toll Like Receptors

Toll protein was originally identified in *Drosophila melanogaster* as an essential receptor for the establishment of the dorso-ventral polarity in developing embryos (Hashimoto et al., 1988). Hoffmann and his colleagues demonstrated that Toll-mutant flies were highly susceptible to fungal infection (Lemaitre et al., 1996). The mammalian homologue of Toll protein was identified as TLR4 (Medzhitov et al., 1997). Up to date, thirteen TLRs have been identified in mammals. In short, TLRs are evolutionarily conserved from the worm *Caenorhabditis elegans* to mammals. TLRs are type I integral membrane glycoproteins. They are characterized by extracellular domains which contain varying numbers of leucine rich repeat (LRR) motifs and a cytoplasmic signaling domain

homologous to that of interleukin 1 receptor (IL-1R), termed the Toll/IL-1R homology (TIR) domain. The LRR domains are composed of 19-25 tandem LRR motifs each of which contains 24-29 amino acids.

TLRs are expressed on various immune cells, including macrophages, DCs, B cells, specific T cells and even on non-immune cells such as fibroblasts and epithelial cells (Akira et al., 2006). Different infections cause expression of different TLRs. To exemplify the point, DCs express TLR1, 2, 6 and 10 as a result of fungal infection, whereas TLRs 1, 2, 4, 5, 6, 9 and 10 are expressed against bacterial infections (Table 1.1)

Each TLR has been indicated to recognize specific components of pathogens. To illustrate the point, TLR2 is essential for recognition of microbial lipopeptides. TLR1 and TLR6 associate with TLR2, and discriminate subtle differences between triacyl- and diacyl lipopeptides. TLR4 recognizes LPS. Bacterial DNAs contain high amount of unmethylated CpG dinucleotides. However, they are methylated and suppressed in mammalian DNA. The mammalian immune system recognizes and responds to the DNA motifs which contain unmethylated CpG via TLR9. CpG DNA binds to and is taken up by immune cells through endocytic pathways, then co-accumulates with TLR9 in phagosome-like vesicles. This process is controlled by PI3 kinase (Ishii et al., 2005). CpG motifs mediate innate immune system activation is characterized by B cell proliferation, DCs maturation, NK cells activation and finally, the production of pro-inflammatory cytokines, chemokines and immunoglobulins. TLR9 is the CpG DNA receptor, whereas TLR3 is implicated in the recognition of viral ds-RNA. TLR5 is a sensor for flagellin (Akira et al., 2006). Hence, TLR family discriminates the differences between specific pathogen associated molecular patterns.

Table 1.1. TLR gene expression patterns against different infection in innate and acquired immunity cells (modified from Takeda et al., 2006 and Akira et al., 2006).

Infection	Cell Types	TLRs									
		1	2	3	4	5	6	7	8	9	10
Viral	Granulocyte	x	x		x						
	Macrophages	x	x	x	x		x	x	x	x	x
	Dendritic Cell	x	x	x	x		x	x	x	x	x
	B Cell	x			x		x	x		x	x
	T cell	x		x	x						
Bacterial	Granulocyte	x	x		x	x					
	Macrophages	x	x		x	x	x			x	x
	Dendritic Cell	x	x		x	x	x			x	x
	B Cell	x			x		x			x	x
	T cell	x			x						
Fungal	Granulocyte	x	x								
	Macrophages	x	x				x				x
	Dendritic Cell	x	x				x				x
	B Cell	x					x				x
	T cell	x									

The activation of TLR signaling pathways originates from the cytoplasmic TIR domains. In the signaling pathway, MyD88, downstream of the TIR domain, was first characterized to play a crucial role in inflammatory responses mediated by all TLR family members. MyD88 possesses the TIR domain in the C-terminal, and a death domain in the N-terminal portion. MyD88 associates with the TIR domain of the TLRs. Upon stimulation, MyD88 recruits IL-1 receptor-associated kinase (IRAK) to TLRs through interaction of the death domains of both molecules. Phosphorylation of IRAK is necessary to activate this pathway. Then, phospho-IRAK associates with TRAF6, which is a member of the tumor necrosis factor receptor (TNFR) associated factor (TRAF) family. It mediates the signaling pathways of cytokines. Phospho-IRAK and TRAF6 association causes the activation of two distinct signaling pathways, leading to the activation of JNK and NF-κB. Finally, the signaling pathways of cytokine expression and secretion are activated.

1.2.2. NOD Like Receptors

Organisms need to be able to defend themselves against pathogens to survive. Many pathogens can kill an organism within a very short period. Hence, the vital initial defense

against pathogens should be a fast response. This is mediated by a range of innate immune mechanisms, many of which are shared by all animals, and some even by plants. As mentioned before, innate immune system has several special sensor proteins which can be found on the extracellular membrane of cells or in the cytoplasm such as NLRs.

In the last 10 years, the NLR family with its 23 members has been determined as novel class of PRRs (Franchi et al., 2009). However, only several members of NLR family such as NOD1, NOD2, Cryopyrin/NLRP3 and Ipaf/NLRC4 have been studied deeply and their molecular mechanisms have been elucidated gradually. It is interesting that many organisms from plants to primitive species have similar proteins like NLRs. For instance, sea urchins lack adequate immune systems but have approximately 200 kinds of NLRs and it is known that their life spans are longer than humans. As a second example, the genome of the zebrafish contains more than 200 genes encoding fish-specific NLR proteins with both conserved and divergent domains.

NLR family members share three characteristic domains. The first one is leucine rich repeats (LRRs) at the C-terminus (Figure 1.4). This domain is conserved in plants to animals and is also found in TLRs. To reflect their close analogy to TLRs, the NLR family are referred to as NOD like receptors. LRRs in NLR proteins are belived to be ligand sensing and auto-regulation domains. The central domain of NLRs is known as NOD (Nucleotide oligomerization domain) or NACHT or NBD (Nucleotide Binding Domain). This is an appropriate domain to make oligomerazation to five multimeric structures. Similar eight or seven NOD domains of Apaf 1 generate the structure of apoptosome (Yuan S. et al., 2010). Finally, there is an N terminus protein-protein interaction domain. This effector part of the protein plays a role in signal transduction and activation of the inflammatory response. This domain can include PYRIN, CARD (Caspase recruitment domain), BIR (Baculoviral inhibitory repeat like domain) or AD (Acidic transactivation domain). The CARD domain is also found in an enzyme family called caspases which have a cleavage role during the execution of apoptosis.

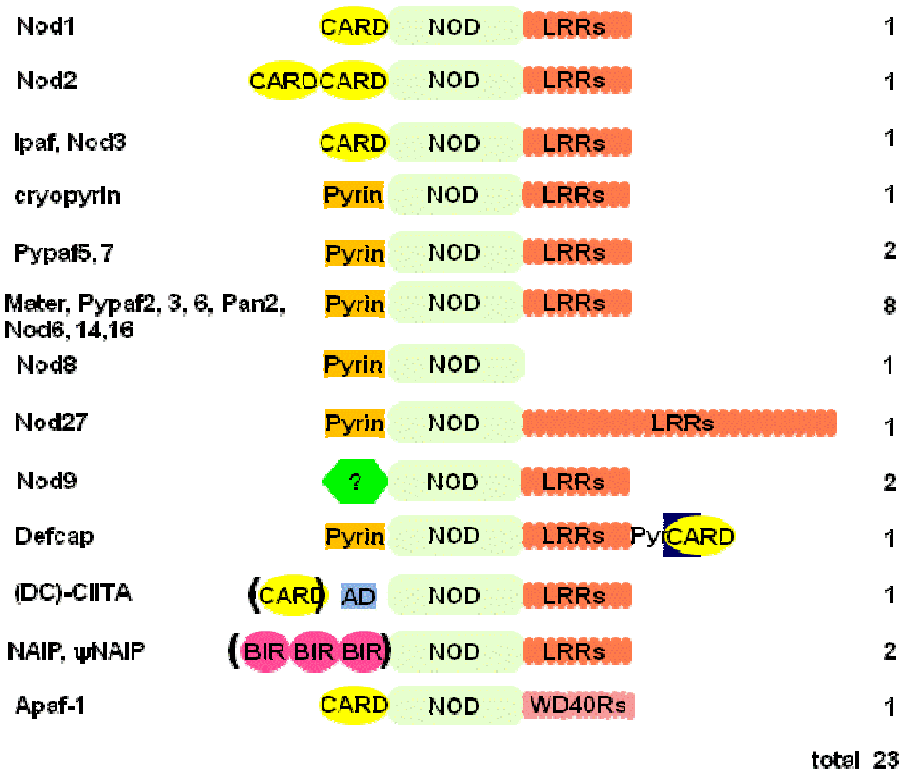

Figure 1.4. Human NLRs and Their Protein Structures. Cryopyrin/NLRP3 and Nod 14/NLRP13 proteins structures are drawn. NOD3/NLRC3 and Ipaf share similar protein structure. The closest family members are shown in a similar way (adopted from Inohara et al., 2003).

Different types of tissues can express different kind of NLR family members. The expression pattern of NLRs can be found in Table 1.2.

Table 1.2. NLR Family Members and Their Tissue Expression Patterns.

Gene	Super Family	Chromosome	Tissue Expression
NOD1	CARD	7p14.3	heart, spleen, placenta, lung, epithelium, ovary, pancreas, skeletal muscle, testis
NOD2	CARD	16q12.1	monocytes, dendritic cells, granulocytes, intestinal epithelial cells, Paneth cells
IPAF	CARD	2p22.3	bone marrow, macrophage, colon, kidney, liver, lung, spleen, placenta, intestine, heart(weak), testis(weak)
APAF 1	CARD	12q22-q23	ubiquitously
CIITA	CARD	16p13	thymic epithelium, B cells, dentritic cells, monocytes
NALP1	CARD-PYRIN	17p13.2	heart, thymus, spleen, peripheral blood leukocytes, monocytes, dentritic cells, B cells, T cells, stomach, gut, neurons, testis
NALP2	PYRIN	19q13.42	thymus, placenta, lung, heart, brain, hematopoirtic-nonhematopoietic lineages, not expressed in skeletal muscle
NALP3	PYRIN	1q44	peripheral blood leukocytes(highly), chondrocytes, monocytes (predominantly), T cells, dendritic cells, oropharynx, esophagus
NALP4	PYRIN	19q13.42	spleen(highest), kidney(highest), lung, liver, placenta, thymus, placenta
NALP5	PYRIN	19q13.42	oocytes
NALP6	PYRIN	11p15	epithelium, granulocytes, monocytes, T cells, B cells, eosinophils, dendritic cells(weak)
NALP7	PYRIN	19q13.42	not express in skeletal muscle, testis, epididymis, lymph, pharynx and placenta
NALP8	PYRIN	19q13.42	testis and oocytes
NALP9	PYRIN	19q13.42	ubiquitously

NALP10	PYRIN	11p15	ubiquitously
NALP11	PYRIN	19q13.42	ubiquitously
NALP12	PYRIN	19q13.41	granulocytes, dentritic cells, monocytes, leukocytes, PBMCs, restricted in myeloid linage
NALP13	PYRIN	19q13.42	placenta
NALP14	PYRIN	11p15.4	ubiquitously
NLRC3	unknown	16p13.3	purified Tcells(highest), Bcells, NK cells, thymus, uterus, kidney
NLRC4	CARD	2p22.3	ubiquitously
NLRC5	CARD	16q13	ubiquitously
NOD9	unknown	11q23.3	ubiquitously
NOD27	PYRIN	16q13	B cells ,T cells, APC, NK cells
NAIP	BIR3X	5q13.1	APC

1.3. Different Features of NLRs

1.3.1. NLRs in Multi-component Platforms: Inflammasomes

Several NLR members can make bigger protein complexes known as inflammasomes. They consist of NLR proteins (NLRP3, NLRP1, NLRC4 or NLRC5), adaptor proteins (ASC/PYCARD or possibly CARDINAL), chaperone proteins (heat shock protein 90, SGT1), and caspases (1 and/or 5).

The NLRP1/NALP1 inflammasome was the first characterized multiprotein complex. NALP1, Caspase 1, Caspase 5 and the adaptors, ASC and CARDINAL are the components of this inflammasome. In humans, a single NLRP1 gene exists encoding an N-terminal PYR domain, a centrally located NOD domain followed by several LRRs, a FIIND domain, and a C-terminal CARD domain. In mice, there are three paralogs (*Nalp1a,*

Nalpb, Nalpc) which are located in tandem in the same chromosomal region and all of which lack the PYD and FIIND domains. Human NLRP1 is particularly expressed in the thymus and spleen. Muramyl dipeptide (MDP), a derivative of bacterial peptidoglycan, triggers the formation of NALP1 inflammasome.

Cryopyrin/NLRP3 is the one of the NLR proteins with a typical NBD-LRR configuration and contains the PYRIN domain. Homotypic interactions occur between the PYRIN domains of NLRP3 and adaptor protein ASC (Apoptosis-associated speck-like protein containing CARD). This interaction bridges the association of Caspase 1 to NLRP3 in a large complex, known as the inflammasome. It regulates the activation of Caspase 1 and the secretion of the pro-inflammatory cytokines such as IL-1β, IL-18 and IL-33. Activated Caspase 1 processes the cytosolic precursors of IL-1β and IL-18. This allows the secretion of the biologically active cytokines. Therefore, Caspase 1 lacking mice are defective in the maturation and secretion of IL-1β and IL-18. Secretion of IL-1β and IL-18 trigger similar biological processes. IL-1β participates in the generation of systemic and local responses to infection, injury and immunological challenges by generating fever. Thanks to fever, lymphocytes are activated and leukocyte infiltration is promoted at the sites of infection or injury (Dinarello et al., 1998). As a result of these regional inflammatory stimuli, edema mechanisms are operated. Furthermore, macrophages, neutrophils and DCs make an effort to destroy the pathogens during edema formation. Simultaneously, these cells move to the nearby lymph nodes and induce the acquired immune system (Schroder et al., 2010). Binding of IL-18 to IL18R complex triggers many signaling cascades that are engaged by the IL-1R including activation of NF-κB, STAT1 and MAPKs. IL-18 also promotes the production of INF-γ in activated T cells and NK cells, thereby contributing to Th1 cell polarization. IL-18 was indicated to induce FAS ligand production and the generation of multiple secondary pro-inflammatory cytokines, chemokines, cell adhesion molecules and NO species.

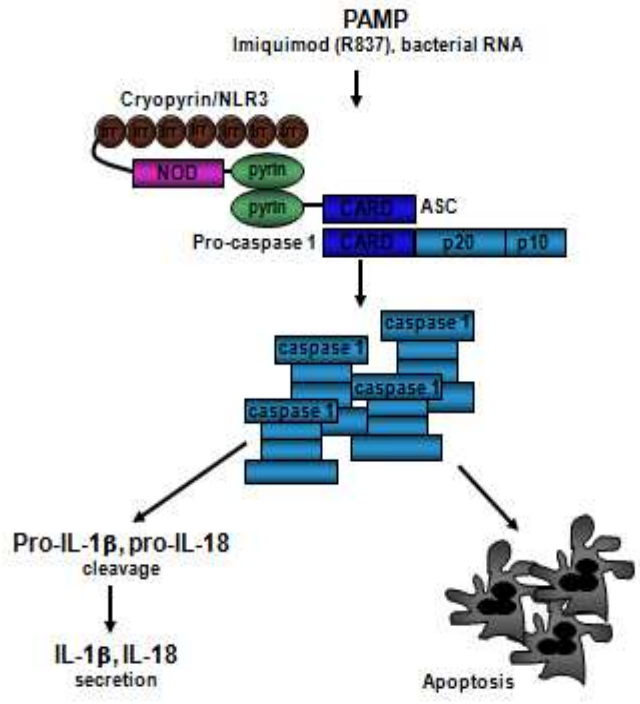

Figure 1.5. Role of Cryopyrin/NLRP3 Inflammasome in Apoptosis and Pro-inflammatory Cytokine Secretion.

Furthermore, NLRP3 inflammasome has a role in programmed cell death, known as pyroptosis. It is a Caspase 1 dependent inflammatory form of cell death (Kepp et al., 2010) (Fernandes-Alnemri et al., 2007). Recently, it has been shown that the immune system can be activated by host derived signals, called DAMPs. Extracellular ATP is one of the DAMPs, perhaps released by dying cells. It was demonstrated that bacterial products alone were not sufficient to trigger the inflammasome. Besides the bacterial products, activation of the purine receptor (P2X7) and subsequent potassium efflux were necessary for this process (Ferrari et al., 2006). Stimulation of potassium efflux in THP-1 cells with potassium-depleting agents induced the formation of the pyroptosome, while increasing potassium concentrations in the culture media or pharmacological inhibition of this efflux inhibited its assembly (Fernandes-Alnemri et al., 2007). Therefore, it can be said that inflammasome has a role in programmed cell death of infected cells. Beside ATP, additional DAMPs can include several particles such as monosodium urate, the crystalline salt of endogenously produced uric acid, and calcium pyrophosphate as a metabolic byproduct. Components of the extracellular matrix such as hyaluronin and biglycan also signal via the inflammasome. The numbers of molecules which have been reported to

activate Cryopyrin/NLRP3 is bigger than the numbers of NOD1 and NOD2 stimulants. RNA, DNA, cholesterol, asbestos, silica, amyloid-β, imiquimod and alum can be also mentioned as ligands of NLRP3 (Schroder et al., 2010) (Dostert et al., 2008) (Eisenbarth et al, 2008) (Kanneganti et al., 2006). Gout-associated uric acid crystals also activate the NALP3 inflammasome (Martinon et al., 2006). However, it is still unknown how Cryopyrin senses these various ligand molecules.

The NLRC4/IPAF/CARD12 inflammasome consists of NLRC4, ASC, Caspase 1 as well as BIR-domain containing protein NAIP5. IPAF recognizes bacterial flagellin from *Salmonella typhimurium*, *Shigella flexneri*, *Legionella pneumophila* and *Pseudomonas aeruginosa*. *Salmonella* mutants lacking flagellin or expressing point mutated flagellin fail in their ability to induce Caspase 1 in an NLRC4 dependent way (Franchi et al., 2007) (Miao et al., 2006).

As a novel player in inflammasome formation, it is suggested that NLRC5 interacts with NLRP3 in order to cooperatively activate inflammasome. RNA interference-mediated knockdown of NLRC5 nearly eliminated the cleavage of Caspase 1, IL-1β, and IL-18 processing in response to bacterial infection, PAMPs, and DAMPs. This outcome was verified in primary human monocytic cells. NLRC5, together with pro-Caspase 1, pro-IL-1β, and the inflammasome adaptor ASC, reconstituted inflammasome activity that showed cooperativity with NLRP3 (Davis et al., 2011).

1.3.2. NLRs as Transcription Factors

Class II trans-activator (CIITA) is a key regulator of MHC class II gene expression that associates and cooperates with transcriptional factors in the MHC class II gene promoter. Loss of CIITA expression in humans and mice results in the severe reduction of only MHC class II expression (Ting et al., 2002).

NLRC5 is a transcriptional regulator of MHC class I genes. MHC class I genes have a role in the immune defense against viruses and tumors by presenting antigens to CD8+ T cells. NLRC5 is an IFN γ inducible nuclear protein, and the expression of NLRC5 resulted in enhancing the expression of MHC class I and related genes such as B2 microglobulin,

transporter associated with antigen processing and large multifunctional protease. They are essential for MHC class I dependent antigen presentations (Meissner et al., 2010).

1.3.3. Associations of NLRs with Diseases

Immune dysregulation linked to genetic variations in NLR genes leads to disease or is associated with increased susceptibility to several inflammatory disorders (Nunez et al., 2009). It has been previously indicated that mutations in the *Cryopyrin/NLRP3* gene can cause auto-inflammatory diseases such as Familial Cold Urticaria (FCU), Familial Cold Auto-Inflammatory Syndrome, Muckle-Well syndrome and Neonatal-Onset Multiple-System Inflammatory Disease (NOMID/CINCA). These three *Cryopyrin* related diseases (FCAS, MWS, and NOMID) are called cryopyrinopathies (CAPS) (Neven et al., 2008). Notably, patients with FCAS, MWS and NOMID have missense mutations that are located in the NOD domain of *Cryopyrin* (Inohara et al., 2003). They are inherited as autosomal dominant disorders. Cryopyrin mutations are found only in 50% of patients with clinically diagnosed CAPS (Aksentijevich et al., 2007). These auto-inflammatory syndromes are closely related, both genetically and in terms of clinical symptoms. Therefore, they are not separate but represent a continuum of subphenotypes since many of their symptoms are overlapping. The symptoms of FCAS are quite more interesting than the others because large red welts form on the skin after being exposed to a cold stimulus. Other diseases have common symptoms like edema formation, episodic fever, chills, and painful joints. So far, no pathogenic bacteria or virus have been determined to be reason of these disorders (Neven et al., 2008).

Several disease associated mutations of *Cryopyrin/NLRP3* have been previously investigated. R260W and D303N *NLRP3* mutants exhibit a gain of function phenotype with enhanced ASC recruitment, NF-κB activation, the cleavage of pro-Caspase 1 and IL-1β secretion when they are compared to the wild type protein (WT). NLRP3 disease related mutants are less soluble than the WT. (Yu et al., 2006) (Dowds et al., 2004).

In addition to CAPS, NLRP3 is associated with gout disease since it can also detect signs of metabolic stress, such as monosodium urate (MSU) crystals (Martinon et al., 2006).

Pyrin is encoded by *MEFV* gene and has a PYD domain that can physically interact with the PYD of ASC. When Pyrin is overexpressed, it specifically inhibits Cryopyrin and IPAF mediated NF-κB activation by disrupting the Cryopyrin-ASC interaction. Hence, Pyrin functions as a negative regulator of Cryopyrin signaling (Dowds et al., 2003). Mutant variants of *MEFV* gene leads to enhanced Cryopyrin signaling and inflammation. Hence, Familial Mediterranean Fever (FMF) is observed. This is an autosomal recessive disease which is characterized by recurrent episodes of fever and localized inflammation.

Behçet Syndrome (BS) is also an auto-inflammatory disease of unknown etiology. It is seen with a frequency of 4 per thousand (0.4%) in the Turkish population (Gül et al., 2005) and is characterized by recurrent inflammatory episodes as a result of aberrant cytokine secretion. Behçet patients have higher serum levels of cytokines such as IL-1β, TNF-α, IL-6, IFN-γ and IL-8 and share same ailments with other auto-inflammatory disorders (Ateş et al., 2005). Recently, variants in the MHC class I, IL10, and IL23R-IL12RB2 regions have been associated with BS via genome-wide association study (Remmers et al., 2010). What is more, we have sequenced all the exonic regions of *Cryopyrin/NLRP3* gene and found two mutations V200M (n=3/104) and T195V (n=1/104) in BS patients but not in control samples (Yuksel et al., manuscript in preparation). However, the molecular mechanism of BS has not been elucidated yet.

CAPS have a major influence on quality of life of patients; they lead to considerable morbidity and even death in severe cases. There are several therapeutic strategies against Cryopyrin related diseases. They depend on IL-1β and Caspase 1 inhibition. One of the IL-1β inhibitor based therapies is treatment with Anakinra. It is a recombinant IL-1 receptor antagonist which blocks the biological activity of the naturally occurring IL-1. IL-1R antagonist is also endogenously expressed and it functions as an inhibitor of IL-1β receptor. FCAS, MWS, CINCA and gout diseases are successfully treated with Anakinra (So et al., 2007) (Fleischmann et al., 2005) (Hoffman et al., 2004) (O'Connell et al., 2007) (Hawkins et al., 2004). Finally, it has been shown that colchicine resistant BS patients give response to Anakinra treatment (Botsios et al., 2008).

Beside *Cryopyrin* related diseases, mutations in the *NOD2* gene were linked to Crohn's disease characterized with symptoms such as colic and intense stomach pain (Ogura et al., 2001). A frame shift mutation and two missense mutations in the LRRs in *NOD2* are associated with Chron's disease. It is a common inflammatory disease of the intestinal tract. These Crohn's disease associated NOD2 variants are defective in their response to bacterial peptidoglycan, resulting in absent or decreased signaling. In addition to Crohn's disease, missense mutations in the NACTH domain of *NOD2* have been associated with Blau syndrome. This is an autosomal dominant trait whose clinical presentations are arthritis, uveitis and skin rashes.

The class II transactivator (CIITA) is mutated in bare lymphocyte syndrome (BLS), a hereditary immunodeficiency disorder characterized by the absence of MHC class II genes expression (Steimle et al., 1993) (Inohara et al., 2003).

Mutations and specific SNPs in *NLRP1* are associated with vitiligo-associated multiple autoimmune diseases, such as hypothyroidism and rheumatoid artiritis (Jin et al., 2007). One *NLRP2* mutation has been recently linked to a case of familial Beckwith-Wiedermann Syndrome, a fetal overgrowth and imprinting disorder (Meyer et al., 2009).

Recently, a link between certain NLRP7 mutations and miscarriage has been reported (Qian J. et al., 2007). Many NLRP7 mutations were found directly to be linked to the hydratidiform mole formation (Kou et al., 2008) (Deveault et al., 2009) (Wang et al., 2009). Moles are abnormal embryonic tissues which may develop in the uterus. Under normal circumstances, it is expected that the maternal immune system will eliminate these tissues.

Lastly, NLRP12 mutations were associated with a fever syndrome resembling FCAS, called FACS2. It is suggested that NLRP12 mutations in these patients disrupt the NF-κB inhibitory activity of NLRP12 (Jeru et al., 2008).

1.3.4. Pro-inflammatory NLR members

NLRs respond to PAMPs and trigger the host's innate immunity. It was previously indicated that NOD1 and NOD2 recognize iE-DAP and MDP, respectively. These molecules are parts of peptidoglycan, the main component of bacterial cell walls of Gram negative and positive bacteria. When NOD1 senses the bacterial PGN in the host cell, it directly recruits the serine-threonine kinase RICK, through their CARD-CARD interactions. RICK is responsible of binding to the NF-κB inhibitor IKK. As a result of this interaction, the ubiqutination of IKK is promoted. Once the pathway is activated, IKK phosphorylates the inhibitor IκB, leading to its degradation via the proteasome, releasing the p50/60 complex which is the active form of NF-κB, allowing it to translocate to the nucleus. As a result of this translocation, the gene expressions of TNF-α, IL-6, pro-IL-1β and 18 are accelerated (Franchi et al., 2009).

NOD2 activates NF-κB via CARD-CARD interaction between the receptor interacting protein 2 (RIP2) and NOD2. The NOD2-RIP2 complex further interacts with the NF-κB. That consequently activates NF-κB by releasing it from the IκB proteins. Activated NF-κB initiates a large number of gene transcripts and triggers the immune response following its translocation into the nucleus. Recently, it has been found that NOD2 core promoter contains a canonical NF-κB binding site in both humans and chimpanzees. Either deletion of the NF-κB binding elements within the *NOD2* promoter or treatment with JSH-23, the inhibitor of NF-κB, could cause a significant decrease in the NOD2 promoter activity. Hence, it can be suggested that there is a positive feedback loop between NF-κB and NOD2. (Chaofeng et al., 2010)**.**

NLRP1, NLRC4 and NLRP3/Cryopyrin can be described as pro-inflammatory NLRs due to their effect on pro-inflammatory cytokines secretion and aberrant inflammasome activity of their mutants.

1.3.5. Anti-inflammatory NLR Family Members

The function of the aforementioned NLRs family members is triggering the inflammatory mechanisms. On the other hand, it has been recently discovered that novel members of the NLRs have the potential to inhibit Caspase 1 dependent IL-1β secretion as well as ASC-mediated NF-κB activation. Therefore, these members were called anti-inflammatory subgroup of NLRs (Kinoshita et al., 2005). To illustrate the point, it was indicated that NLRC3 suppressed the activity of NF-κB signaling pathway when it was over-expressed in Jurkat cells (Conti et al., 2005). Moreover, human NLRP10 (PYNOD) suppressed the assembly of ASC dependent inflammasome and decreased the secretion of IL-1β (Imamura et. al., 2010). When NLRP7/PYPAF3 protein was over-expressed in HEK293T cells, the activation of Caspase 1 and the secretion of IL-1β declined (Kinoshita et al., 2005). Therefore, it can also be mentioned as a member of anti-inflammatory NLR subgroup.

Recently, NLRC5 has been identified as a negative regulator of NF-κB and Type I interferon signaling pathway (Cui et al, 2010). It can inhibit the IKK complex and RIG-I/MDA5 function. NLRC5 interacted with IKKα and IKKβ and blocked their phosphorylation and inhibited NF-κB dependent responses. Specific siRNA knockdown of NLRC5 not only induced the activation of NF-κB and its responsible genes, TNF-α and IL-6, but also promoted type I interferon signaling and antiviral immunity (Cui et al., 2010). Overexpression of NLRC5 failed to trigger inflammatory responses such as the NF-κB or interferon pathways in HEK293T cells (Neerincx et al., 2010).

NLRP12/Monarch-1/Pypaf-7 is a negative regulator of inflammatory responses (Lich et al., 2007). This inhibition effect is based on the sequence of Walker A/B motifs of Monarch-1. They lead to self-oligomerization of Monarch-1, degradation of NIK, and inhibition of IRAK-1 phosphorylation. The stable expression of a Walker A/B mutant NLRP12 in THP-1 monocytes results in increased production of pro-inflammatory cytokines and chemokines. This phenotype was confirmed with siRNA mediated silencing (Ye at al., 2008). It has been shown that Monarch-1 inhibited CD40-mediated activation of NF-κB. This inhibition stems from the ability of Monarch-1 to induce proteasome mediated degradation of NIK. Congruently, silencing of Monarch-1 with shRNA enhanced

the expression of p50-dependent chemokines (Lich et al., 2011). There are still very few reports about these anti-inflammatory family members and in this thesis, we investigated that NLRC3 and NLRP13 can be anti-inflammatory NLRs.

1.4. Cancer, Inflammasome and Inflammation

Inflammation is linked to cancer and NF-κB appears to have a crucial role in tumorigenesis. Inflammatory molecules can provide growth signals that promote the proliferation of the malignant cells. To illustrate the point, IL-6 is upregulated in breast and prostate cancers (Sanser et al., 2008) (Wegiel et al., 2008). Pro-inflammatory cytokines have been demonstrated to exert key roles in inducing gut inflammation and colorectal tumor formation. Their synthesis and secretions are controlled by STAT, NF-κB and AP-1 families. NF-κB is generally related to the survival of the cells. It regulates the expression of anti-apoptotic genes and activates pro-inflammatory cytokines and chemokines. Hence, NF-κB can be a key molecular link between inflammation and oncogenesis initiation and progression (Naugler et al., 2008). Hence, inhibition of NF-κB reduces tumorigenesis. Accumulated genetic and biochemical evidence in mouse models suggest that NF-κB has a causative role in malignant conversion and progression (Luedde et al., 2007). However, the molecular linkage between inflammation and cancer has not been elucidated completely. Ongoing studies indicate that microRNAs can make a connection between inflammation and cancer. miRNAs play critical roles in many biological processes including cancer by directly interacting with specific messenger RNAs (mRNAs) (Bartel et al., 2009). miRNAs can undergo aberrant regulation during carcinogenesis and they can act as oncogenes or tumor suppressor genes. To exemplify the point, Let-7 was found to be deleted in several human cancers (Calin et al., 2004). It was also demonstrated that there was an epigenetic switch which involved NF-κB, Lin28, Let-7 mi-RNA and IL-6 links inflammation to cell transformation (Iliopoulos et al., 2009).

TLR and NLR families initiate the activation of NF-κB and the induction of additional inflammatory signaling cascades. The role of TLRs in the recruitment of immune cells at mucosal surfaces and in protection against tumorigenesis in the gut is well established. For instance, the activation of TLR5 in a mouse xenograft model of human colon cancer elicited powerful antitumor activity (Rhee et al., 2008). In addition to TLRs,

NLRs play an important role in defending human beings against tumorigenesis. To illustrate the point, NOD1 is important for protection against colitis associated colorectal tumor formation (Chen et al., 2008).

Additionally, the NLRP3 inflammasome was recently shown to confer protection against experimental colitis and colitis related cancer model in mice (Zaki et al., 2010) (Allen et al., 2010). IL-18 is one of the downstream products of NLRP3 inflammasome. IL-18 secretion was found to exert a protective role against colorectal tumor formation. NLRP3 iflammasome dependent IL-18 production prevented the neoplastic event, possibly though the induction of IFN-γ production and STAT1 signaling (Zaki et al., 2010). Anticancer chemotherapies are targeted to activate DC cells because they play an important role in presenting antigens from dying cancer cells to T lymphocytes. They produce tumor specific IFN-γ. Dying tumour cells also release several DAMPs such as ATP, activating P2X7 purinergic receptors of DCs and this triggering the formation of the NLRP3 inflammasome, causing the secretion of IL-1β. Activation of the NLRP3 inflammasome in DCs enhanced IL-1β dependent adaptive immunity against tumors. The priming of INF-γ producing CD8+ T cells by dying tumor cells failed in the absence of functional IL1R in *Nlrp3*$^{-/-}$ or *Casp-1*$^{-/-}$ mice. However, when exogenous IL-1β was provided, CD8+ T cells managed to prime IFN γ. In addition to this, when the purigenic receptor *P2RX7* or *Nlrp3* or *Casp-1* of hosts were knocked out, anticancer chemotherapy was inefficient against tumors (Ghiringhelli et al., 2009). It was also reported that anhracycline treated breast cancer patients with a loss of function P2RX7 allele enhanced metastatic disease much more rapidly than the patient with the normal allele (Krelin et al., 2007) (Balkwill et al., 2005).

Loss of inflammasome components lead to tumorigenesis in several tissues. To exemplify the point, Caspase 1 is down-regulated in human colon adenocarcinomas not only at the mRNA but also at the protein level (Jarry et al., 1999). *Casp1*$^{-/-}$ mice, *NLRC4*$^{-/-}$ mice featured significantly enhanced proliferation in both steady state and the early phase of inflammation-induced tumor formation and reduced apoptosis in colorectal cancers (Bo et al., 2010). Mice lacking the inflammasome adaptor protein PYCARD/ASC and Caspase 1 demonstrate enhanced tumorigenesis and they are highly susceptible to inflammation-driven colon tumorigenesis (Allen et al., 2010).

When all of these outcomes are taken into consideration, inflammasome-deficient mice can be suggested to feature enhanced tendency for tumorigenesis and inflammasomes links the innate and adaptive immune responses against dying tumor cells.

1.5. Novel NLRs as Cytoplasmic Immune Sensors

1.5.1. NLRC3

NLRC3, *Caterpiller* gene, *CLR16.2* is located on human chromosome 16. It has seventeen exons (Figure 1.6). The protein which is encoded by this gene has a typical NBD-LRR configuration. It includes a CARD domain as the effector domain. Real time PCR analysis of *CLR16.2* indicated that the gene was highly expressed in T lymphocytes. In addition, the *NLRC3* expression was detected in NK cells, B lymphocytes and several types of tissues such as the thymus, uterus, kidney and the brain. Querying microarray studies in the public databases showed that *CLR16.2* was significantly (>90%) down-regulated 6h after anti-CD3 and anti-CD28 stimulation of primary T lymphocytes. Indeed CLR16.2 decreased NF-κB, NFAT, and AP-1 induction of reporter gene constructs in response to T cell activation by anti-CD3 and anti-CD28 antibodies or PMA and ionomycin (Conti et al., 2005).

The suppression of T cell activation is one of the mechanisms that all immune privilege areas share. Therefore, NLRC3 may be important in immune tolerance to inhibit the activation of T cells.

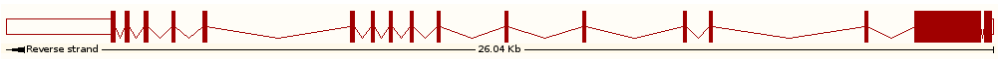

Figure 1.6. Gene Structure of NLRC3.

1.5.2. NLRP13

NLRP13 gene encodes a receptor protein with the characteristics NBD-LRR structure. PYRIN is found at its N terminus as the effecter domain. It is located on human chromosome 19. It has eleven exons (Figure 1.7). According to bioinformatics tools, the

NLRP13 protein should be located in the cytoplasm. Placenta is the only known tissue with expression of NLRP13. It was determined that NLRP13 was highly expressed in oocytes and then gradually decreased in embryos with a very low expression level in day5 (D5) embryos (Zhang et al., 2008). There is no further information about NLRP13 in the literature. Inflammation against allografts are greatly limited or prevented in certain organs, a phenomenon called immune privilege. Placenta is one of the regions where immune privilege is well developed. Therefore, it can be hypothesized that NLRP13 activity might be important for immune privilege in the placenta.

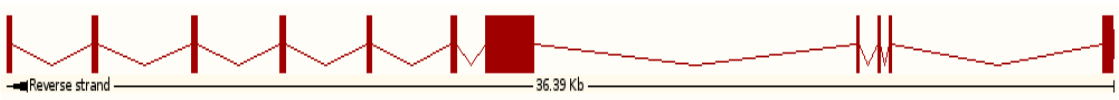

Figure 1.7. Gene Structure of NLRP13.

1.6. Immune Tolerance

The most interesting feature of our immune system is that it is able to distinguish self antigens from non-self and it does not react against self antigens. This unresponsiveness to self antigens is called immunological tolerance. During infection, secretion of pro-inflammatory cytokines and inflammation are the central orchestrators of immunity against various classes of pathogens because they are necessary to induce the activation of immune cascades. However, immune mediated inflammation is greatly limited or prevented in certain organs. This phenomenon is called immune privilege. Placenta and testis are two of the regions where immune privilege is well developed. Apart from these, brain, ovary, pregnant uterus, hair follicle and eyes can be labeled as immunologically privileged regions (Niederkorn JY., 2006). It was observed that edema formation and inflammatory mechanisms which can also destroy the healthy tissues are blocked in immunologically privileged regions. There are several mechanisms, which have an impact on reduction of the immune response.

The first mechanism is related to the physiological features of the privileged organs, such as the eye. The lymphatic vessels do not go deep into eyes and lymph drainage out of the tissue is not adequate to sense the foreign molecules. Hence, the limited lymphatic

drainage of the eye limits the access of antigens to the regional lymph nodes (Niederkorn JY., 2006).

The second feature is about the expression pattern of HLA proteins in the eye. By and large, MHC Ia is a membrane protein expressed by all nucleated cells. Nonetheless, the levels of its expression in the eye and brain decline (Niederkorn JY., 2006). MHC Ia proteins are indispensable to activate cytotoxic T cells. Due to the low amount of MHC Ia in the eye and brain, viral and bacterial infected retina or brain cells are not targeted and killed. In addition to that villous cells in trophoblast which are generated by the embryo do not express classical MHC I proteins; hence, embryo can be protected from maternal cytotoxic T cells (Riteau et al., 2001).

The eyes, brain and trophoblast cells lack MHC I. However, they express MHC Ib molecules such as HLA-G and HLA-E in humans, and Qa-2 in mice. These molecules work together and have a capacity to engage the NK cell inhibitory receptor CD94-NKG2 and suppress NK cell mediated lysis (Riteau et al., 2001).

The third protection mechanism against the immune system is the expression of certain type of proteins localized on the cell membrane. TRAIL and FasL can be given as examples for these strongest ligands. After three of each ligand bind to their receptor molecules, the cells which express respectively FAS, DR4 and DR5/KILLER undergo programmed cell death immediately (Strasser et al., 2009). In other words, active T cells contain FAS receptors on their cell surface. After a complex formation between FasL and Fas, activated T cells undergo apoptosis. In this way, the eyes and fetus can be protected from the immune system (Green et al., 2009).

Last but not least, immune privileged sites can express several immunosuppressive factors to block the inflammatory cascades. Such immunosuppressive factors have an impact on inhibiting cellular parts of immunity. To illustrate the point, transforming growth factor β (TGF-β) can be expressed by eye, brain and fetus. It suppresses the activation of T cells, NK cells, and macrophages. Like TGF-β, soluble FasL suppresses neutrophil recruitment and activation. In addition to that some of immunosuppressive molecules can inhibit the elaboration or release of inflammatory factors such as calcitonin

gene-related peptide (CGRP) and α-melanocyte stimulating hormone (α-MSH) (Niederkorn JY., 2006).

Tumors are abnormal tissue formations which the immune system should also investigate and eliminate from healthy human beings. Normally, the immune system can deal with these problems successfully. However, evolution is an ongoing process for the pathogenic factors like the host. As a result of the microevolution of tumors, they can develop several strategies against the immune system in order to locate, grow, and metastasize to other tissues. Tumors should be targeted for destruction by cytotoxic T cells and NK cells while still developing. However, tumor cells can express FAS and TRAIL to kill the attacking T-cells. This mechanism plays a critical role in establishing tumor immune tolerance (Lu et al., 2008). What is more, Several MHC Class Ib proteins like human leukocyte antigen (HLA)-G, Qa-2, CD1d and NKG2D ligands can bind to either stimulatory or inhibitory receptors expressed on T, NK and NKT lymphocytes, and thereby modulate their anti-tumor activity (Gomes et al, 2007). Interestingly, the numbers of regulatory T cells in cancer patients (T-reg) is quite higher than the numbers in healthy individuals. Regulatory T cells are a unique CD4 (+) T cell lineage that plays a crucial role in the maintenance of immunological tolerance.

The contribution of NLRs to the immune tolerance or immune privilege mechanisms has not been investigated to date. We plan to discover any possible links between NLRC3 and NLRP13 signaling and immune tolerance.

2. PURPOSE

The aim of this study was to investigate the functions of NLRC3 and NLRP13 in innate immunity.

To start with, NLRC3 and NLRP13 genes were cloned into modified pcDNA3 plasmid vectors.

Furthermore, to understand the cellular localization of the NLRC3 and NLRP13 proteins in HEK293FT cells, *NLRC3* and *NLRP13* genes were cloned into pEGFP C3 vector and pEGFP C3 NLRC3 and NLRP13 plasmids were co-transfected with different fluorescently labeled organelle markers to investigate the cellular localizations of NLRC3 and NLRP13 proteins.

Both NLRC3 and NLRP13 share NLR family characteristic domains, respectively CARD and PYRIN. To test the possible interactions of NLRC3 and NLRP13 with inflammasome components, co-immunoprecipitation experiments were performed. Under confocal microscopy, transfected HEK293FT cells were visualized to indicate whether EGFP NLRC3 and NLRP13 could co-localize with their candidate fluorescently labeled protein partners or not. Finally, we performed luciferase reporter gene assay to test the effects of NLRC3 and NLRP13 on NF-κB signaling pathway.

The suppression of T cell activation is one of the mechanisms that all immune privilege areas share. NLRC3 may be important in immune tolerance to inhibit the activation of T cells. Additionaly, placenta is one of the regions where immune privilege is well developed and it can be suggested that NLRP13 might be important for immune privilege in the placenta. Lastly, we can suggest that both NLRC3 and NLRP13 can be anti-inflammatory NLRs. Therefore, this thesis will be a good initiator to discover any existing links between NLRC3 and NLRP13 signaling and immune tolerance.

.

3. MATERIALS

3.1. Cell Lines

3.1.1. Human Embryonic Kidney Cells (HEK293FT)

HEK293FT cells were kindly provided by Assoc. Prof. Maria Soengas from the Spanish National Cancer Research Center (CNIO, Madrid-Spain).

3.1.2. Jurkat cell line

Jurkat cells were kindly provided by Assoc. Prof. Bünyamin Akyol from the Department of Molecular Biology and Genetics at Izmir Institute of Technology.

3.2. Chemicals, Plastic and Glass Ware

All solid and liquid chemicals used in this study were purchased from Sigma (USA), AppliChem (Germany) and Merck (German). Plasticware from TPP (Switzerland) were preferentially used throughout the whole study unless otherwise stated. Glassware was sterilized by autoclaving at 121^0 C for 20 minutes before use.

3.3. Buffers and Solutions

3.3.1. Cell Culture

Table 3.1. Cell Culture Materials.

0.5 per cent Trypsin-EDTA 1X	:	GibcoBRL, USA
DMSO	:	AppliChem, Germany
Dulbecco's Modified Eagle Medium (DMEM)	:	GibcoBRL, USA

Table 3.1. Cell Culture Materials (continued).

Fetal Bovine Serum (FBS)	:	GibcoBRL, USA
Freezing Medium	:	25 per cent FBS 1 per cent Pen Strep 1 per cent GlutaMAX 1 per cent NEAA 1 per cent DMSO
GlutaMAX I 100X	:	GibcoBRL, USA
MEM Non-essential amino acid (NEAA) 100x	:	GibcoBRL, USA
Penicillin/Streptomycin	:	GibcoBRL, USA
RPMI 1640	:	GibcoBRL, USA

3.3.2. Cloning and Diagnostic Digestion

Table 3.2. Cloning and Diagnostic Digestion Materials.

Restriction Enzymes	:	NEB, England
T4 DNA Ligase	:	NEB, England

3.3.3. DNA Electrophoresis

Table 3.3. DNA Electrophoresis Materials.

50X Tris-acetic acid EDTA (TAE)	:	2 M Tris-acetate 50 mM EDTA pH 8.5
DNA Ladder	:	DNA Ladder Mix Fermentas, Canada
Ethidium bromide (EtBr)	:	Merck
Loading buffer	:	6x DNA Loading Dye Fermentas, Canada

3.3.4. Transformation and Transfection

Table 3.4. Transformation and Transfection Materials.

2X HBS Buffer	:	1.6 g NaCl 0.074 g KCl 0.027 g Na_2HPO_4 0.2g Glucose 5 ml 1 M HEPES Make up to 100 ml with dd H_2O Adjust pH 7.05
Ampicillin	:	AppliChem, Germany
Chloroquine	:	AppliChem, Germany
HEPES	:	GibcoBRL, USA
Kanamycin	:	Sigma, USA
LB Agar	:	1 L LB medium 15 g Agar
LB medium (1 L)	:	10 g Tryptone 5 g Yeast Extract 5 g NaCl
SOC Media	:	20 g Tryptone 5 g Yeast Extract 2 ml of 5 M NaCl 2.5 ml of 1 M KCl

3.3.5. Protein Isolation

Table 3.5. Protein Isolation Materials.

Cell Lysis Buffer	:	10 mM NaH_2PO_4 140 mM NaCl 3 mM $MgCl_2$ 0.5 % NP40 Adjust pH 8.0 Before using add 1 tablet Protease Inhibitor cocktail
Protease Inhibitor Cocktail	:	Roche, Germany

3.3.6. RNA Isolation

Table 3.6. RNA Isolation Materials.

PBS-DEPC Water	:	4 g NaCl 0.10 g KCl 0.12 g KH_2PO_4 0.72 g Na_2HPO_4 Make up to 500 ml with DEPC water Autoclave
Red Blood Lysing Buffer-DEPC	:	4.15 g NH_4Cl 0.5 g $KHCO_3$ 1 mM EDTA Make up to 500 ml with DEPC water Autoclave

3.3.7. Western Blot (WB)

Table 3.7. Western Blot Materials.

Acrylamide:Bisacrylamide	:	29.2 g/100 ml acrylamide 0.8 g/100 ml N`N`-bis-methylene-acrylamide
Ammonium Persulfate	:	10 % APS (w/v) in dd H_2O
Blocking Solution	:	5 % non-fat milk powder in TBST
Chemiluminescence	:	Roche
Coomassie Brilliant Blue Staining	:	125 ml Ethanol 100% 0.625 g Coomassie Brilliant Blue 25 ml Glicial acetic acid 100 ml dd H_2O
Coomassie Blue Destaining Solution:		37.5 ml Glicial acetic acid 25 ml Ethanol 100% 437 ml dd H_2O
Non-Fat Dry Milk	:	Bio-Rad
Ponceau Staining Solution	:	1 g Ponceau (AppliChem) 50 ml acetic acid Make up to 1 L with ddH_2O
Protein Marker	:	PageRuler^{TM} Plus Prestained Protein Ladder Fermentas
Resolving Gel (15%) Stock	:	33.3 ml Acryalmide 30% 20 ml Tris-base 1.875 M pH 8.8 1 ml SDS 10% 45.7 ml H_2O Store at $+4^0$ C
Resolving Gel (15%) for mini gel	:	10 ml Resolving Gel (15%) Stock 100 µl APS 10% 10 µl TEMED

Table 3.7. Western Blot Materials (continued).

Running Buffer	:	250 ml 10x Tris-Glycine buffer 25 ml SDS 10% 2250 ml dd H_2O
6xSample Buffer	:	1.2 g SDS 0.9 g DTT 6 mg bromophenol blue 4.7 mL glycerol 1.2 mL Tris 0.5 M pH 6.8 2.1 mL dd H_2O
SDS	:	AppliChem, Germany
Stacking Gel (4%) Stock	:	3.3 ml Acryalmide 30% 6.3 ml Tris- HCl 0.5 M pH 6.8 250 µl SDS 10% 15 ml H_2O Store at $+4^0$ C
Stacking Gel for mini gel	:	5 ml stacking gel stock (4%) 50 ml APS 10% 5 ml TEMED
Stripping Solution	:	62.5 mM Tris-HCl, pH 6.8 2% SDS 0.7% β-Mercaptoethanol
TBS 10X	:	90 g NaCl 121.14 g Tris-Base Make up to 1 L with dd H_2O Adjust pH 7.5
TBS-TWEEN	:	100 ml TBS 10X 899 ml dd H_2O 1 ml TWEEN 20

Table 3.7. Western Blot Materials (continued).

Transfer Buffer	:	2.93 g Glycine 5.81 g Tris-Base 6.25 ml SDS 10% 1 L dd H_2O
Tris-Glycine Buffer 10X	:	15 g Tris-Base 72 g Glycine 500 ml dd H_2O
TWEEN	:	CalbioChem, Canada

3.3.8. Co-Immunoprecipitation (Co-IP)

Table 3.8. Co-Immunoprecipitation Materials.

Protein A Matrix	:	Pierce
Protein G Matrix	:	Thermo Scientific
Lysing Buffer	:	10 mM NaH_2PO_4 140 mM NaCl 3 mM $MgCl_2$ 0.5% NP40 Adjust pH 8.0 Before using add 1 tablet Protease inhibitor cocktail (Roche)
Isotonic Lysing Buffer	:	10 mM NaH_2PO_4 50 mM NaCl 3 mM $MgCl_2$ 0.5% NP40 Adjust pH 8.0 Before using add 1 tablet Protease

3.4. Fine Chemicals

3.4.1. Plasmids

Several plasmids were kindly provided from our department or several universities. There are the table of used plasmids and their sources.

Table 3.9. Plasmids.

Ds RED MTS	AKLAB (BOUN MBG)
FLAG pcDNA3	AKİL
FLAG pcDNA3 Caspase 1	Nunez Lab. (University of Michigan)
MYC pcDNA3	AKİL
pEGFP C3	Retina Lab. (BOUN MBG)
pTag RFPC3	AKİL
pcDNA3 TagRFP-T	Tsien Lab. (MIT)
HA pcDNA3	AKİL
pECFP C1 Caspase 1	AKİL
pECFP ER	Batu Erman Lab. (Sabancı University)
pECFP Golgi	Batu Erman Lab. (Sabancı University)
pCFP Rab 5	Batu Erman Lab. (Sabancı University)
pCFP Rab 9	Batu Erman Lab. (Sabancı University)
pCFP Rab 11	Batu Erman Lab. (Sabancı University)

3.4.2. Primers

Primers used in this study were synthesized by Harvard DNA Core Facility (Boston, USA). The primers listed in Table 3.10 were used for cloning studies. The plasmids listed in Table 3.11 were used for sequencing the positive colonies, which contained the gene of interests as insert.

Table 3.10. Primer Sequences for Cloning Part of the Study.

Primer Name	RE Cutting Sites	Tm	Sequence
NALP13_F	Spe I	58,4	TAAG ACTAGT AAC TTT TCT GTA ATC ACC
NALP13_R	Not I	75,2	GATAGAC GCGGCCGC TTA CCC GAG TTT CTG CAG
NLRC3_F	Xba I	67,1	TAAG TCTAGA AGG AAG CAA GAG GTG CGG
NLRC3_R	Not I	74,2	GATAGAC GCGGCCGC TCA CAT TTC AAC AGT GCA
BNLRC3_F	BamH I	69	TAAG GGATCC ATG AGG AAG CAA GAG GTG C
BNLRP13_F	Mfe I	59,9	TAAG CAATTG ATG AAC TTT TCT GTA ATC ACC TGC C

Table 3.11. Primer Sequences for Sequencing Part of the Study.

SEQ NLRC3_F	1	5’ CTGCAGCAATGACTCAAGGA 3’
	2	5’ CAAGGTGTGTTTGGAGCAGA 3’
	3	5’ TCTTGTCTCCGAGGGTCAAT 3’
	4	5’ CTGCACCTGCAGAAGAACAG 3’
	5	5’ ACAGGAGCCTCACCAGCTTA 3’
NLRP13 SEQ_F	1	5’ AGAAGCAGCAGCAGGGAATA 3’
	2	5’ GGTTCCCCTGGCTACCTTAC 3’
	3	5’ CATTCCACAAAGCCACAAGA 3’
	4	5’ ACGTGCAAATCGGTAACTCCT 3’
	5	5’ CAGAACAGGAGCCTGACACA 3’
T7	5’ TAATACGACTCACTATAGGG 3’	
SP6	5’ ATTTAGGTGACACTATAG 3’	
CMV	5’ CGCAAATGGGCGGTAGGCGTG 3’	
M13_F	5’ TGTAAAACGACGGCCAGT 3’	
M13_R	5’ CAGGAAACAGCTATGAC 3’	
GAPDH_F	5’ ATGGGGAAGGTGAAGGTCG 3’	
GAPDH_R	5’ GGGGTCATTGATGGCAACAATA 3’	

3.4.3. Antibodies

Table 3.12. Antibodies Used in Western Blot Analysis and Co-IP.

Antibody	Source	Company	Dilution Used	Usage
GFP antibody (ab290)	Rabbit	Abcam	1:2500	WB
beta actin antibody	Rabbit	Cell Signaling	1:1000	WB
Anti-rabbit IgG	Gout	Cell Signaling	1:1000	WB
Anti-mouse IgG	Rabbit	Cell Signaling	1:1000	WB
FLAG	Rabbit	Cell Signaling	1:1000	WB
FLAG	Rabbit	Cell Signaling	1:250	IP
MYC	Rabbit	Cell Signaling	1:1000	WB
ASC	Rabbit	Novus	1:250	IP
ASC	Rabbit	Novus	1:1000	WB
Caspase 1	Rabbit	Santa Cruise	1:1000	WB
Caspase 1	Rabbit	Cell Signaling	1:250	IP
IκB alpha subunit	Rabbit	Cell Signaling	1:1000	WB
Phospho-IκB alpha subunit	Rabbit	Cell Signaling	1:1000	WB

3.5. Kits

3.5.1. PCR Purification

High PCR Purification Kit : Roche, Germany

3.5.2. RNA isolation

High Pure RNA Isolation Kit : Roche, Germany

3.5.3. Plasmid Miniprep-Midiprep-Maxiprep

QIAfilter Plasmid Midi Kit : Qiagen, USA

3.5.4. Luciferase Reporter Gene Assay

Dual-Glo Luciferase Reporter Gene Assay : Promega, USA

3.5.5 Reverse Transcription System

Reverse Transcription System : Promega, USA

3.5.6. Agarose Gel Extraction

Agarose Gel Extraction kit : Qiagen, USA

3.5. Equipment

Table 3.13. Equipment Used in This Thesis.

Equipments	Models
Autoclave	Model MAC-601, Eyela, Japan Model ASB260T, Astell, UK
Balances	Precisa XT4200C
Centrifuges	Allegra X22-R, Beckman Coulter, USA Centrifuge 1-15, Sigma, USA Centrifuge 2-16K, Sigma, USA Centrifuge 16 M, Spectrafuge Himac CT4200C, Hitachi Koki, Japan J2-MC Centrifuge, Beckman Coulter, USA J2-21 Centrifuge, Beckman Coulter, USA Micro 200R Centrifuge
Cover Slips	22x22 mm, ISOLAB Laborgeräte, Germany
Cold room	Birikim Elektrik Soğutma, Turkey
Deep Freezers	2021D (-20^{0}C), Arçelik, Turkey
Documentation System	Gel Doc XR System, Bio Doc, ITALY
Electrophoretic Equipments	Mini-PROTEAN 3 Cell, BIO-RAD, USA Trans-Blot Semi Dry Cell, BIO-RAD, USA Agarose Gel System, Thermo Scientific
Ice Machine	Scotsman Inc., AF20, ITALY
Incubator	Hepa Class II Forma Series, Thermo Electron
Heat Bloker	Standart heat blocker, VWR
Laminar flow cabinet	Class II A Tezsan, Turkey Class II B Tezsan, Turkey
Luminometer	Fluoraskan Ascent FL and Fluoroskan Askent, Thermo Scientific
Magnetic Stirrer	Yellowline MSH Basic

Table 3.13. Equipment Used in This Thesis (continued).

Microscopes	Zeiss, Axio Observer Z1 Inverted Mic., USA LeicaTCSSP5II Leica Confocal Microscopy Nikon Eclipse TS100 Flourescent Mic.
Microscope slides	ISOLAB Laborgeräte, Germany
Microwave oven	Arçelik
pH Meter	H221 Calibration Check Nicroprocessor, Hanna Instruments
Pipettes	Pipetman, Gilson, USA
Pipettor	Greiner-bio one RatioLab acupetta
Refrigerator	4250T, Arçelik, Turkey
Power Supplies	EC135-90, Thermo Electron Corporation Power Pac Universal, BIO-RAD, USA
Shakers	Polymax 1040, Heildophl Polymax 1010, Heildophl
Spectrophotometer	NanoDrop ND-1000, Thermo, USA
Protein Visualization	Stella, Raytest, Germany
Thermocyclers	C1000 thermal cycler, BIO-RAD, USA
Vortex	Fisons Whirli Mixer GmcLab, Gilson
Water Bath	Water bath, GFL Water bath, Memmert
Water Purification	UTES, Turkey

4. METHODS

4.1. Cell Culture

4.1.1. Maintenance of HEK293FT Cell Lines

Human embryonic kidney cell lines HEK293FT were kindly provided by Prof. Maria Soengas at Spanish National Cancer Research Center. They were grown in DMEM supplemented with 10% FBS, 1X L-Glutamine, 1X Penicillin/Streptomycin and 1X MEM Non-Essential Amino Acids. Cell lines were grown at 37^0 C and 5% CO_2. HEK293FT cells can be frozen with 10% DMSO at -80^0C.

4.1.2. Maintenance of Jurkat Cell Lines

Jurkat cells are one of the T lymphocytes kindly provided by Assoc. Prof. Bünyamin Akyol Department of Molecular Biology and Genetics at Izmir Institute of Technology. They are non-adherent cells. The cells were grown in RPMI 1640 supplemented with 10% FBS, 1X L-Glutamine, 1X Penicillin/Streptomycin and 1X MEM Non-Essential Amino Acids. Cell lines were grown at 37^0C and 5% CO_2. They could grow fast. Therefore, the cells should be passaged in every 48 hours. Jurkat cells can be stored in 10% DMSO at -80^0C.

4.2. Plasmids

4.2.1. Chemically Competent Cell Preparation by Calcium Chloride Method

A single colony of Top10 strain of *E. coli* cells was inoculated in 5 ml LB medium. This culture was incubated overnight at 37ºC with shaking at 200 rpm. After 16 hours, 25 ml LB was inoculated with 250 µl of the grown culture to make 1:100 dilution. Cells were grown in the shaker till OD 600 reached 0.4. Cells were harvested by centrifuging at 3000 rpm for 10 minutes at 4ºC. The pellet was resuspended in 12.5 ml of ice-cold sterile 50 mM $CaCl_2$ and incubated on ice for 30 min. Cells were centrifuged again (3000 rpm for 10

min at 4ºC) and the pellet was resuspended in 2.5 ml of ice-cold sterile 50 mM $CaCl_2$. 100-150 µl of this preparation was used for transformations. For long term storage at -80 ºC, glycerol was added to make 10 per cent final concentration and cells were rapid-frozen in liquid nitrogen.

4.2.2. Heat Schock Transformation of Bacteria

In the transformation experiment, first, competent cells were incubated on ice for 15 minutes. Then, 50 µl of competent *E.coli*, cells which placed in calcium chloride solution were mixed with 10 ng of plasmid DNA and then; incubated on ice for 10 minutes, in 42°C water bath for 2 minutes and again on ice for 4 minutes. The bacteria containing the plasmids were grown in antibiotic-free liquid SOC medium for 1 hour at 37°C, in order to allow expression of antibiotic resistance. Next, the bacteria were plated on a 100 mg/ml antibiotic-containing LB agar plate and incubated overnight at 37°C. On the next day, colonies from the plate was selected and grown in 250 ml of 100 mg/ml antibiotic-containing liquid LB medium for overnight at 37°C.

4.2.3. Plasmid Isolation

Overnight inoculated 250 ml bacteria were used for plasmid isolation process. QIAfilter Plasmid Midi Kit was used for purification of plasmid DNA. The kit combines QIAfilter Midi cartridges to separate bacterial lysates by filtration. Plasmid isolation was performed according to manufacturer's instructions. In the final step, plasmid was eluted in TE buffer. Concentration of the eluted plasmid DNA was determined by the NanoDrop Spectrophotometer. The plasmid DNA was stored at -20°C for further applications.

4.3. RNA Isolation

RNA was always handled with equipments previously wiped with RNase inhibitor. Isolation was performed with Roche High Pure RNA Tissue Kit. Blood cells were used as a source of total RNA. 10 ml blood was taken from two volunteers. In the first step, blood cells were incubated with 20 ml Red Blood Cell (RBC) lysing buffer which was prepared with DEPC water. The incubation was done on the shaker at room temperature. Then, cells

were centrifugated at 3000 rpm for 8 minutes. The pellet was resuspened in RBC-DEPC lysing buffer. This step was repeated until the colour pellet started to be white. After final washing, the pellet was resuspended in 400 µl sterile 1x PBS-DEPC.

400 µl of cells were transferred to Eppendorf tubes and mixed with 400 µl Lysis/-Binding Buffer and vortexed for 15 seconds. Next, the lysate was transferred to High Pure Filter Tubes and centrifuged for 15 seconds at 10000 rpm at 4^0C. Master DNase mix, containing 90 µl DNase incubation buffer and 10 µl DNase working solution were applied onto the filters of the High Pure Filter Tubes, followed by incubation at room temperature for 15 minutes. Then, 500 µl of Wash Buffer I was added, which was centrifuged for 1 minute at 10000 rpm at 4^0C; the flow-through was discarded. In the second wash, 500 µl of Wash Buffer II was added, followed by centrifugation for 1 minute at 10000 rpm; again the flow-through was discarded. In the last wash, 300 µl of wash buffer II was added, followed by centrifugation for 2 minutes at 13000 rpm at 4^0C. The filter was carefully removed and put into a sterile Eppendorf tube. Finally, 50 µl Elution Buffer was applied to the filter and centrifuged for 1 minute at 13000 rpm at 4^0C. The concentration of the eluted RNA was determined by the NanoDrop Spectrophotometer and it was stored at -80^0C for further use.

4.4. c-DNA Synthesis

c-DNA synthesis followed the process of total RNA isolation. 1 µg total RNA was prepared in each Eppendorf tube and 1 µl poly-dT primer was added and the RNA-primer mixes were incubated at 72^0C for 5 minutes. Then, the mixture was immediately chilled in ice-water for at least 5 minutes. Next, the tubes were spinned for 10 seconds in a microcentrifuge to collect the condensate and maintain the original volume. The tubes were closed and incubated on ice until the reverse transcription reaction master mix was added. In the master mix, 4µl 5x reaction buffer, 5 µl $MgCl_2$, 1 µl dNTP mix, 0.5 µl RNase inhibitor and 1 µl reverse transcriptase were added. 11.5 µl master mix was distributed to each Eppendorf. Reaction took place at 42^0C for 1 hour and as a final step reverse transcriptase was inactivated at 70^0C for 15 minutes.

4.5. Gene Specific PCR of NLRC3 and NLRP13

Total RNA from lymphocytes was used to clone the *NLRC3* gene. The primers' annealing temperatures were listed in Table 3.9 in the Materials part. *NLRC3* gene source was the c-DNA library of total blood cells. *NLRP13* gene was purchased from GeneCopoeia (GeneCopoeia, USA) in the pENTR223.1 vector. This vector was used as a template in PCRs. To clone NLRC3 and NLRP13, high fidelity Taq polymerase (Finzymme, Finland) was preferred to amplify the genes. Firstly, gradient PCR was performed to choose the most suitable annealing temperatures for NLRC3 and NLRP13 primers. 60^0C was found to be the most appropriate temperature. The concentration of NLRC3 and NLRP13 primers were 10 μM per reactions. To eliminate any nonspecific amplification of NLRC3 and NLRP13, 3% DMSO was used in the PCR. In addition to that, $MgCl_2$ concentration was optimized to 2.5 mM. 10 μl c-DNA was used to amplify *NLRC3* gene and 200 ng pENTR223.1 NLRP13 was added to the PCR reactions as a template.

Table 4.1. PCR Conditions for NLRC3 and NLRP13.

98^0C	30 seconds	
98^0C	15 seconds	X 30
60^0C	30 seconds	
72^0C	3 minutes	
72^0C	10 minutes	
4^0C	15 minutes	

4.6. Agarose Gel Electrophoresis

DNA fragments were fractionated by horizontal electrophoresis using standard 1x TAE-based agarose gels (1 per cent to 2 per cent). Agarose is mixed with 1x TAE Buffer and allowed to boil in a microwave oven. After cooling for a couple of minutes, ethidium bromide was added to final concentration of 30 ng/ml and the solution was poured into the gel casting tray. Appropriate amounts of the DNA samples were mixed with 6x loading

buffer to get 1x final concentration. The solidified gels were run in 1x TAE buffer at varying voltage and time depending on the size the fragments.

4.7. Generation of NLRC3 and NLRP13 Plasmid Vectors

4.7.1. Cloning into FLAG, HA or MYC pcDNA3

pcDNA3 was modified to insert FLAG, HA and MYC tags after starting codon. These modified plasmids included several specific cutting sites that made the cloning process easy. Firstly, ORFs of NLRC3 and NLRP13 genes were found from NCBI database. NM_178844.2 was the NCBI reference sequence of NLRC3 and NM_176810.2 was the NCBI reference sequence of NLRP13. These sequences were analysed with NEB Cutter V2.0 online programme *(http://tools.neb.com/NEBcutter2/index.php)* to get their restriction maps. After web based restriction digestion, XbaI restriction enzymes cutting site was added into 5' end of NLRC3 forward primer and NotI digestion sequence was added to 5' end of NLRC3 reverse primer. 3 nucleotides were added before cutting sites to increase the cutting efficiency. The same process was performed for NLRP13. SpeI cutting site was added to 5' of NLRP13 forward primer and NotI was inserted in 5' ends of NLRP13 reverse primer. The expected PCR products were loaded in 1% agarose gel and they were extracted and purified with QIAGEN Agarose Gel Extraction kit. Purified NLRC3 PCR product included 5' XbaI and 3' NotI cutting sites. FLAG, HA or MYC pcDNA3 plasmids contain XbaI and PspOMI restriction sites. PspOMI creates compatible sticky ends for NotI and SpeI creates sticky compatible ends for XbaI. 2 µg PCR products and plasmids were digested by 5 units each restriction enzyme. After sequential digestion of vectors and PCR products, digested PCR products and linear vectors were prepared. To purify the digestion reaction, each first reaction was extracted from agarose gel and the second reactions were purified with PCR purification kit.

Ligation reactions were held as follows: 1 µl digested vector, 3 µl digested insert, 1.5 µl ligase buffer and one unit ligase. Final volume was 15 µl and the tubes were incubated at room temperature for 2 hours. Ligation reaction was transformed into Top10 competent bacteria. Colonies were scanned with T7 and SP6 universal primers in colony PCR. Diagnostic digestion was performed for purified plasmids. One unit EcoRI and XbaI were

used to digest the 1 µg plasmids. DNA fragments were run in the 1% agarose gel (100 V, 40 minutes, 250 A). Fragments were visualized in Gel-Doc (Bio-Rad, USA). To verify the sequence, positive plasmids were sent to Macrogen (Macrogen, Korea) for sequencing.

4.7.2. Generation of EGFP NLRC3 and EGFP NLRP13 Fusion Proteins

pEGFP C3 plasmid (Clontech, USA) was kindly provided from Retina Laboratory in our department. *NLRC3* gene is cloned from pET30 a (+) NLRC3 plasmid into pEGFP-C3 vector by BgIII and NotI sites. *NLRP13* gene was cloned from FLAG pcDNA3 NLRP13 plasmid into pEGFP C3 vector by XhoI and XmaI sites. Colonies were scanned with CVM forward primer and NLRC3 or NLRP13 cloning reverse primers. Positive colonies were inoculated into 6 ml Kanamycin (50 µg final concentration) LB media. Diagnostic digestion was performed for purified plasmids. One unit EcoRI and XbaI were used to digest the 1 µg plasmids. DNA fragments were run in the 1% agarose gel (100 V, 40 minutes, 250 A). Fragments were visualized in Gel-Doc (Bio-Rad, USA). To verify the sequence, positive plasmids were sent to Macrogen (Macrogen, Korea) for sequencing.

4.8. $Ca_3(PO_4)_2$ Transfection

HEK293FT cells were seeded at $1x10^6$ cells/wells in 6-well plate and incubated overnight at 37^0C, 5% $C0_2$. In each well, the volume included 2 ml cell and media mixture. On the next day, 5 µl chloroquine (25 µM final concentration) was added to each well. 2 µg modified pcDNA3 NLRC3 or NLRP13 plasmids and 0.5 µg pEGFP C3 empty vector were added to the microcentrifuge tubes and the volume was completed to 219 µl. After DNA-water mixes were prepared, 30.5 µl 2 M $CaCl_2$ was added and finally the volume was completed to 500 µl 2x HBS buffer. The tubes were incubated at room temperature for 10 minutes to precipitate the DNA molecules with $PO4^{-3}$ ions. After incubation, the mixture was added to the cell media and incubated at 37^0C, 5% CO_2 for 8-12 hours. The medium was replaced with fresh complete DMEM after 8-12 hours to remove choroquine.

4.9. SDS-Polyacrylamide Gel Electrophoresis (PAGE) and Western Blotting

One day before transfection, 10^6 cells per well were plated into 6 well plates. Cells are transfected with respective plasmids and 24 hours later, they were harvested with 100 µl of cell lysing buffer. Cells were incubated on ice for 1 hour and they were vortexed lightly and periodically. After 1 hour incubation, cells were centrifuged at 13000 rpm, $+4^0$C and 30 minutes. Supernatants were collected and the 6x sample buffer was added. Samples were boiled at 95°C for 10 minutes and run on a 15 per cent polyacrylamide gel with a 4 per cent stacking gel. The gel was run in running buffer at 55V until the samples reach the resolving gel and the voltage was increased to 110V.

Blotting papers (Sigma-Aldrich, USA) and PVDF membrane (Milipore, Ireland) were cut the size of the gel to be transferred and wetted in methanol for 1 minutes, in ddH_2O for 1 minutes and in cold transfer buffer for 3 minutes. Semi-dry transfer was done at (area of polyacrylamide gel x 5) mA for 45 minutes. The membrane was incubated in 5 per cent fat-free milk powder in TBST for 1 hour and in 1° antibody in 1 per cent milk powder in TBST overnight. On the next day membrane was washed in TBST for 3x10 minutes and incubated with the 2° antibody conjugated to horse radish peroxidase (HRP) in 5 per cent milk powder in TBST for 1h. The previous washing steps were repeated. Lumi-light Western Blotting Substrate (Roche, Germany) was applied onto the membrane for five minutes and the bands were visualized on the Stella. Very sensitive image program was chosen to detect the proteins on the membrane.

4.10. Confocal Analysis

One day before transfection, a cover slips was put in each well of 6 well plates and 10^6 cells per well were plated into 6-well plates. Cells were transfected with respective plasmids and 24 hours later, cells were washed with 1 ml 1x PBS for 2 times and 1 ml 10% paraformaldehyte was added and incubated for 5 minutes at room temperature to fix the cells. Cells were washed with 1 ml 1xPBS for 3 times. Mounting media was put on slide and cover slip was closed on the mounting media without making bubbles. The slides were left to dry before analyses.

Slides were visualized with Leica TCS SP5 II upright confocal microscope. All images used for speck counting were taken under identical conditions. Cells were monitored with 20x objective and 20x magnification (755 μm x 755 μm visual field) at locations with 100% cell confluency, pinhole= 30.5 μm. RFP or DsRED, EGFP and ECFP were monitored by sequential scan in which EGFP is excited by 488 nm laser line and ECFP by 458 nm laser line of argon laser. For EGFP, 525-600 nm and for ECFP 465-475 nm windows were used for capturing images.

4.11. Co-Immunoprecipitation

HEK293FT cells were seeded at $5x10^6$ cells/10 cm culture plates and incubated overnight at 37^0C, 5% $C0_2$. Cells were transfected with plasmids and 24 hours later, they were harvested. The pellet of cells was washed with cold 1x PBS. This washing step was repeated 3 times. Pellets were resuspended in 500 μl 0.5% NP40 lysing buffer. Resuspended pellets were incubated on ice for 1 hour and vortexed gently and periodically. After 1 hour, cell lysates were centrifuged at 13000 rpm at 4^0C for 30 minutes. The supernatant was removed and 100 μl was stored as total lysate. 15 μl Protein A and 15 μl protein G beats were washed with 0.5% NP40 lysing buffer for 3 times. 400 μl supernatant was incubated with the mixture of washed protein A-G beads on the rotator at cold room for 30 minutes. In a parallel way, 25 μl Protein A and 25 μl protein G was washed with 0.5% NP40 lysing buffer for 3 times. At the end of incubation period, beads-supernatant mixture was centrifuged at 13000 rpm at 4^0C for 15 seconds. Supernatant was collected and added to cleaned beads. 2 μl antibody was added to supernatant-beads and incubated at cold room on rotator for overnight.

Beads-supernatant-antibody mixture was centrifuged at 13000 rpm at 4^0C for 15 seconds and beads were washed with isotonic lysing buffer for 3 times. Each time, beads-lysing buffer mixture was centrifuged at 13000 rpm at 4^0C for 15 seconds.

In the final step, beads were resuspended in 30 μl of sample buffer and Western Blot analyses were performed.

4.12. Luciferase Reporter Gene Assay for NF-κB Activity

$1x10^6$ HEK293FT cells were plated in 6 well plates and co-transfected with pBVIx-Luc fire fly luciferase reporter plasmid (50 ng), pRL-TK Luc renilla luciferase (5 ng) as an internal control, FLAG pcDNA3 NLRC3 or MYC pcDNA3 NLRC3 (10-50-100 ng), pcDNA3 HA NOD1 (100 ng) and pEGFP C3 (150 ng) via calcium phosphate method. The total amount of DNA (750 ng) was kept constant by inclusion of empty pcDNA3 vector. Twenty four hours post-transfection, NF-κB dependent transcription was determined by using a Dual-Glo Luciferase Assay System (Promega, USA). pRL-TK Luc renilla luciferase was used for normalizing transcription efficiencies. Assays were performed in triplicates. Statistical analyses of the results were performed with online tool *(http://www.graphpad.com/quickcalcs/ttest1.cfm?Format=C).*

4.13. Phylogenetic Analysis

The phylogenetic trees presented in this thesis were constructed with Mega version 3.1 software. The sets of genes or amino acids were aligned with ClustalX2 and the phylogenetic trees were constructed with Mega version 3.1 software. Minimum evolution, neighbor-joining, and maximum parsimony methods were used with Poisson correction for multiple amino acid or nucleic acid substitution with 1000 random bootstrap replicates. The figures were shown in the Minimum evolution or Neighbor Joining tree (the three methods produced very similar topologies).

5. RESULTS

5.1. The Structures of NLRC3 and NLRP13 proteins

Sequence comparisons of NLRC3 show the same overall multi-domain configuration composed of the N-terminal effector domain, central NACHT domain and LRR domains found in all other human NLRs (Figure 5.1.A). On the other hand, NLRP13 shares similar architecture with NLRC3 but it has characteristic PYRIN domain. The NLRC3 effector domain included the amino acid residues from 1 to 138 and shows no sequence homology to CARD or PYRIN domains (Figure 5.1.C and 5.1.D). Besides CARD and PYRIN domain, apoptosis related molecules also share several domains like death domain (DD) and death effector domain (DED). All of these modules form a six or seven antiparelel α-helical bundle that has been termed the death domain (Bouncheir-Hayes et al., 2002). NLRC3 has characteristic a 6 α-helical bundle. This indicates that NLRC3 effector domain is structurally similar to CARD or PYRIN domains, whereas features a different interface. The NACHT domain of NLRC3 (residues 139-302) contains a consensus sequence GVAGMGKT known as P-loop (Walker A box). This domain represents high homology with the NACHT domain of Cryopyrin (Figure 5.1.E). The carboxyl terminal of NLRC3 share similar LRR configuration. This domain has 14 LRRs (Figure 5.1.A).

The effector domain of NLRP13 has typical PYRIN domain. NLRP13 is composed of an amino terminal PYRIN domain fused to a region of 60 amino acids (residues 13-72) (Figure 5.1.B). The PYRIN of NLRP13 was most similar to PYPAF protein (Figure 5.1.C). One of the conserved domains in the NLRP13 protein is NACHT domain. This domain represents high homology with the NACHT domain of NALP1 (Figure 5.1.E). In the NACHT domain, there is a consensus P-loop sequence, GRAGVGKT. The carboxyl terminal region of NLRP13 contained 11 LRRs that have a role in sensing pathogens and protein-protein interaction (Figure 5.1.B).

A

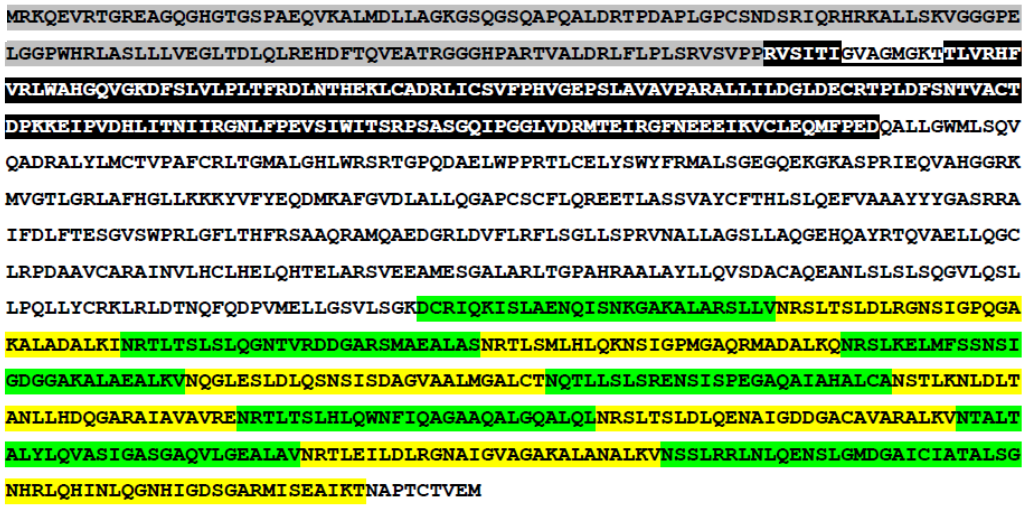

B

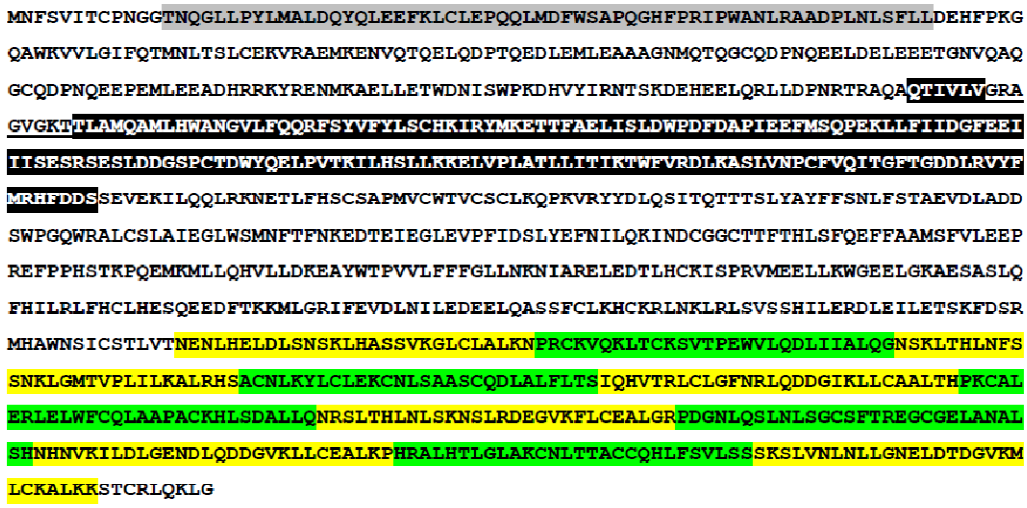

Figure 5.1. Alignments of Human NLRC3, NLRP13 and Related Proteins. (A) NLRC3 protein structure. (B) Protein structure of NLRP13. (C) Alignment of PYRINs and CARDs (D) of NLR family members. (E) Alignment of NACHT domains of NLRs.

C

```
MEFV          ---------------------PSDHLLSTLEELVPY-DFEKFKFKLQNTSVQKEHSRIPRS 39
CRYOPYRIN     ---------------------TRCKLARYLEDLEDV-DLKKFKMHLEDYPPQKGCIPLPRG 39
PYPAF         ---------------------ARDAILDALENLTAE-ELKKFKLKLLSVPLREGYGRIPRG 39
NLRP13        ---------------------TNQGLLPYLMALDQY-QLEEFKLCLEPQQLMD-FWSAPQG 38
NALP1         ---------------------AWGRLACYLEFLKKE-ELKEFQLLLANKAHSRSSSGETPA 39
NLRP2         ---------------------MGFNLQALLEQLSQD-ELSKFKYLITTFSLAHELQKIPHK 39
NLRC3         MRKQEVRTGREAGQGHGTGSPAEQVKALMDLLAGKGSQGSQAPQALDRTPDAPLGPCSND 60
                                      :   :  *    .  .                  .

MEFV          QIQRARPVKMATLLV--TYYGEEYAVQLTLQVLRAINQRLLAEELHR------------- 84
CRYOPYRIN     QTEKADHVDLATLMI--DFNGEEKAWAMAVWIFAAINRRDLYEKAKR------------- 84
PYPAF         ALLSMDALDLTDKLV--SFYLETYGAELTANVLRDMGLQEMAGQLQA------------- 84
NLRP13        HFPRIPWANLR----------AADPLNLSFLL---------------------------- 60
NALP1         QPEKTSGMEVASYLV--AQYGEQRAWDLALHTWEQMGLRSLCAQAQE------------- 84
NLRP2         EVDKADGKQLVEILT--THCDSYWVEMASLQVFEKMHRMDLSERAKD------------- 84
NLRC3         SRIQRHRKALLSKVGGGPELGGPWHRLASLLLVEGLTDLQLREHDFTQVEATRGGGHPAR 120
                       :                     :

MEFV          ------------------
CRYOPYRIN     ------------------
PYPAF         ------------------
NLRP13        ------------------
NALP1         ------------------
NLRP2         ------------------
NLRC3         TVALDRLFLPLSRVSVPP 138
```

D

```
PYPAF         -----LHFIDQHRAALIARV-----TNVEWLLDALYG---------KVLTDEQYQAVRAE 41
NALP1         -----LHFVDQYREQLIARV-----TSVEVVLDKLHG---------QVLSQEQYERVLAE 41
NOD1          -----IQLLKSNRELLVTHI-----RNTQCLVDNLLKN--------DYFSAEDAEIVCAC 42
NLRC4         -----MNFIKDNSRALIQRMGM---TVIKQITDDLFVW--------NVLNREEVNIICCE 44
APAF1         -----RNCLLQHREALEKDI------KTSYIMDHMISD--------GFLTISEEEKVRNE 41
CASPASE1      ---MADKVLKEKRKLFIRSMGE---GTINGLLDELLQT--------RVLNKEEMEKVKRE 46
NOD2          ----SQEAFQAQRSQLVELLVSGSLEGFESVLDWLLSW--------EVLSWEDYEGFHLL 48
CASPASE9      MDEADRRLLRRCRLRLVEEL------QVDQLWDALLSR--------ELFRPHMIEDIQRA 46
CASPASE5      STSVKKDNHKKKTVKMLEYLGK---DVLHGVFNYLAKH--------DVLTLKEEEKKKYY 49
NLRC3         ---MRKQEVRTGREAGQGHGTGSPAEQVKALMDLLAGKGSQGSQAPQALDRTPDAPLGPC 57
NLRP13        --------------------------TNQGLLPYLMA-----------LDQYQLEEFKLC 23
                                        :   :           :

PYPAF         --PTNPSKMRKLFSFTPAWN--------WTCKDLLLQALRE----SQSYLVEDLERS--- 84
NALP1         --NTRPSQMRKLFSLSQSWD--------RKCKDGLYQALKE----THPHLIMELWEK--- 84
NOD1          --PTQPDKVRKILDLVQSKG--------EEVSEFFLYLLQQL---ADAYVDLRPWLL--- 86
NLRC4         --KVEQDAARGIIHMILKKG--------SESCNLFLKSLKEW---NYPLFQDLNGQ---- 87
APAF1         --PTQQQRAAMLIKMILKKD--------NDSYVSFYNALLHE---GYKDLAALLHDG--- 85
CASPASE1      N-ATVMDKTRALIDSVIPKG--------AQACQICITYICE----EDSYLAGTLGL---- 89
NOD2          G-QPLSHLARRLLDTVWNKG--------TWACQKLIAAAQEA---QADSQSPKLH----- 91
CASPASE9      GSGSRRDQARQLIIDLETRG--------SQALPLFISCLEDT---GQDMLASFLRT---- 91
CASPASE5      --DTKIEDKALILVDSLRKN--------RVAHQMFTQTLLNM---DQKITSVKPL----- 91
NLRC3         SNDSRIQRHRKALLSKVGGGPELGGPWHRLASLLLVEGLTDLQLREHDFTQVEATRGGGH 117
NLRP13        -----LEPQQLMDFWSAPQG---------HFPRIPWANLRA----ADPLNLSFLL----- 60
                                .

PYPAF         ----------------------
NALP1         ----------------------
NOD1          ----------------------
NLRC4         ----------------------
APAF1         ----------------------
CASPASE1      ----------------------
NOD2          ----------------------
CASPASE9      ----------------------
CASPASE5      ----------------------
NLRC3         PARTVALDRLFLPLSRVSVPP 138
NLRP13        ----------------------
```

Figure 5.1. Alignments of Human NLRC3, NLRP13 and Related Proteins. (A) NLRC3 protein structure. (B) Protein structure of NLRP13. (C) Alignment of PYRINs and CARDs (D) of NLR family members. (E) Alignment of NACHT domains of NLRs (cont.).

E

```
Cryopyrin       HTVVFQGAAGIGKTILARKMMLDWASGTLYQDRFDYLFYIHCREVSLVTQR---SLGDLI 57
NLRP1           RIVILQGAAGIGKSTLARQVKEAWGRGQLYGDRFQHVFYFSCRELAQSKVV---SLAELI 57
NLRP13          QTIVLVGRAGVGKTTLAMQAMLHWANGVLFQQRFSYVFYLSCHKIRYMKET---TFAELI 57
NLRC3           RVSITIGVAGMGKTTLVRHFVRLWAHG-QVGKDFSLVLPLTFRDLNTHEKL---CADRLI 56
NOD1            ETIFILGDAGVGKSMLLQRLQSLWATG-RLDAGVKFFFHFRCRMFSCFKESDRLCLQDLL 59
NOD2            DTVLVVGEAGSGKSTLLQRLHLLWAAG-QDFQEFLFVFPFSCRQLQCMAKP--LSVRTLL 57
NLRC5           RVTVLLGKAGMGKTTLAHRLCQKWAEG-HLN-CFQALFLFEFRQLNLITRF--LTPSELL 56
CIITA           RVIAVLGKAGQGKSYWAGAVSRAWACG-RLP-QYDFVFSVPCHCLNRPGDA--YGLQDLL 56
NLRX1           QTVVLYGTVGTGKSTLVRKMVLDWCYG--RLPAFELLIPFSCEDLSSLGPAP-ASLCQLV 57
NLRC4           SPCIIEGESGKGKSTLLQRIAMLWGSG-KCKALTKFKFVFFLRLSRAQGGLFETLCDQLL 59
                      *  * **:         *  *          : .  .               *:

Cryopyrin       MSCC----PDPNPPIHKIVRKPSRILFLMDGFDEL--QGAFDEHI--GPLCTDWQKAERG 109
NLRP1           GKDG----TATPAPIRQILSRPERLLFILDGVDEP--GWVLQEPS--SELCLHWSQPQPA 109
NLRP13          SLDW----PDFDAPIEEFMSQPEKLLFIIDGFEEIIISESRSESLDDGSPCTDWYQELPV 113
NLRC3           CSVF----PHVGEPS-LAVAVPARALLILDGLDECRTPLDFSNTV----ACTDPKKEIPV 107
NOD1            FKHYCYPERDPEEVFAFLLRFPHVALFTFDGLDELHSDLDLSRVP----DSSCPWEPAHP 115
NOD2            FEHCCWPDVGQEDIFQLLLDHPDRVLLTFDGFDEFK--FRFTDRE----RHCSPTDPTSV 111
NLRC5           FDLYLSPESDHDTVFQYLEKNADQVLLIFDGLDEALQPMG-------------PDGPGPV 103
CIITA           FSLGPQPLVAADEVFSHILKRPDRVLLILDGFEELEAQDGFLHST----CGPAPAEPCSL 112
NLRX1           AQRY----TPLKEVLPLMAAAGSHLLFVLHGLEHLNLDFRLAGTG----LCSDPEEPQEP 109
NLRC4           DIPG---TIRKQTFMAMLLKLRQRVLFLLDGYNEFK--------------------PQNC 96
                                      *: :.* :.

Cryopyrin       DILLSSLIRKKLLPEASLLITTRPVALEKLQHLLDHPRHVEILGFSEAKRKEYFFKYFSD 169
NLRP1           DALLGSLLGKTILPEASFLITARTTALQNLIPSLEQARWVEVLGFSESSRKEYFYRYFTD 169
NLRP13          TKILHSLLKKELVPLATLLITIKTWFVRDLKASLVNPCFVQITGFTGDDLRVYFMRHFDD 173
NLRC3           DHLITNIIRGNLFPEVSIWITSRPSASGQIPGGLVD-RMTEIRGFNEEEIKVCLEQMFPE 166
NOD1            LVLLANLLSGKLLKGASKLLTARTG--IEVPRQFLR-KKVLLRGFSPSHLRAYARRMFPE 172
NOD2            QTLLFNLLQGNLLKNARKVVTSRPAAVSAFLRKYIR-TEFNLKGFSEQGIELYLRKRHHE 170
NLRC5           LTLFSHLCNGTLLPGCRVMATSRP-GKLPACLPAEA-AMVHMLGFDGPRVEEYVNHFFSA 161
CIITA           RGLLAGLFQKKLLRGCTLLLTARPRGRLVQSLSKAD-ALFELSGFSMEQAQAYVMRYFES 171
NLRX1           AAIIVNLLRKYMLPQASILVTTRPSAIGRIPSKYVG-RYGEICGFSDTNLQKLYFQLR-- 166
NLRC4           PEIEALIKENHRFKNMVIVTTTTECLRHIRQFGALT---AEVGDMTEDSAQALIREVLIK 153
                  :   :     .       *                    : .:     .    .

Cryopyrin       E 170
NLRP1           E 170
NLRP13          S 174
NLRC3           D 167
NOD1            R 173
NOD2            P 171
NLRC5           Q 162
CIITA           S 172
NLRX1           -
NLRC4           E 154
```

Figure 5.1. Alignments of Human NLRC3, NLRP13 and Related Proteins. (A) NLRC3 protein structure. (B) Protein structure of NLRP13. (C) Alignment of PYRINs and CARDs (D) of NLR family members. (E) Alignment of NACHT domains of NLRs (cont.).

NLRC3 is one of the evolutionarily conserved NLR family members. Several *NLRC3* genes from different organisms share high homology. Human *NLRC3* gene shares 97.9% identity with *NLRC3* gene of *P. troglodytes*; 85.4% identity with *Canis lupus familiaris*; 86.4 % identity with *Bos taurus*; 81.3% identity with *R. norvegicus* and 81.4% identity with *Mus musculus*. If the protein sequences are taken into consideration, the identity is conserved. The human NLRC3 proteins shares 97.6 % identity with NLRC3 protein of *P. troglodytes*; 84.9% identity with *Canis lupus familiaris*; 85.3 % identity with

Bos taurus; 80.5% identity with *R. norvegicus* and 80.3% identity with NLRC3 protein of *Mus musculus* (Figure 5.2.A)

NLRP13 gene represents a different evolution any pattern. Limited number of species carries the *NLRP13* gene. Human NLRP13 gene shows high homology with NLRP13 gene of *P. troglodytes*. The nucleotide sequence of human *NLRP13* gene has 99.5% identity with the sequence of *P. troglodytes* and the protein sequence identity is 99.2%. *Canis lupus familiaris* shares 73.1% identity in DNA sequence and 59.9% identity in protein sequence. *Bos taurus* has 63.1% identity in DNA sequence and 52.3% identity in protein sequence (Figure 5.2.B)

A

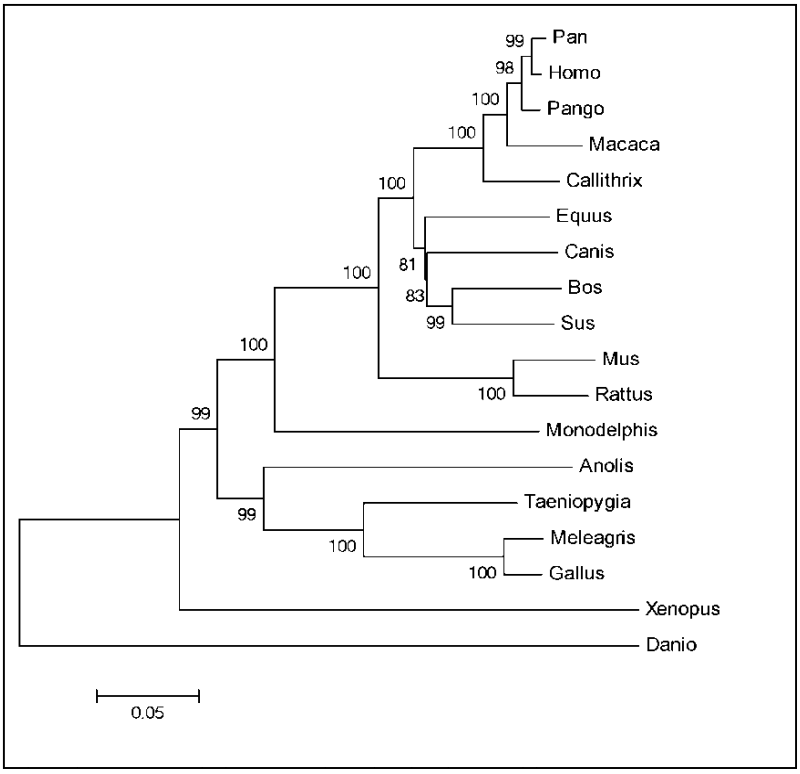

Figure 5.2. Phylogenetic analysis (Neighbor Joining) of *NLRC3* and *NLRP13* genes among species. (A) Comparison of the species according to *NLRC3* gene. (B) Comparison of the species according to *NLRP13* gene.

B

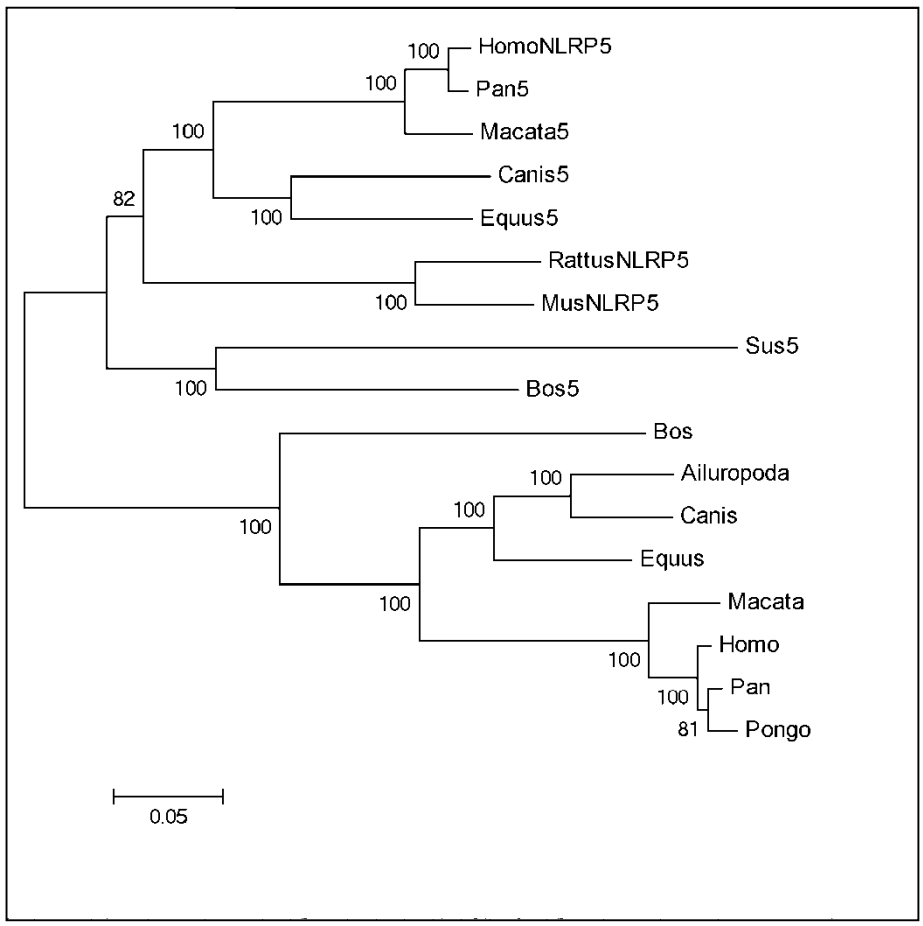

Figure 5.2. Phylogenetic analysis (Neighbor Joining) of *NLRC3* and *NLRP13* genes among species. (A) Comparison of the species according to *NLRC3* gene. (B) Comparison of the species according to *NLRP13* gene (cont.).

Mouse and rat genomes do not contain *NLRP13* gene. However, they have the *NLRP5* gene. When the nucleotides of NLRP5 and NLRP13 genes are aligned, it can be suggested that NLRP13 and NLRP5 have a common ancestor (Figures 5.2.B and 5.3). Human *NLRP13* gene shares 59% identity with human and *Pan NLRP5* gene; 58% identity with *Macatta* and *Mus NLRP5* gene; 56 % identity with *Canis* and *Equus NLRP5* gene; 55 % identity with *Bos taurus*; 54% identity with *Rattus NLRP5* gene.

To further analyze NLR family members, amino acid sequences of NOD1, NOD2, Cryopyrin, NLRX1, NLRC5, CIITA, NLRC4, NLRP13, NLRP5, NLRC3, APAF1, NALP1 and NALP2 were aligned with ClustalX2 programme. As a next step, the phylogenetic trees were constructed with Mega version 3.1 software. Minimum evolution,

neighbor-joining, and maximum parsimony methods were used with Poisson correction for multiple amino acid substitution and with 1000 random bootstrap replicates.

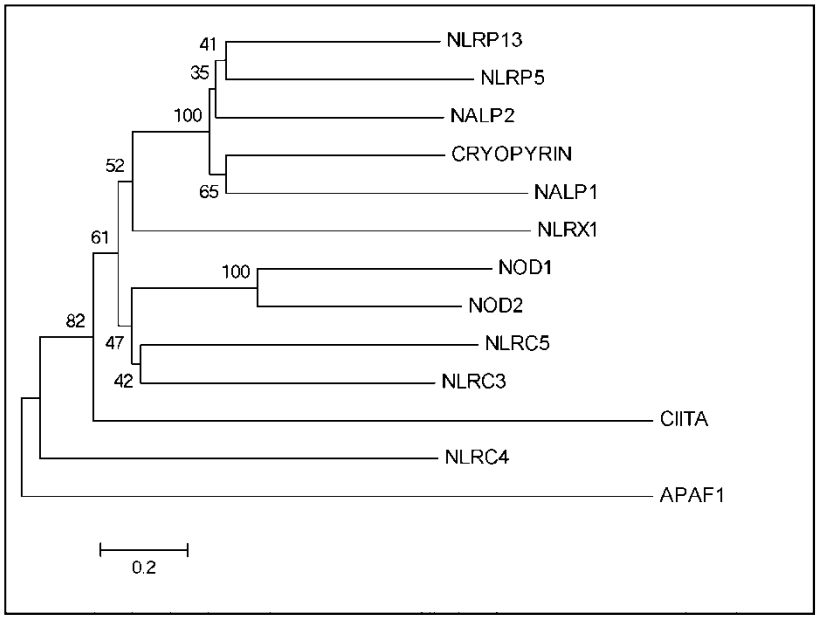

Figure 5.3. Phylogenetic analysis of human NLR proteins**.** The figure represents the Minimum evolution tree (the three methods produced very similar topologies).

NLR family members share high homology with respect to their NACHT domain and LRRs motifs. However, their amino terminal effector domains can represent different amino acid compositions. When the alignment of amino acid sequence is taken into consideration, NLRC3 is most similar to NLRC5 whereas NLRP13 is mostly close to NLRP5. This can suggest that NLRP5 and NLRP13 gene can have a common ancestor (Figure 5.3).

5.2. Preparation of Mammalian Expression Vector Constructs for NLRC3 and NLRP13

5.2.1 Cloning of Full Lenght NLRC3

Blood cells are one of the major sources of NLRC3 mRNA. Therefore, 10 ml blood was taken from two volunters and total blood RNA was isolated by using Roche High Pure RNA isolation kit and blood c-DNA library was constructed via Promega First Strand cDNA synthesis kit. To amplify the NLRC3 gene, NLRC3_ORF forward and reverse primers with flanking XbaI and NotI restriction sites were designed and synthesized at Harvard DNA Core Facility. These cutting sites were chosen to ligate in modified pcDNA3 vectors including HA, MYC and FLAG tags. NLRC3 gene specific PCR conditions were optimized and the gene was amplified for the cloning purpose. All PCR reactions were performed with Finnzyme Phusion High Fidelity Taq polymerase enzyme. PCR analyses of NLRC3 in two different reactions are indicated in Figure 1. NLRC3 PCR product was digested with XbaI and NotI one by one and modified pcDNA3 vectors were digested with XbaI and PspOMI. After ligation and transformation reactions, the positive colonies were selected by colony PCR. Positive colonies were inoculated in Ampicillin LB media and plasmids were isolated. The sequences of the isolated plasmids were confirmed firstly by diagnostic digestion with EcoRI and the plasmids sent to Macrogen in Korea for sequencing. In conclusion, HA, FLAG and MYC pcDNA3 NLRC3 plasmids were generated.

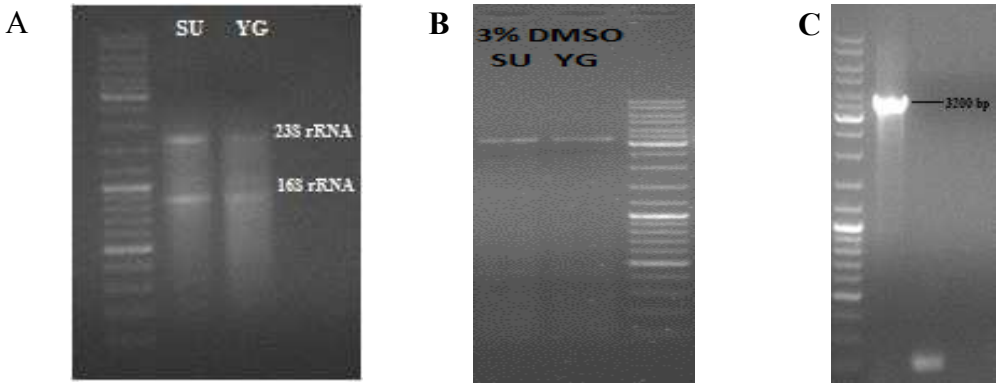

Figure 5.4. Cloning Strategy for NLRC3. (A) Agarose gel electrophoresis of isolated total blood RNA. (B) PCR amplification of NLRC3 gene. (C) T7 and SP6 universal primers were used in colony PCR reactions. (D) Diagnostic digestion.

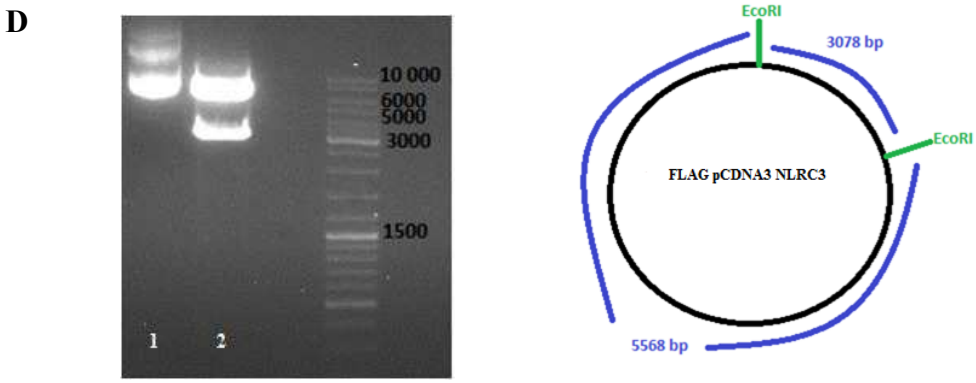

Figure 5.4. Cloning Strategy for NLRC3. (A) Agarose gel electrophoresis of isolated total blood RNA. (B) PCR amplification of NLRC3 gene. (C) T7 and SP6 universal primers were used in colony PCR reactions. (D) Diagnostic digestion (cont.).

5.2.2. Cloning of Full Lenght NLRP13

NLRP13_ORF inserted in pENTR223.1 vector was purchased from OriGene. To amplify the NLRP13 gene, NLRP13_ORF forward and reverse primers with flanking SpeI and NotI restriction sites were designed and synthesed at Harvard DNA Core Facility. These cutting sites were chosen to ligate in modified pcDNA3 vectors including HA, MYC and FLAG tags. NLRP13 gene specific PCR conditions were as some as NLRC3 ones and the gene was amplified for the cloning purpose. Finnzyme Phusion High Fidelity Taq polymerase enzyme was used in all of the PCR reactions.

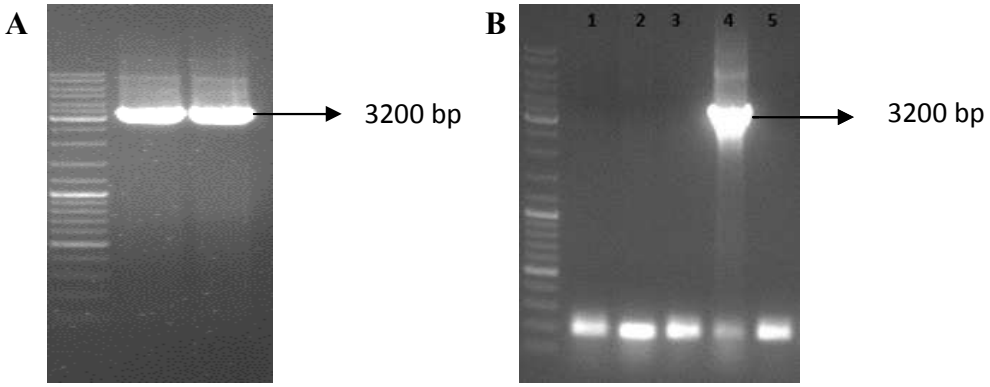

Figure 5.5. General Steps of NLRP13 Cloning. (A) PCR amplification of NLRP13 gene. (B) Colonies were scanned with PCR using T7 and SP6 primers. (C) Positive colony was confirmed with EcoRI diagnostic digestion.

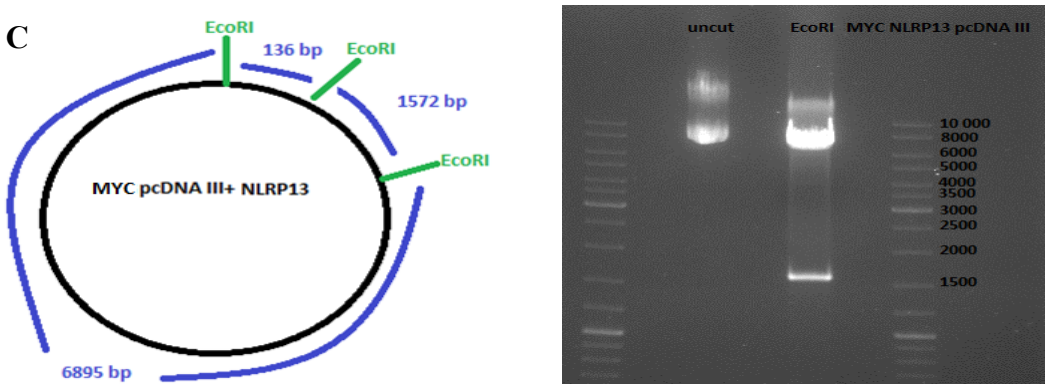

Figure 5.5. General Steps of NLRP13 Cloning. (A) PCR amplification of NLRP13 gene. (B) Colonies were scanned with PCR using T7 and SP6 primers. (C) Positive colony was confirmed with EcoRI diagnostic digestion (cont.).

As a result of sub-cloning of NLRP13, HA, FLAG or MYC tag versions of NLRP13 vectors were prepared (Figure 5.4 and 5.5)

5.3. Expression of Tagged NLRC3 and NLRP13 Proteins in HEK293FT Cell Line

The HEK293FT cell line is a very suitable host for mammalian expression vectors and can be easily transfected via calcium phosphate. 2 µg FLAG pcDNA3 NLRC3 and 2 µg MYC pcDNA3 NLRP13 plasmids were transfected in $1x10^6$ HEK293FT cells. 0.5 µg pEGFP C3 vector was also cotransfected with gene of interests to indicate the transfection efficiency. Transfection was successful at 85% efficiency. After 24 hours, transfected cells were collected and cell lysates were used to perform Western blotting.

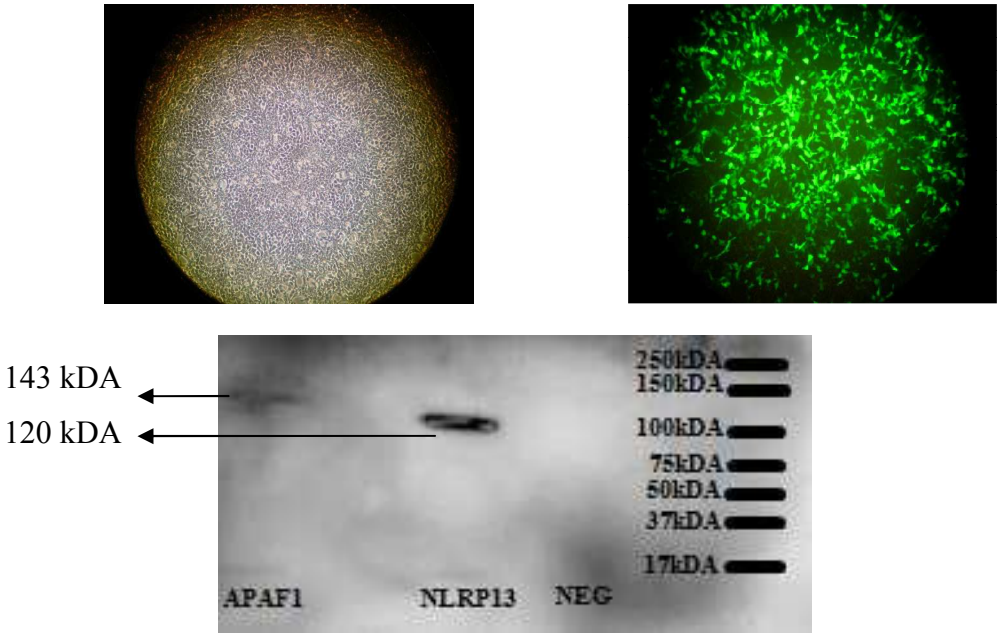

Figure 5.6. Expression of FLAG pcDNA3 NLRP13 in HEK293FT cells. (A) $1x10^6$ HEK293FT cells were transfected via calcium phosphate. (B) Overexpressed proteins were visualized using anti-flag antibody.

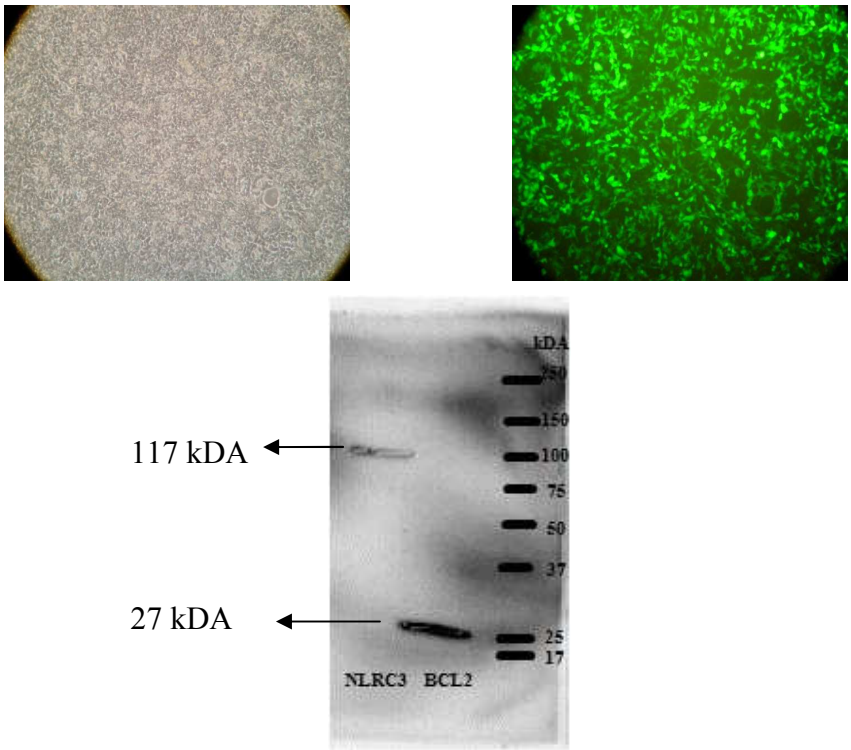

Figure 5.7. MYC pcDNA3 NLRC3 Expression in HEK293FT cells. (A) Calcium phosphate transfection was used for $1x10^6$ HEK293FT cells. Western Blotting was performed with anti-MYC antibody.

In conclusion, MYC pcDNA3 NLRC3 and Flag pcDNA3 NLRP13 expressed the tagged proteins in HEK293FT cells and they were detected via Western blotting (Figure 5.6 and 5.7).

5.4. Cellular Localization of NLRC3 and NLRP13

5.4.1. Generation of Fusion EGFP NLRC3 and NLRP13 Proteins

NOD like receptor family members are generally localized in the cytoplasm. However, several of them can represent different features and they can be found in mitochondria such as NLRX1 or nucleus like CIITA or NLRC5. To test the subcellular localization of NLRC3 and NLRP13 in the HEK293FT cells, NLRC3 and NLRP13's ORF were inserted into pEGFP C3 and EGFP fusion NLRC3 and NLRP13 were generated. To check the expression of the fusion proteins, HEK293FT cells were transfected with 2 μg pEGFP C3 NLRC3 or NLRP13 plasmids. 24 hours, the cells were collected and lysed with 0.2 % NP40 lysis buffer and Western blotting protocol was applied with anti-GFP antibody and beta actin protein was used as a loading control (Figure 5.8 and 5.9).

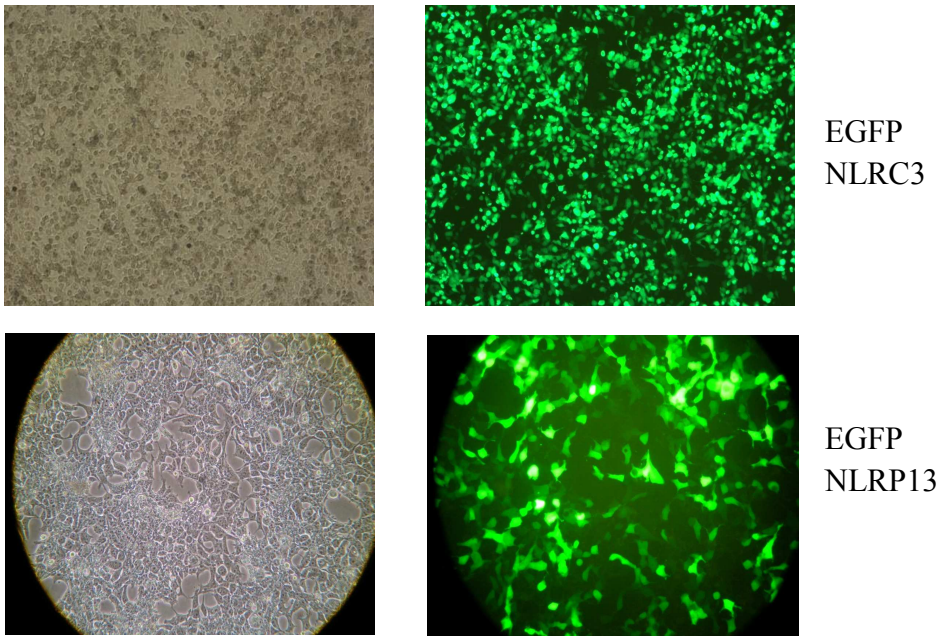

Figure 5.8. Transfection Efficiency of pEGFP C3 NLRC3 and pEGFP C3 NLRP13. $1x10^6$ HEK293FT cells were transfected via $Ca_3(PO_4)_2$.

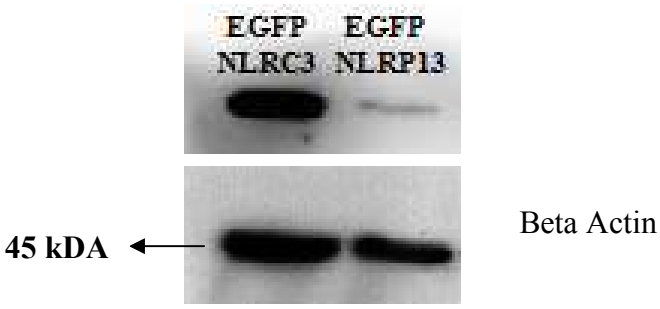

Figure 5.9. Expression of EGFP NLRC3 and NLRP13 in HEK293FT cells. Western blot analysis of EGFP NLRC3 and NLRP13 proteins. Anti-GFP antibody was used to detect the fusion versions of the proteins.

EGFP NLRC3 and EGFP NLRP13 fusion protein expression was detected via Western blotting. The calculated molecular weight of EGFP NLRC3 is 143 k DA and EGFP NLRP13 is 146 k DA.

5.4.2. Confocal Microscopy Analysis of Subcellular Localization of EGFP NLRC3 and EGFP NLRP13

$1x10^6$ HEK293FT cells were co-transfected with 2 μg pEGFP C3 NLRC3 and 1.5 μg DsRED MTS (a gift from Ahmet Koman's Laboratory) vectors. Beside Ds RED MTS mitochondral target plasmid, 1.5 μg CFP tagged organel plasmids such as ER, Golgi, early endosomal plasmid Rab5 and Rab11, late endosomal Rab9 plasmid were co-transfected in these cells. After 24 hours, transfected HEK293FT cells were fixed with 10% paraformaldehyte and slides were analysed with confocal microscopy.

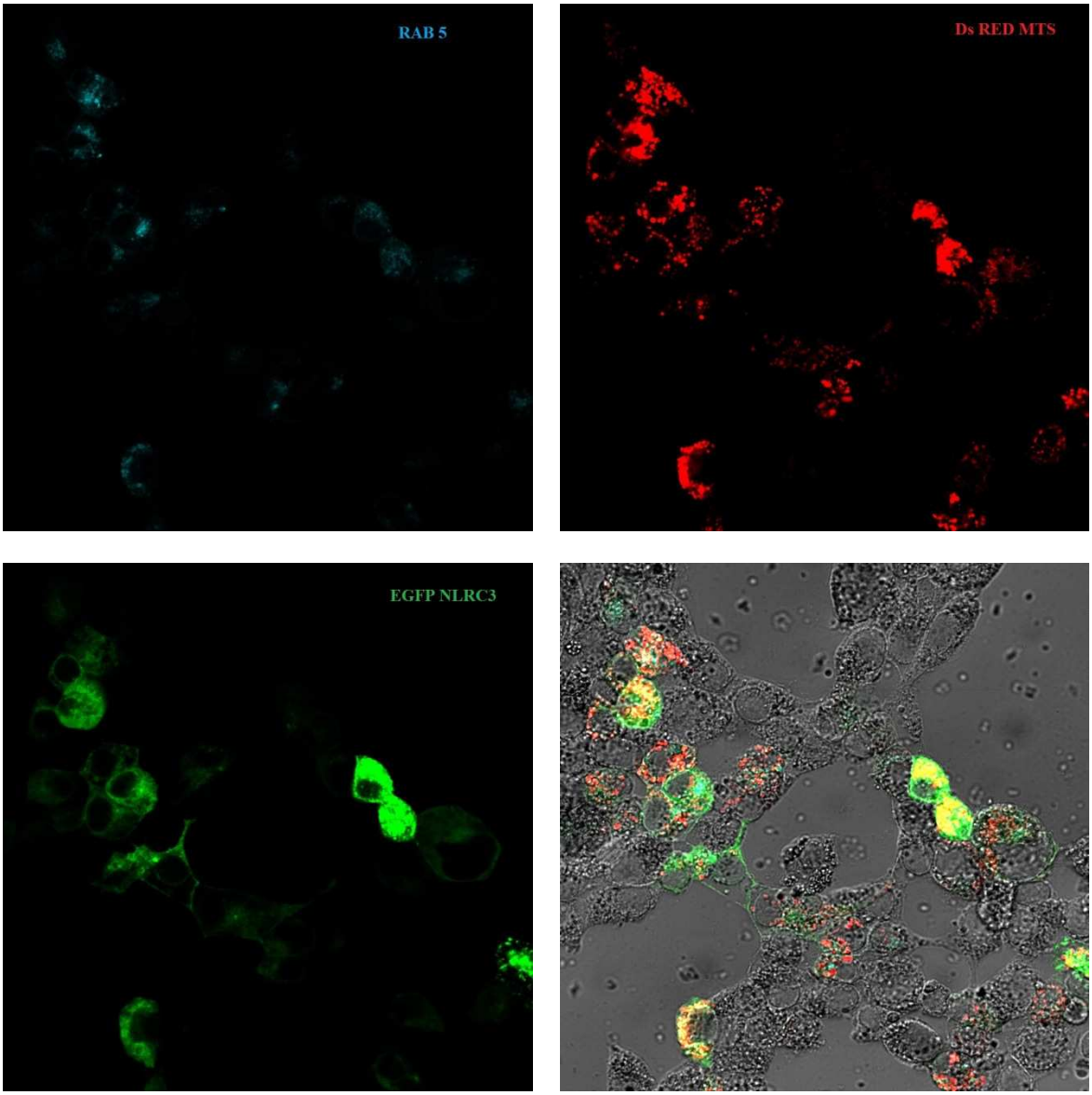

Figure 5.10. Subcelular Co-localization of EGFP NLRC3 with CFP Rab5 Endosomal Marker and Ds RED MTS Mitochondrial Marker in HEK293FT Cells.

Rab5 is a small GTPase that is the marker of early endosomes. It regulates the fusion between endocytic vesicles and early endosomes (Olkkonen et al., 1997). Rab11 is the other early endosomal marker that regulates the compartmentalization of early endosomes and is necessary to transport efficiently from early endosomes to the trans-Golgi network (Wilcke et al., 2000). Finally, Rab9 is known as a late endosomal marker protein.

We tested whether EGFP NLRC3 could be found in endosomal vesicles by co-transfecting CFP tagged endosomal marker plasmids with EGFP NLRC3 into HEK293FT

cells. To conclude, EGFP NLRC3 could be found in the endosomal vesicles (Figures 5.10, 5.11 and 5.12). However, the ratio was not high to consider that endosomal vecihles had an impact on NLRC3 function because endosomal trafficing is such a common transportation in protein synthesis.

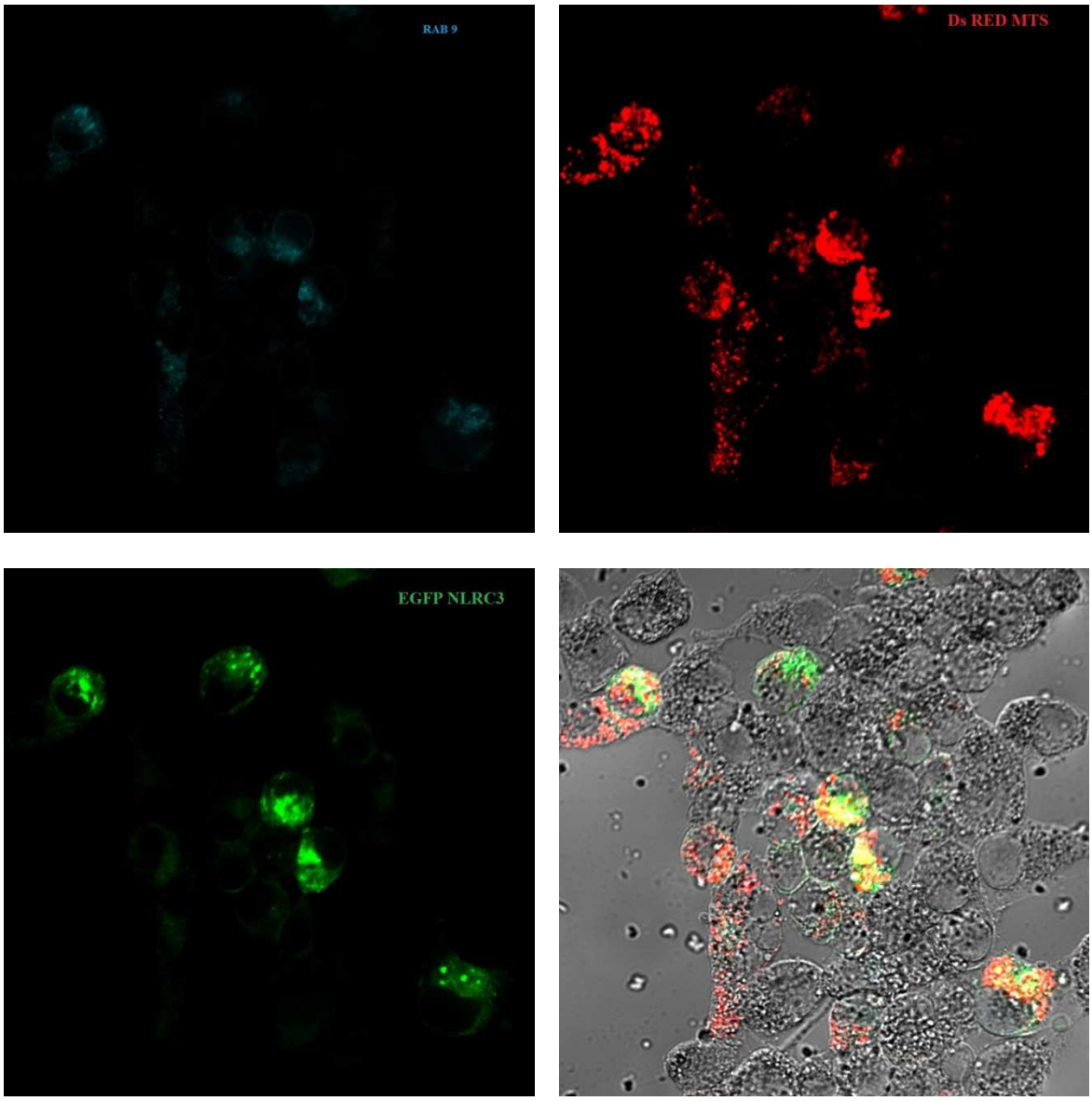

Figure 5. 11. Subcellular Co-localization of EGFP NLRC3 with CFP Rab9 Endosomal Marker and Ds RED MTS Mitochondrial Marker in HEK293FT Cells.

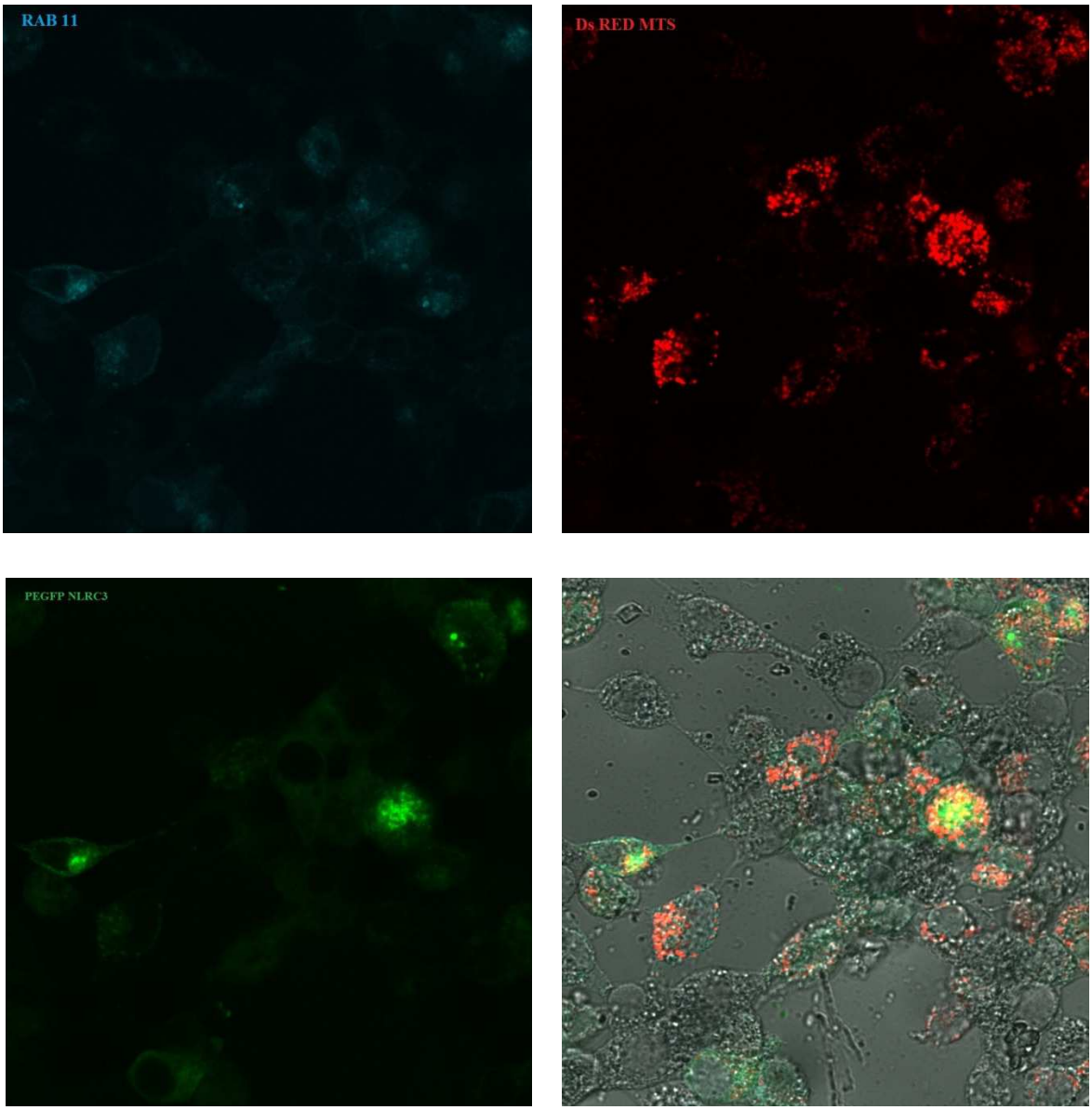

Figure 5.12. Subcellular Co-localiation of EGFP NLRC3 with CFP Rab11 Endosomal Marker and Ds RED MTS Mitochondrial Marker in HEK293FT Cells.

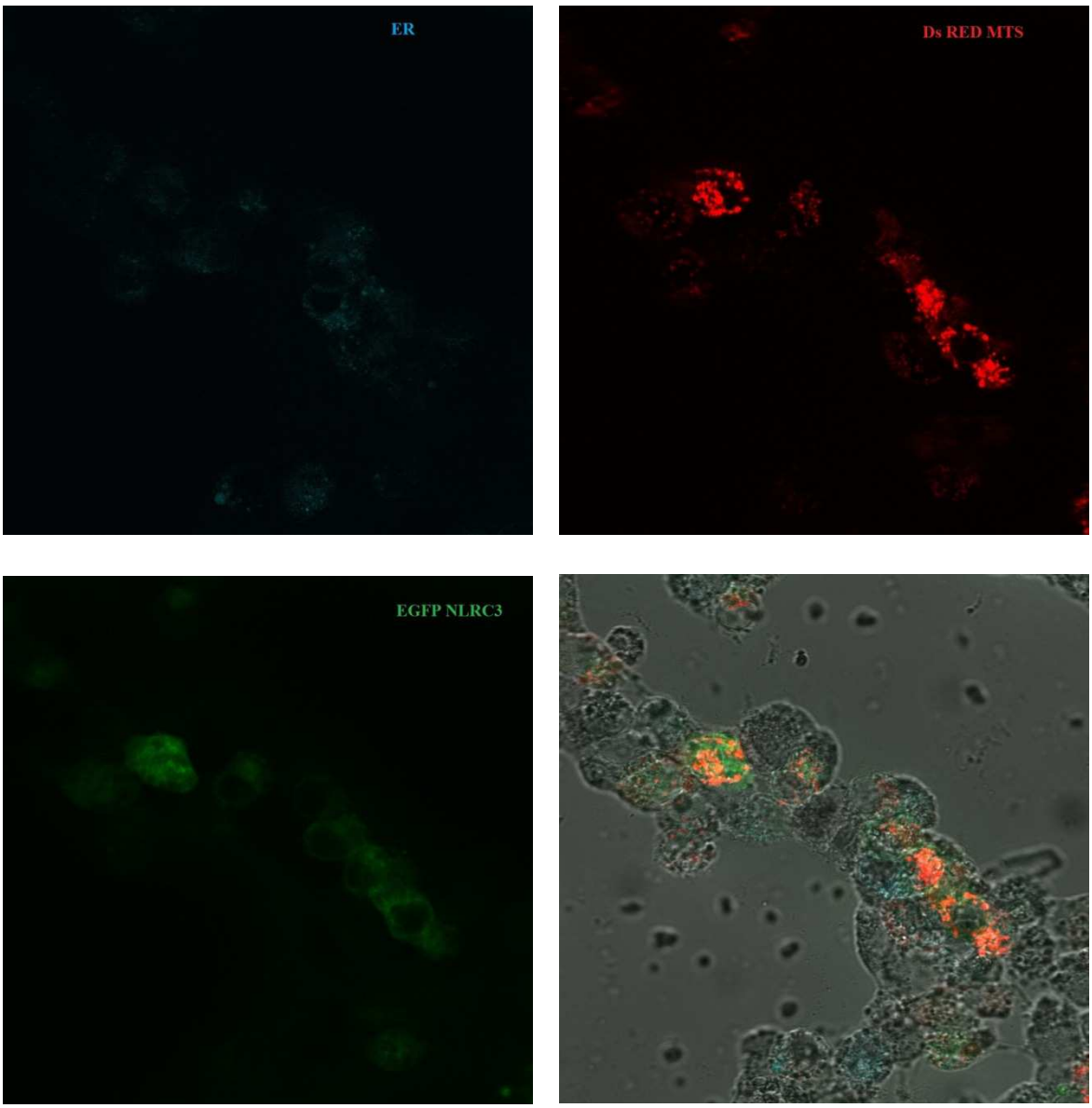

Figure 5.13. Subcellular Co-localiation of EGFP NLRC3 with ECFP ER Marker and Ds RED MTS Mitochondrial Marker in HEK293FT Cells.

Besides endosomal vehicles, we tested whether EGFP NLRC3 could be found localized in endoplasmic reticulum or not. For this purpose, HEK293FT cells were co-transfected with ECFP ER and pEGFP C3 NLRC3 plasmids. Under confocal microscopy, we did not find any co-localization between ER marker and the gene of interest (Figure 5.13)

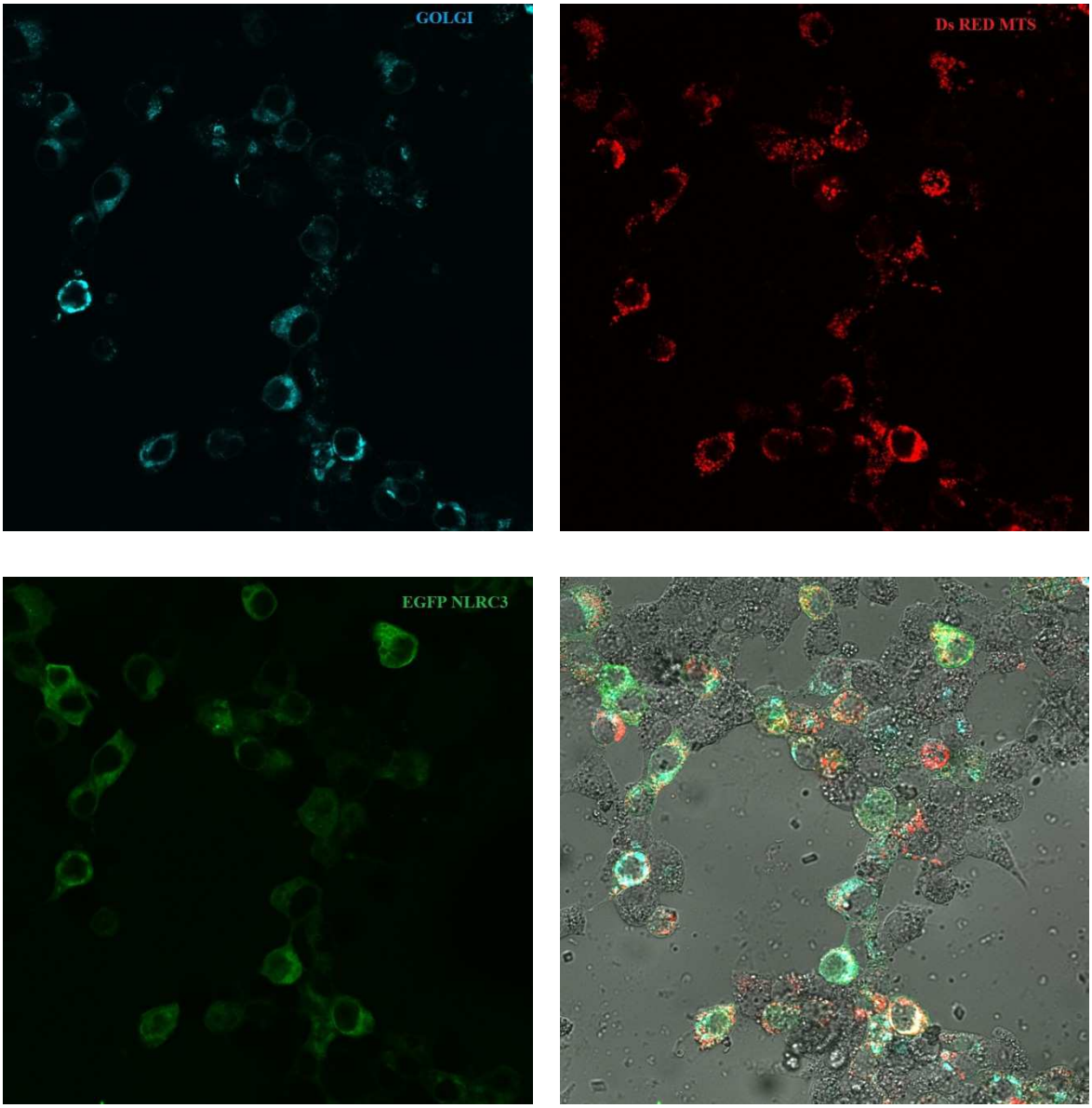

Figure 5.14. Subcellular Co-localiation of EGFP NLRC3 with ECFP Golgi Marker and Ds RED MTS Mitochondrial Marker in HEK293FT Cells.

To determine the localization of EGFP NLRC3 in Golgi, HEK293FT cells were co-transfected with ECFP Golgi and pEGFP C3 NLRC3 plasmids. We found that EGFP NLRC3 could be found in Golgi. However, the ratio was only 12%. Golgi is one of the places that proteins are packaged (Figure 5.14). Therefore, location in the Golgi seems not to be important for NLRC3 functions.

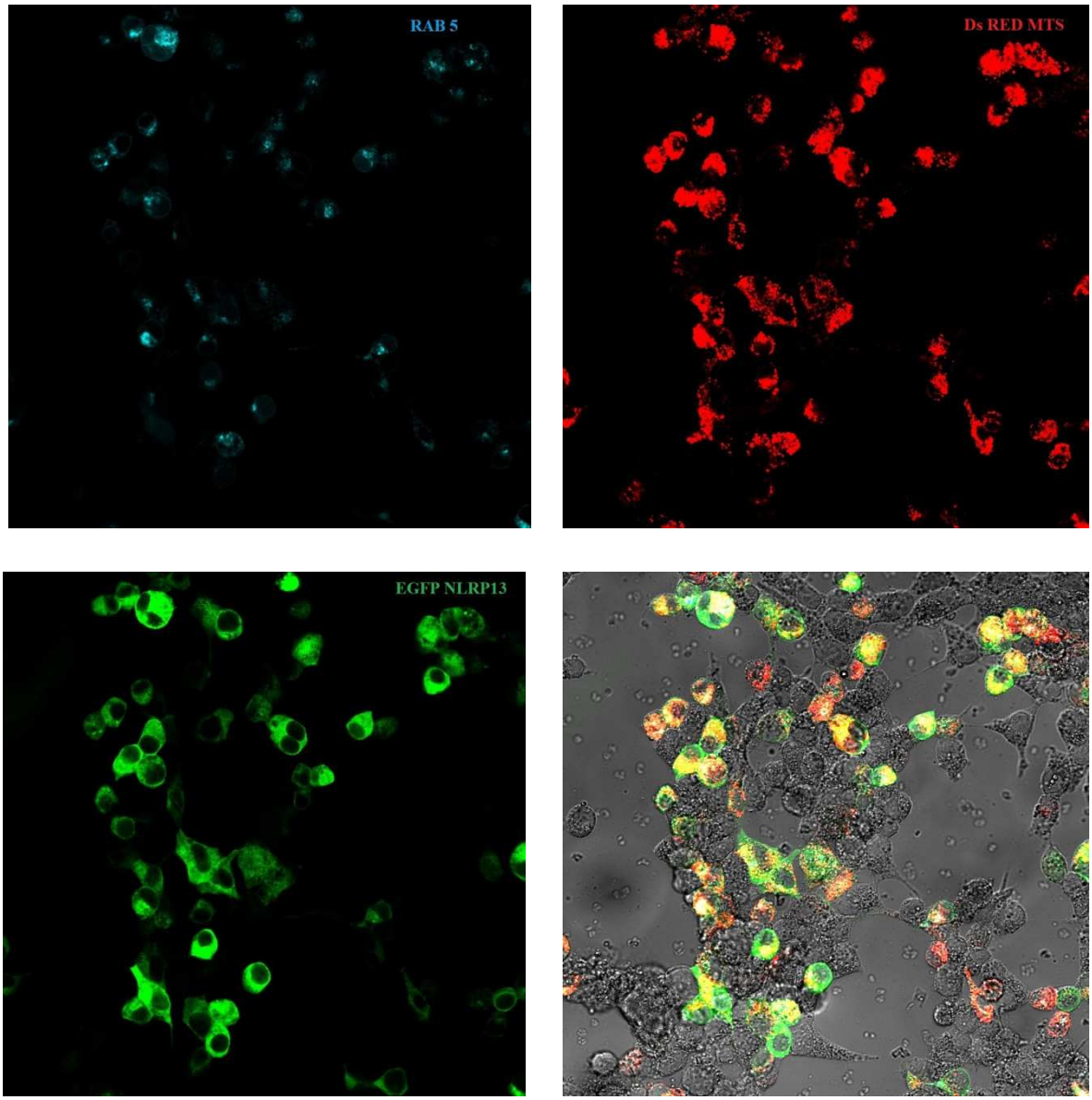

Figure 5.15. Subcellular Co-localiation of EGFP NLRP13 with CFP Rab5 Endosomal Marker and Ds RED MTS Mitochondrial Marker in HEK293FT Cells.

To test whether EGFP NLRP13 could be found in the endosomal vesicles, HEK293FT cells were co-transfected with CFP tagged endosomal marker plasmids and EGFP NLRP13. It is clear that EGFP NLRP13 could be found in the early endosomal vesicles (Figures 5.15). The ratios were 8% for Rab5. The majority of cells showed no-colocalization, suggesting NLRP13 function is carried out outside the endosomes.

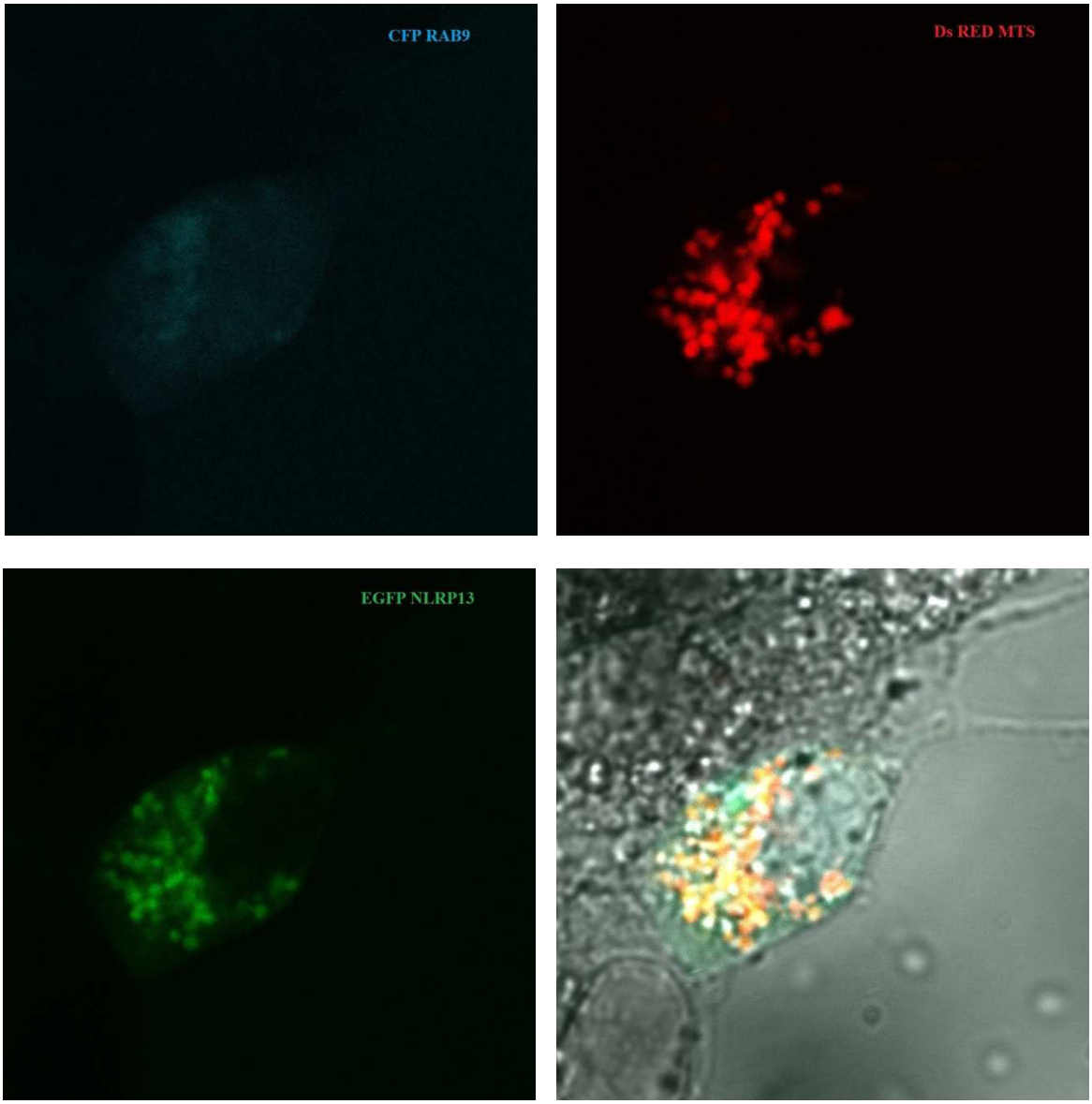

Figure 5.16. Subcellular Co-localization of EGFP NLRP13 with CFP Rab9 Endosomal Marker and Ds RED MTS Mitochondrial Marker in HEK293FT Cells.

It is clear that EGFP NLRP13 could be found in the late endosomal vesicles (Figure 5.16). The ratios were 9% Rab9 and the majority of the EGFP NLRP13 proteins were in the cytoplasm.

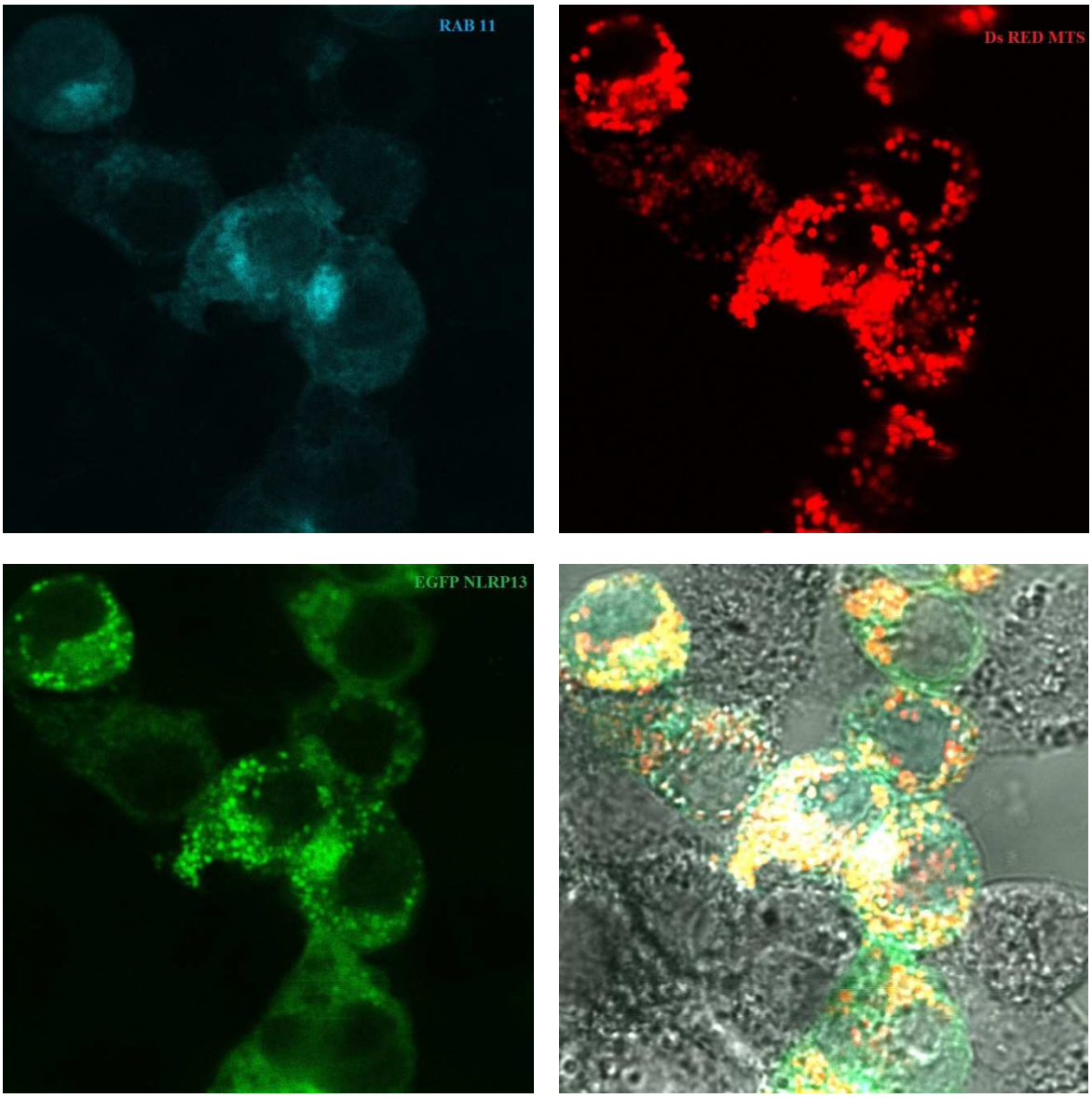

Figure 5.17. Subcellular Co-localization of EGFP NLRP13 with CFP Rab11 Endosomal Marker and Ds RED MTS Mitochondrial Marker in HEK293FT Cells.

It is clear that EGFP NLRP13 could be found in the late endosomal vesicles (Figure 5.17). The ratios were 14% Rab11 and the majority of the EGFP NLRP13 proteins were free and localized in the cytoplasm.

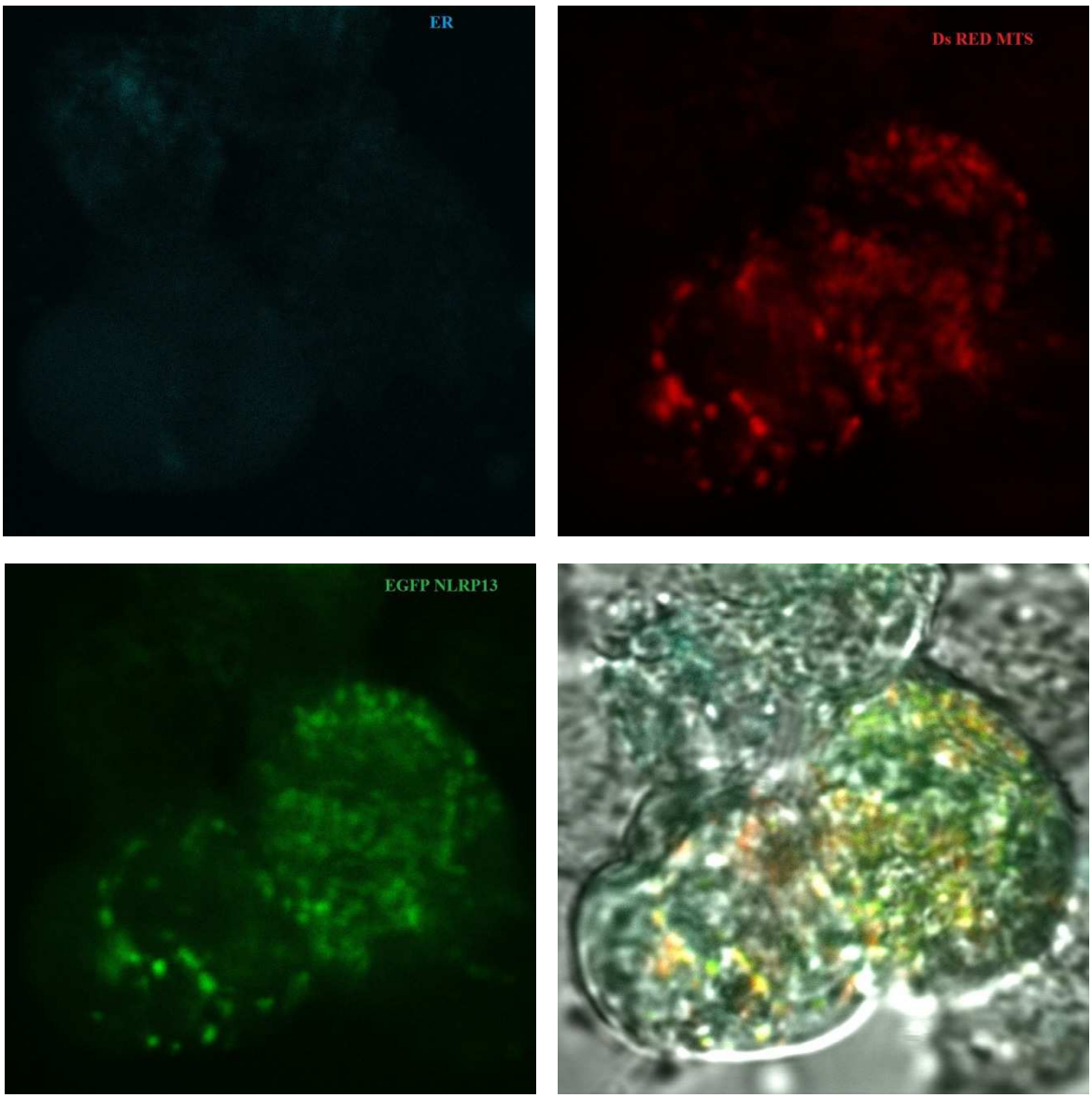

Figure 5.18. Subcellular Co-localization of EGFP NLRP13 with ECFP ER Marker and Ds RED MTS Mitochondrial Marker in HEK293FT Cells.

HEK293FT cells were co-transfected with ECFP ER and pEGFP C3 NLRP13 plasmids to test whether EGFP NLRP13 could localize in the ER or not. We found that EGFP NLRP13 did not localize in the ER (Figure 5.18).

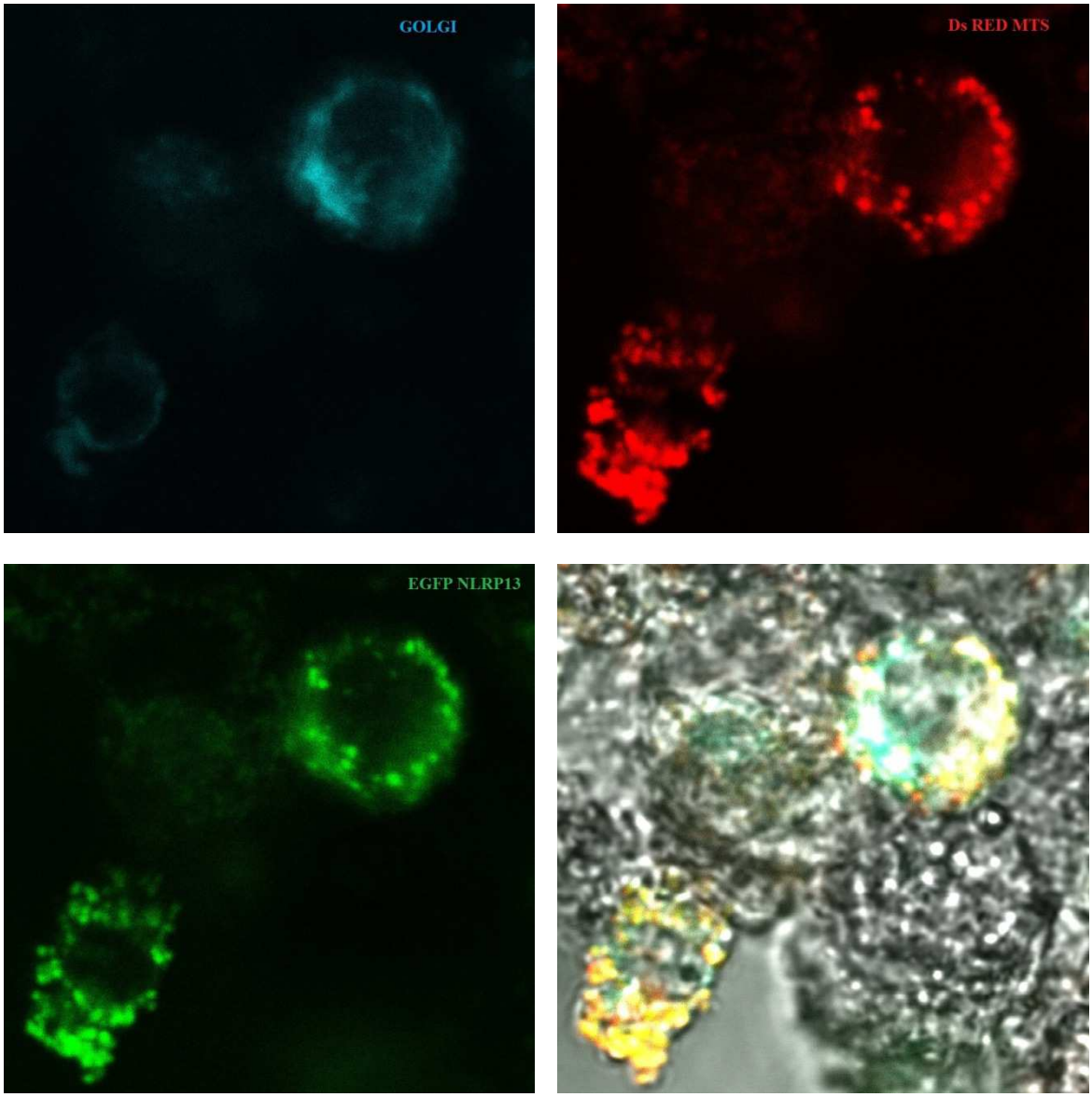

Figure 5.19. Subcellular Co-localization of EGFP NLRP13 with ECFP Golgi Marker and Ds RED MTS Mitochondrial Marker in HEK293FT Cells.

HEK293FT cells were co-transfected with ECFP Golgi and pEGFP C3 NLRP13 plasmids to test whether EGFP NLRP13 could localize in the Golgi complex or not. We found that EGFP NLRP13 could be found in the Golgi (Figure 5.14). The ratio was 15%. Golgi is one of the places where proteins are packaged. Additionally, several post-translational modifications can be done in Golgi. Thus, the location of NLRP13 in the Golgi may not be important for the function of NLRP13. It seems NLRP13 proteins are mainly independent from the Golgi complex.

Mitochondria are one of the important cellular organelles that have several functions. They have a role in ATP generation, calcium homeostasis, biosynthesis of amino acids, lipids, nucleic acids. Finally, programmed cell death can be mentioned as the last function of mitochondria. Recently, several studies reported that mitochondria had an important role in innate immunity signaling pathways. In addition to the functions of mitochondria in apoptosis and immunity, several NLR family members can lead to apoptosis. Therefore, testing the potential localization of NLRC3 and NLRP13 in mitochondria gained much more importance for the functions of the proteins. To determine the localization of EGFP NLRC3 and EGFP NLRP13 in mitochondria, HEK293FT cells were co-transfected with Ds RED MTS and pEGFP C3 NLRC3 or pEGFP C3 NLRP13 plasmids. We found that both EGFP NLRC3 and EGFP NLRP13 could be found in mitochondria (Figures 5.10 to 5.19). However, the main localization of the protein seemed to be in the cytoplasm. There were certain photos to indicate that NLRC3 and NLRP13 could be mitochondrial protein but in general they were localized in cytoplasm (Figures 5.16, 5.17 and 5.19). The mitochondrial co-localization ratio was 22% for NLRC3 and 35% for NLRP13. To conclude, both NLRC3 and NLRP13 are cytoplasmic proteins and both of them can also localize in mitochondria.

5.5. Possible Interactions of NLRC3 and NLRP13 with Inflammasome Components

5.5.1. ASC can Interact with both NLRC3 and NLRP13

The adaptor protein ASC bridges the association of Caspase 1 to NLRP3 in the inflammasome. It has an N terminal PYRIN domain and C terminal CARD domain. Both NLRC3 and NLRP13 share an effector domain with ASC. To test the binding ability of NLRC3 and NLRP13 to ASC, a co-immunoprecipitation experiment was performed. $5x10^6$ HEK293FT cell were transfected with 2.5 μg pcDNA3 ASC and 10 μg FLAG pcDNA3 NLRC3 or FLAG pcDNA3 NLRP13. As a positive control 10 μg FLAG pcDNA3 Cryopyrin was also transfected with pcDNA3 ASC to HEK293FT cells. After 24 h, transfected cells were collected and immunoprecipitation was performed. To precipitate the lysate, anti-ASC antibody was used. In the immunoblotting part, anti-FLAG antibody

was used to detect FLAG tag NLRC3, NLRP13 and Cryopyrin. FLAG Cryopyrin's molecular weight is 120 kDA, FLAG NLRC3 is 117 kDA and FLAG NLRP13 is 120 kDA.

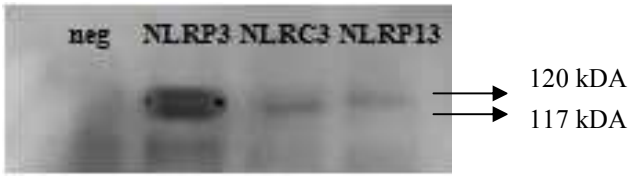

Figure 5.20. ASC can Weakly Interact with NLRC3 and NLRP13. Protein lysates of transfected HEK293FT cells were precipitated with anti-ASC antibody and Western blotting was performed with anti-FLAG antibody.

As a result of CO-IP experiments, it can be suggested that both NLRC3 and NLRP13 can interact with ASC when they are overexpressed in HEK293FT cells (Figures 5.20). According to the Co-IP result, it can be concluded that both NLRC3 and NLRP13 can weakly interact with ASC when compared to Cryopyrin/NLRP3.

To confirm the interactions of ASC-NLRC3 and ASC-NLRP13, cellular co-localization of ASC-NLRC3 and ASC-NLRP13 were tested. $1x10^6$ HEK293FT cells were co-transfected with 1 μg pTagRFP C3 ASC and 2 μg pEGFP C3 NLRC3 or pEGFP C3 NLRP13. 24 hours after transfection, cells were fixed with 10% paraformaldehyte and visualized under confocal microscopy.

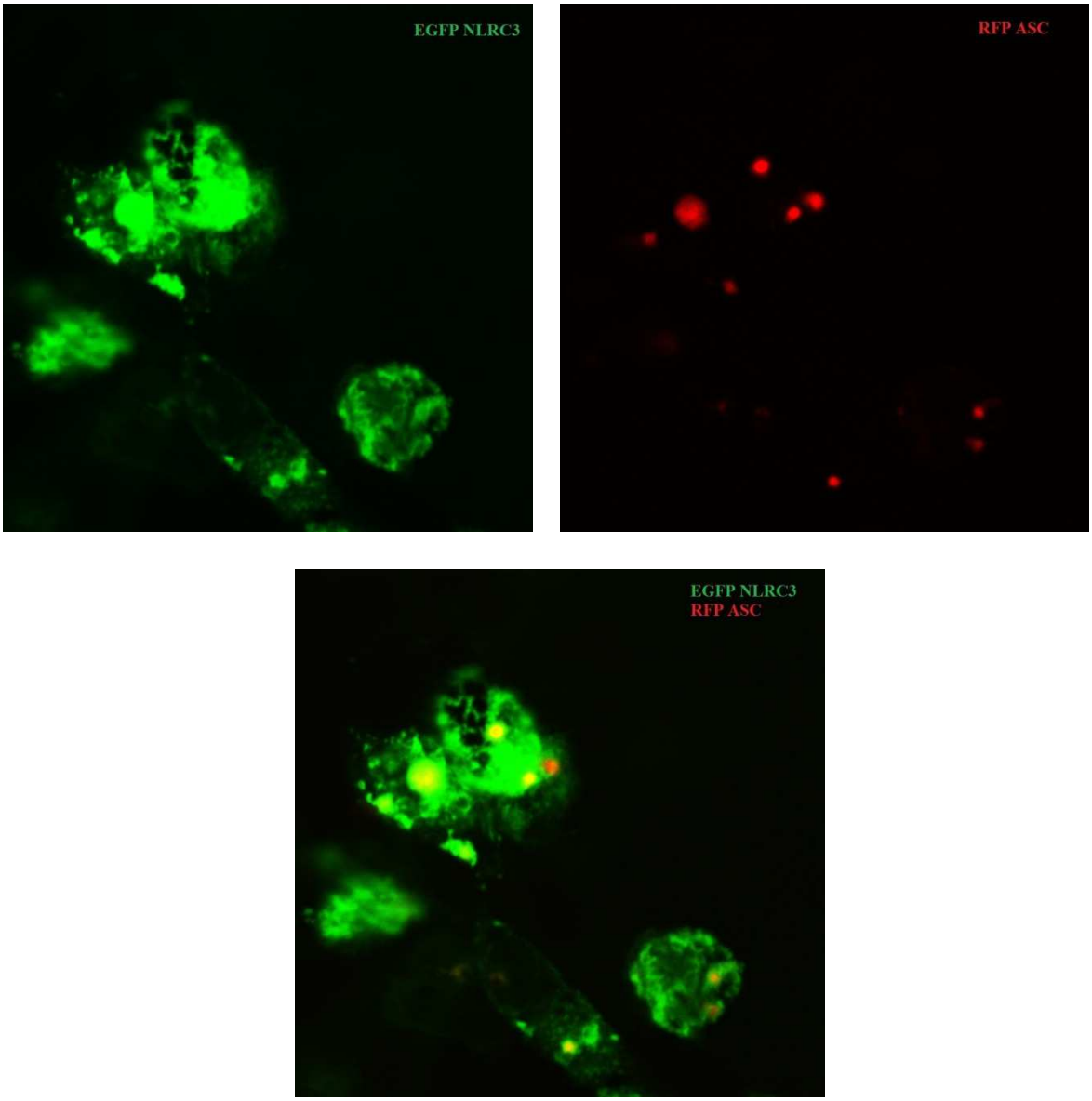

Figure 5.21. Cellular Co-localization of RFP ASC and EGFP NLRC3 in HEK293FT cells.

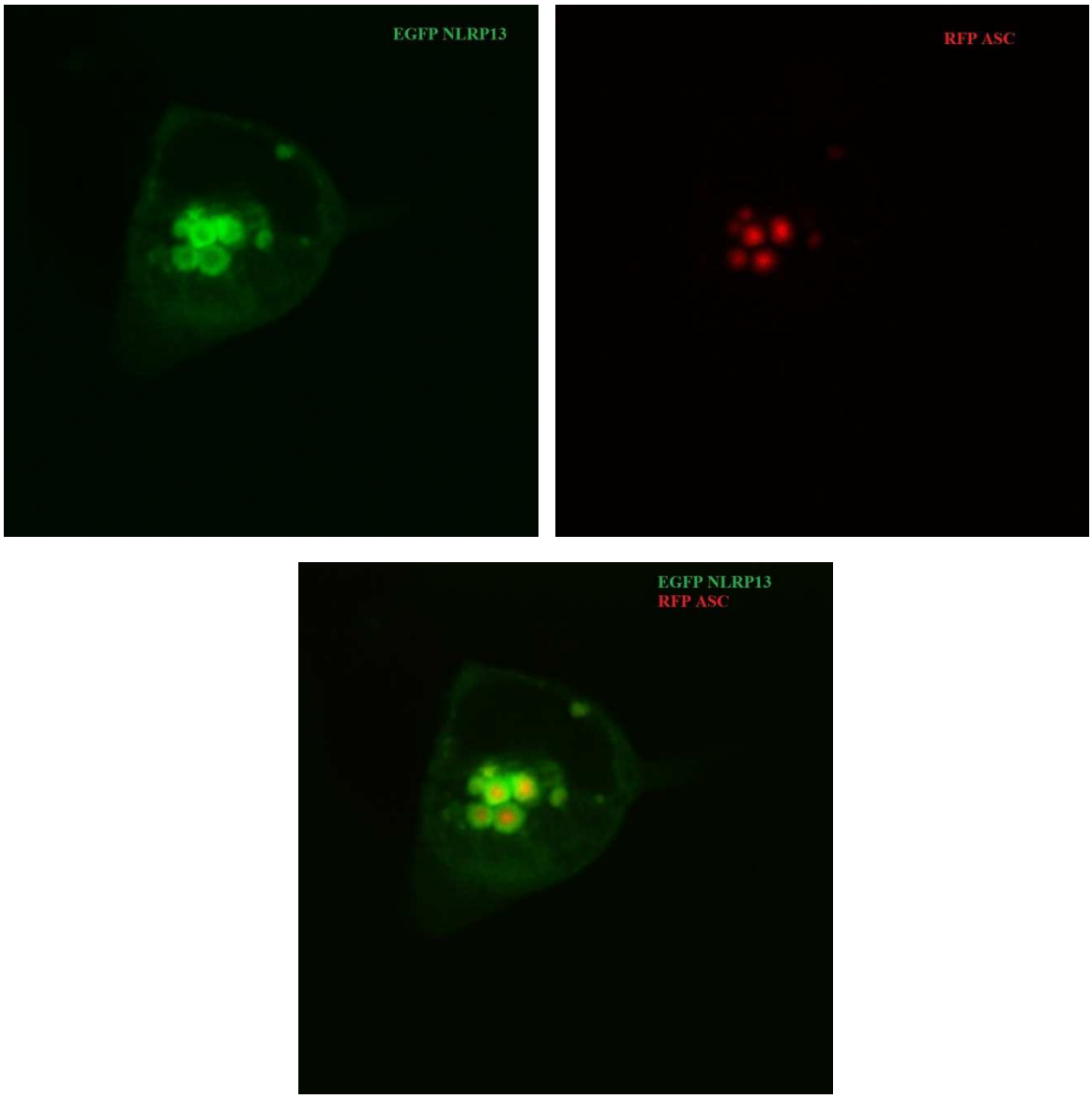

Figure 5.22.A. Cellular Co-localization of RFP ASC and EGFP NLRP13 in HEK293FT cells.

Supporting the result of Co-IP, cellular co-localization experiment suggests that both NLRC3 and NLRP13 can interact with ASC under overexpression conditions (Figures 5.21 and 5.22). However, there were also several specks like structures of ASC which did not appear to have NLRC3 or NLRP13 in them.

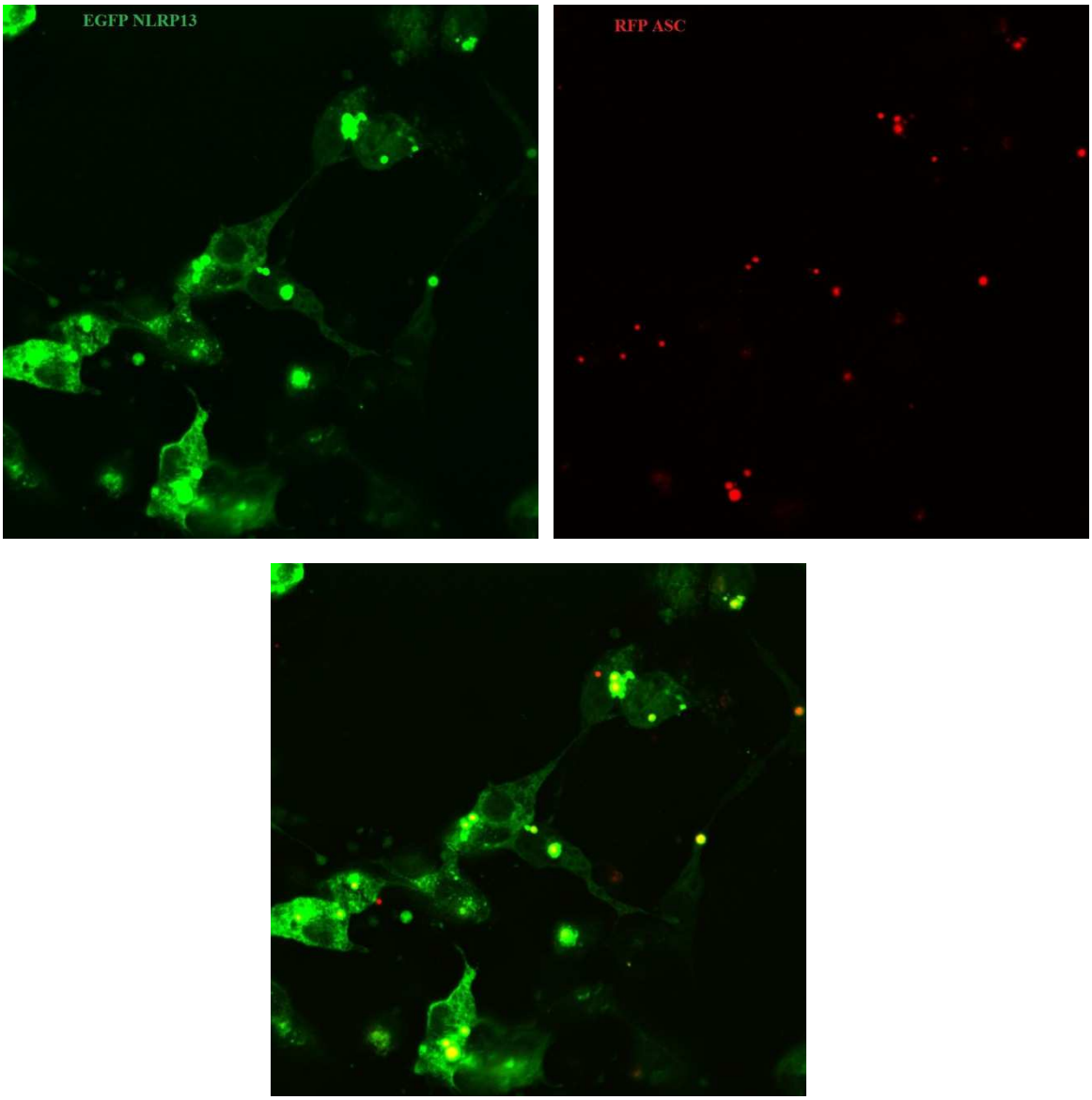

Figure 5.22.B. Cellular Co-localization of RFP ASC and EGFP NLRP13 in HEK293FT cells.

Co-localization of RFP ASC and EGFP NLRC3 or EGFP NLRP13 represented different features when compared to ASC- Cryopyrin co-localization. In Cryopyrin-ASC co-localization, there was only one ASC speck formation in each cell and there were no free cytoplasmic Cryopyrin proteins (Figure 5.26). All Cryopyrin proteins were in the speck formations of ASC. In contrast, the majority of NLRC3 and NLRP13 could be found in the cytoplasm and they could make more than one speck formation in one cell. Additionally, the co-localization ratio was 88% for ASC and NLRC3 and 89% for ASC and NLRP13 (Figures 5.21 and 5.22).

5.5.2. Caspase 1 Interacts with NLRC3 or NLRP13

Caspase 1 is one of the components of inflammasomes. It has a CARD domain and it is known that during inflammasome assembly, Caspase 1 interacts with ASC through its CARD domain. NLRC3 has a CARD domain, whereas NLRP13 has a PYRIN domain. To investigate the possible interaction between NLRC3 and Caspase 1 or NLRP13 and Caspase 1, co-immunoprecipitation experiment was performed. $5x10^6$ cells HEK293FT cells were counted and seeded in 10 cm plates 24 hours before transfection. 3 μg pECFP C3 Caspase 1 and 10 μg FLAG pcDNA3 NLRP13 or pECFPC3 Caspase 1 and FLAG pcDNA3 NLRC3 plasmids were co-transfected into HEK293FT cells. The negative control plate was transfected with empty Flag pcDNA3and pEGFP C3 vectors. 24 hours after the transfection, the Co-IP procedure was applied. Transfection effeciencies of CO-IP experiments were close to 85 %.Total protein lysates were precipitated with anti-FLAG antibody and Western blotting was performed with anti-Caspase 1 antibody.

Figure 5.23. NLRC3 and NLRP13 Interact with Caspase 1. Figure A represents CO-IP part and figure B represents total lysates. Immunoprecipitation was performed with anti-FLAG antibody and Western blotting was applied with anti Caspase 1 antibody. ECFP Caspase 1 fusion protein is 78 kDA.

Co-IP results suggest that both NLRC3 and NLRP13 can interact with Caspase1 (Figure 5.20). To verify the outcome of the Co-IP experiment, cellular co-localizations of ECFP Caspase 1 and EGFP NLRP13 or NLRC3 were analysed via confocal microscopy. $1x10^6$ HEK293FT cells were co-transfected with 1 μg pECFP C3 Caspase 1 and 2 μg pEGFP C3 NLRP13 or 2 μg pEGFP C3 NLRC3 plasmids. 24 hours later, transfected cells were fixed with 10% paraformaldehyde and visualization was performed under confocal microscopy.

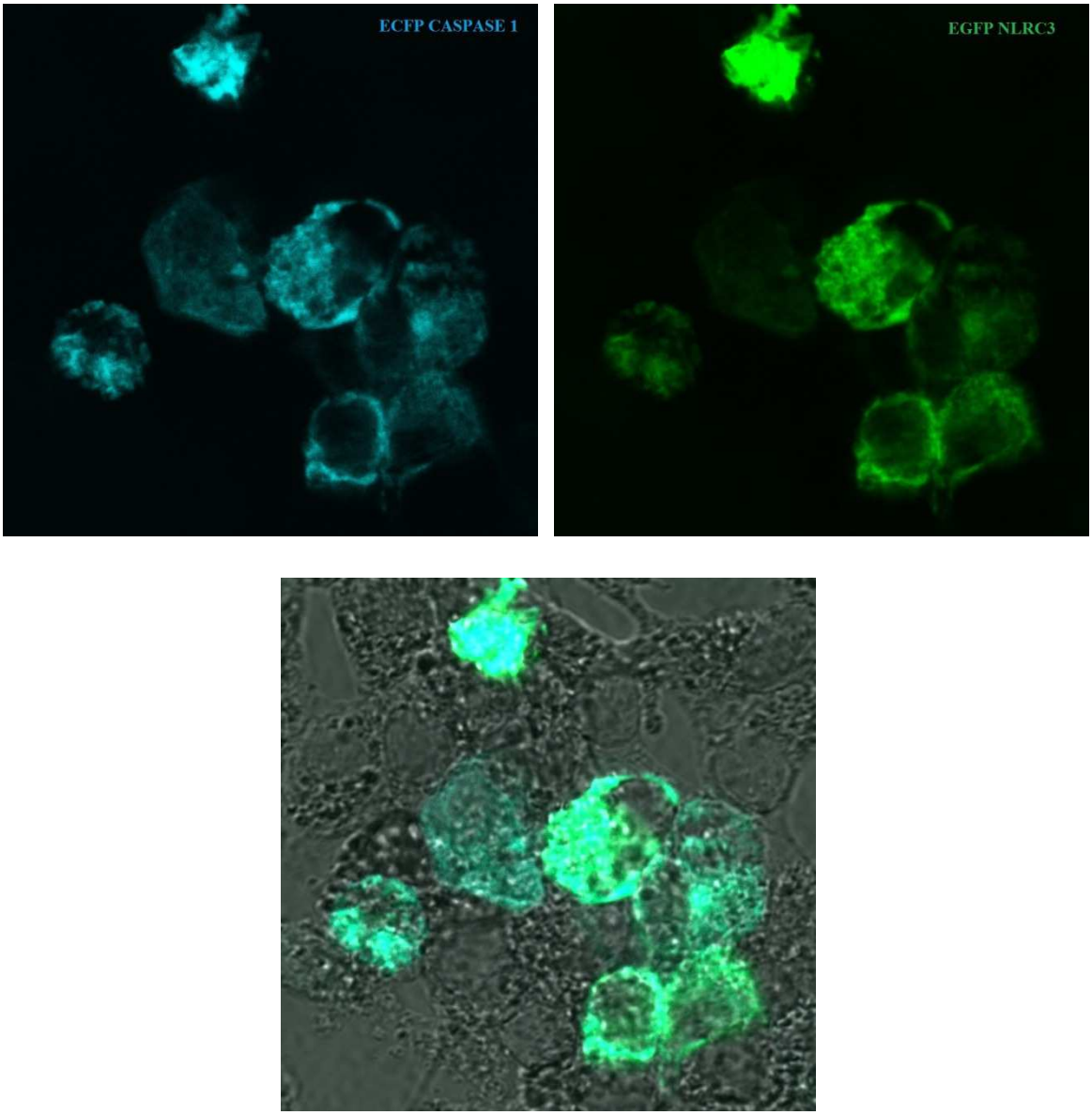

Figure 5.24. Cellular Co-localization of ECFP Caspase 1 and EGFP NLRC3 in HEK293FT cells.

To conclude, Caspase 1 can interact with both NLRC3 and NLRP13 when overexpressed in HEK293FT cells. This outcome was verified with Co-IP experiment and co-localization studies (Figures 5.23, 5.24 and 5.25).

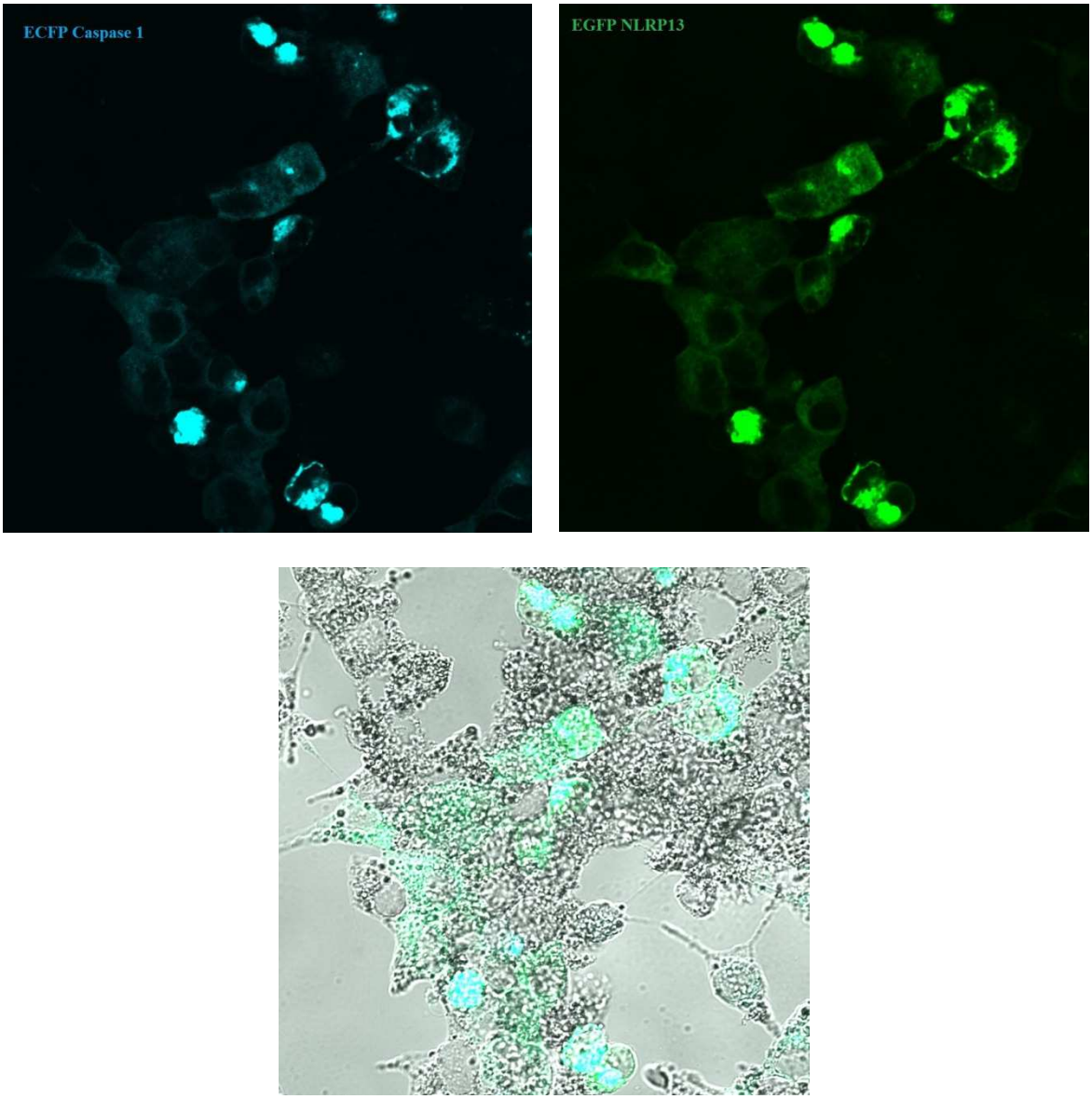

Figure 5.25. Cellular Co-localization of ECFP Caspase 1 and EGFP NLRP13 in HEK293FT cells.

Both NLRC3 and NLRP13 were completely co-localized with Caspase 1 in the cytoplasm of the cell and they did not make any speck formations. Co-transfected HEK293FT cells had 100% EGFP NLRC3 or EGFP NLRP13 and ECFP Caspase 1 signals and the co-localization ratio was 100% in HEK293FT cells.

Both Caspase 1 and ASC are known components of inflammasomes and they come together to assemble this large complex. For example, when homotypic interactions occur between the PYRIN domains of Cryopyrin/NLRP3 and adaptor protein ASC, this

interaction bridges the association of Caspase 1 to Cryopyrin/NLRP3 in the inflammasome complex (Figure 5.26).

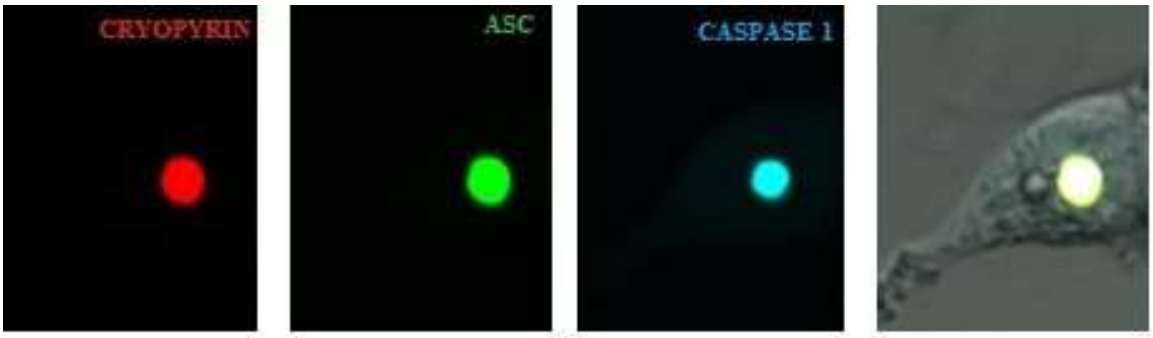

Figure 5.26. Cryopyrin, the Adaptor Protein ASC and Caspase 1 are the Components of Inflammasome.

Our Co-IP and cellular co-localization data indicate that both NLRC3 and NLRP13 can interact with ASC and Caspase 1 one by one, without the need for the third component. It can be thus suggested that both NLRC3 and NLRP13 can make an inflammasome-like complex by interacting with ASC and Caspase 1. To determine the co-localization of NLRC3-ASC and Caspase 1 or NLRP13-ASC and Caspase 1 in an inflammasome like complex, $1x10^6$ HEK293FT cells were co-transfected with 2 μg pEGFP C3 NLRC3 or pEGFP C3 NLRP13, 1 μg pTagRFP C3 ASC and 1 μg pECFP C3 Caspase 1. After 24 hours, transfected HEK293FT cells were fixed with 10% paraformaldehyte and cells were visualized with confocal microscopy.

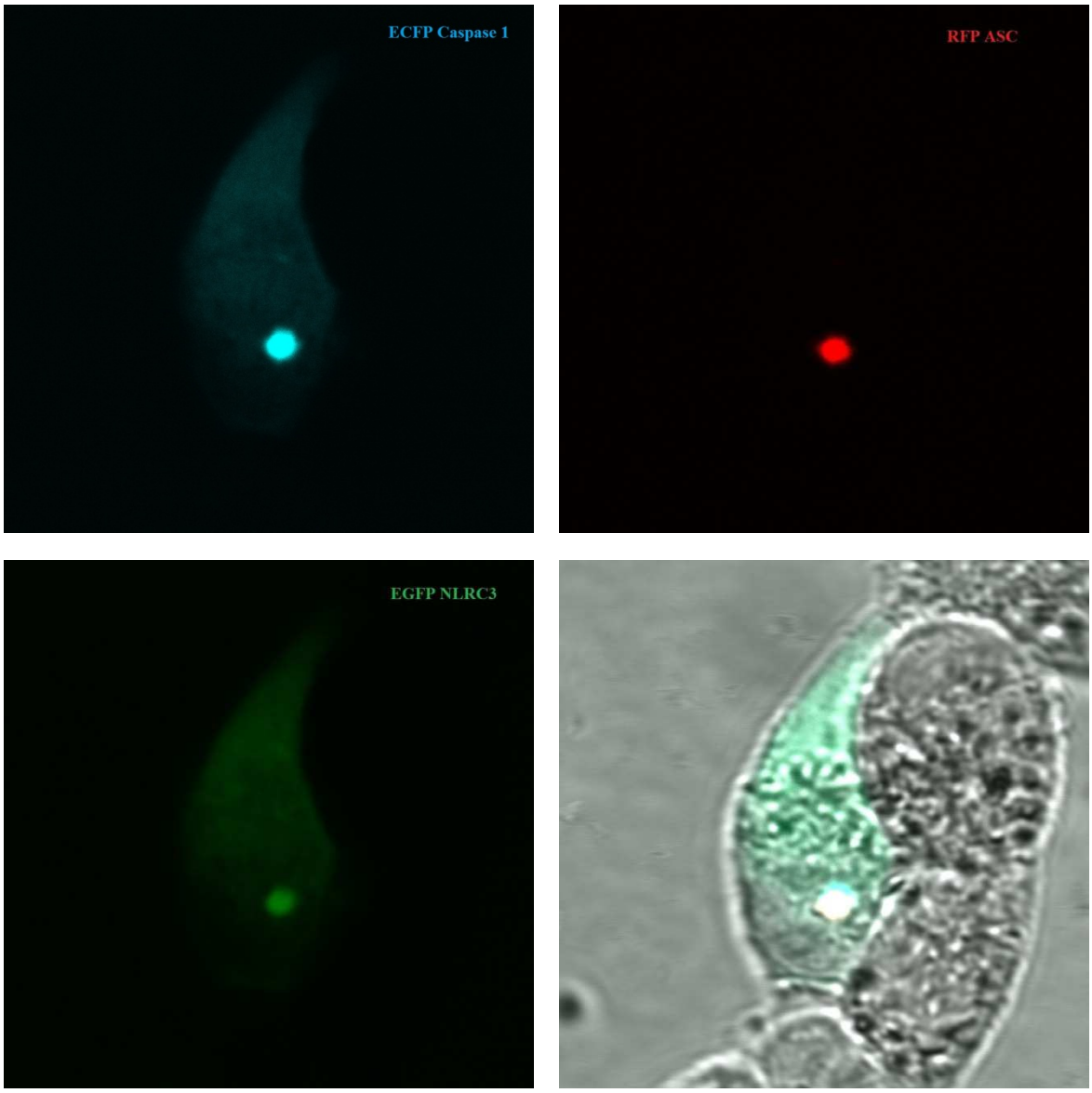

Figure 5.27. Inflammasome Like Complex of NLRC3-ASC and Caspase 1.

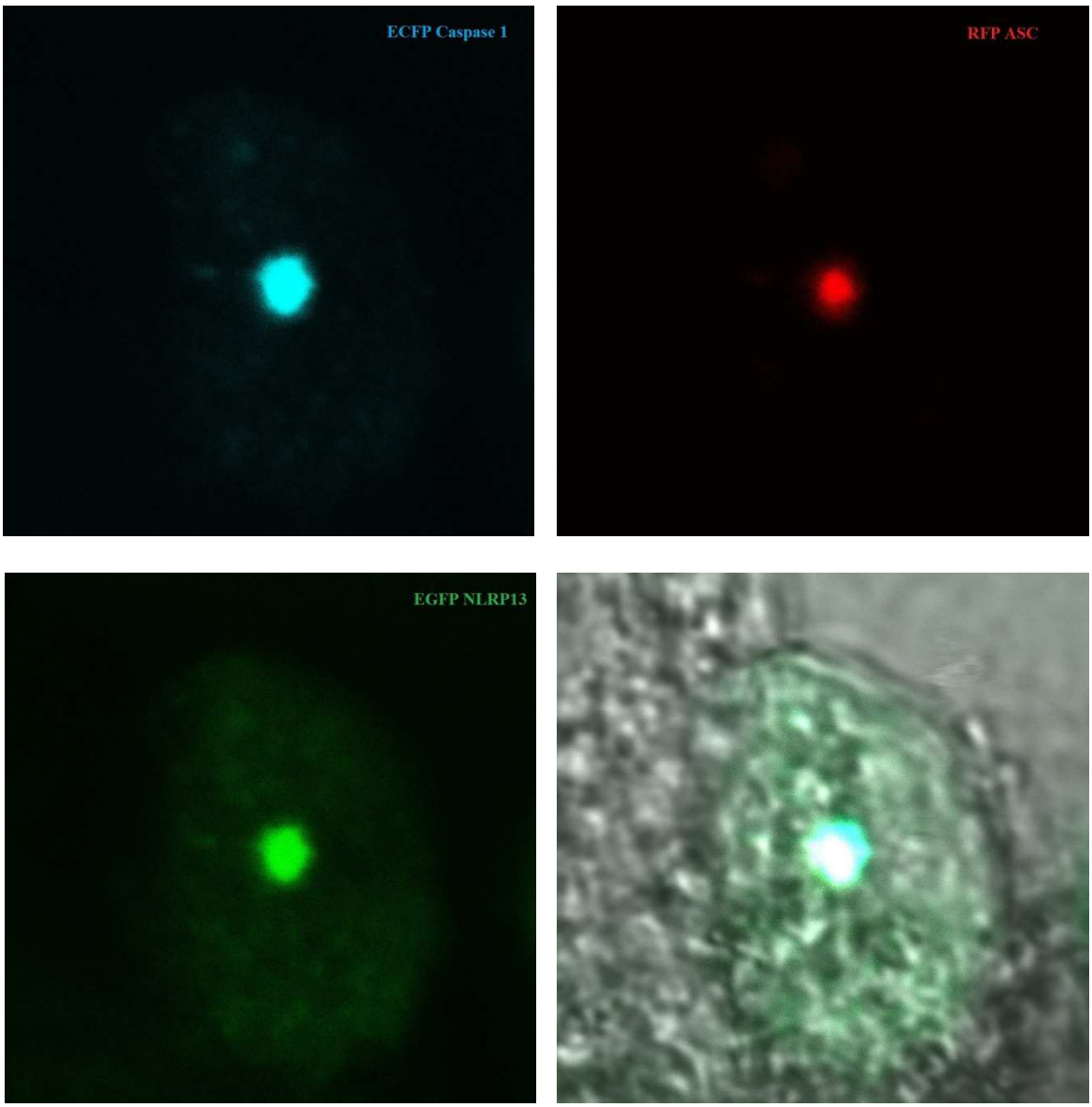

Figure 5.28. Inflammasome Like Complex of NLRP13-ASC and Caspase 1.

To sum up, it can be concluded that both NLRC3 and NLRP13 can assemble inflammasome like complexes, when they are co-transfected with ASC and Caspase 1 in HEK293FT cells. It was clear from the pictures that NLRC3 and NLRP13 proteins were not only found in the speck formation. It can be seen that Caspase 1 can interact with NLRC3 and NLRP13 even in areas where ASC is absent. On the contrary, when Cryopyrin makes the inflammasome assembly, all Cryopyrin proteins are found in the speck structure (Figure 5.26, 5.27 and 5.28).

5.5.3. NLRC3 can Interact with Caspase 5

Caspase 5 is one of the inflammatory enzymes that have the ability to digest the target proteins after their aspartic acid residues, similar to Caspase 1. Our CO-IP and co-localization data indicate that NLRC3 and NLRP13 can interact with Caspase 1 when overexpressed in HEK293FT cells. Therefore, to investigate the similar interaction ability of NLRC3 and NLRP13 with Caspase 5, co-immunoprecipitation experiments were carried out. $5x10^6$ HEK293FT cells were co-transfected with 2.5 μg FLAG pcDNA3 Caspase 5 and 10 μg MYC pcDNA3 NLRC3 or NLRP13. After 24 hours, transfected cells were collected and their cell lysates incubated with anti-FLAG antibody to precipitate the target proteins. Western blotting was performed with anti-MYC antibody.

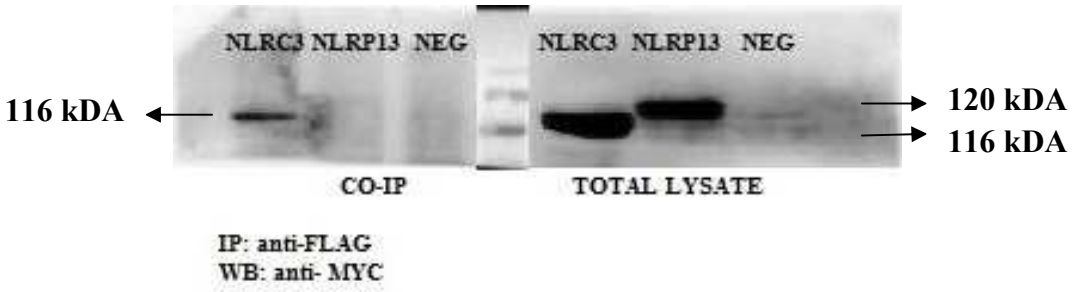

Figure 5.29. NLRC3 but not NLRP13 Interacts with Caspase 5. Protein lysates of transfected HEK293FT cells were incubated with anti-FLAG antibody to precipitate the target protein and Western blotting was performed with anti-MYC antibody.

As a result of the Co-IP experiment, we saw that NLRC3 interacts with Caspase 5, whereas NLRP13 may not interact with Caspase 5 when overexpressed in HEK293FT cells (Figure 5.29).

To verify the potential interaction, cellular co-localization of Caspase 5 and NLRC3 was performed. For this purpose, both MYC pcDNA3 Caspase 5 and pEGFP C3 plasmids were digested with XhoI and XmaI and digested Caspase 5 fragment was ligated into XbaI- XmaI digested pEGFP C3. Thus, pEGFP C3 Caspase 5 plasmid was generated. Parelelly, both pET30 NLRC3 and pTagRFP C3 plasmids were digested with KpnI and NotI or PspOMI and KpnI-Not digested NLRC3 fragment was ligated into KpnI-PspOMI digested plasmid. Hence, pTagRFP C3 NLRC3 plasmid was generated. To test the co-

localization of NLRC3 and Caspase 5, 2 μg pTagRFP C3 NLRC3 and 1 μg pEGFP C3 Caspase 5 plasmids were co-transfected in $1x10^6$ HEK293FT cells. After 24 hours, transfected cells were fixed with 10% paraformaldehyte and slides were analyzed under confocal microscopy.

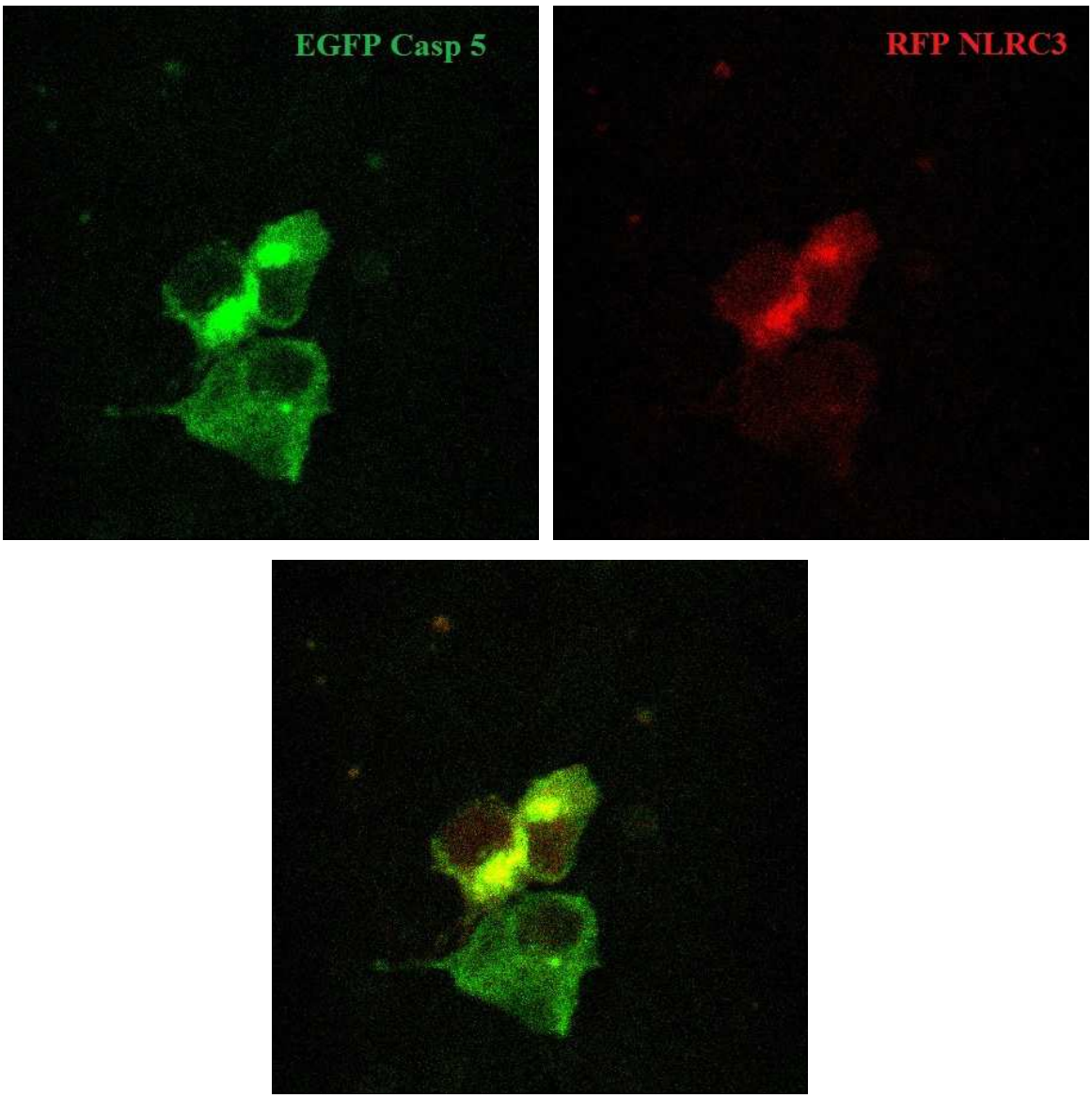

Figure 5.30. EGFP Caspase 5 Co-localized with RFP NLRC3 in HEK293FT cells.

To summarize, NLRC3 can interact with NLRC3 under overexpression conditions (Figure 5.29). This interaction was further confirmed with co-localization experiment in HEK293FT cells. NLRC3 was completely co-localized with Caspase 5 in the cytoplasm of the cell and they did not make any speck formations (Figure 5.30). Co-transfected HEK293FT cells had 100% RFP NLRC3 and ECFP Caspase 5 signals.

5.6. Induction of ASC Speck Formation

ASC is known as apoptosis-association speck-like protein containing a CARD domain. It plays an adaptor role in the inflammasome. Under physiological conditions, ASC can be found as a soluble protein in the cytosol of healthy cells. On the other hand, it forms ring-like speck structures with hallow center in apoptotic cells. In addition to that Cryopyrin can enhance the speck formation when overexpressed. Our co-immunoprecipitation and co-localization data suggest that NLRC3 and NLRP13 can interact with ASC when overexpressed in HEK293FT cells. To test the effect of NLRC3 and NLRP13 on the speck formation of ASC, stable EGFP ASC HEK293FT cells were transfected with NLRC3 and NLRP13 in a dose dependent manner. Each of the FLAG pcDNA3 NLRC3, NLRP13 and Cryopyrin plasmids were transfected at 50 ng, 100 ng and 250 ng per well. Flag pcDNA3 Cryopyrin was selected as a positive control. Speck formation of the EGFP ASC stable cells were visualized under inverted fluorescent microscopy in a time dependent manner. The numbers of speck structures were quantified from photos taken after 24 hours, 48 hours and 72 hours post-transfection.

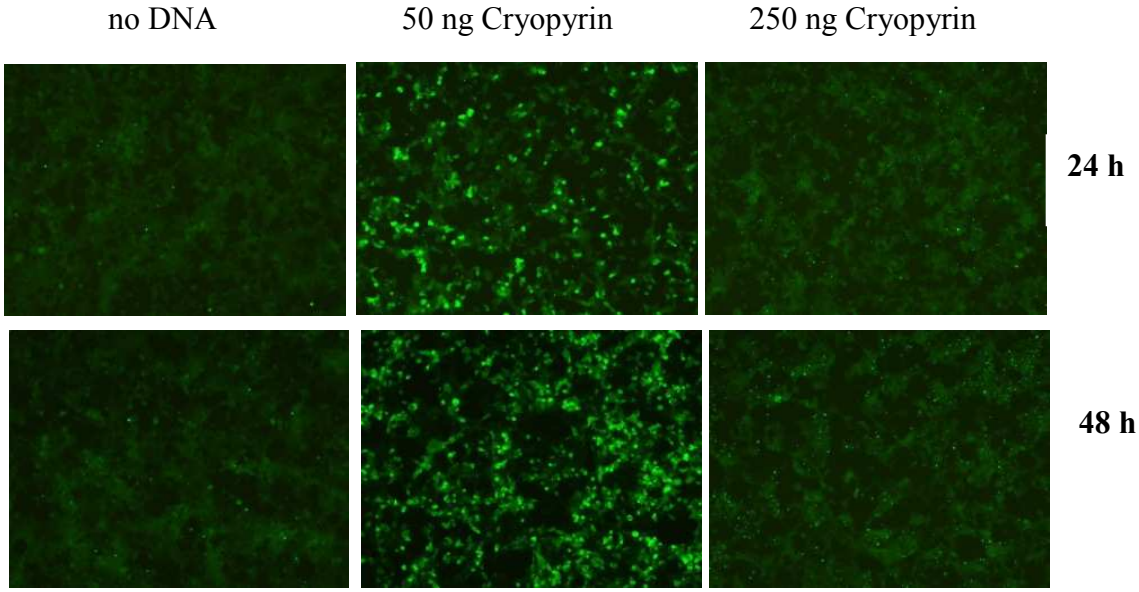

Figure 5.31. Dose and Time Dependent Increase in Speck Formation in Cryopyrin/NLRP3 Transfected Cells. $1x10^6$ cells were seeded 24 hours before transfection, performed with 50 ng, 100 ng and 250 ng plasmid per well.

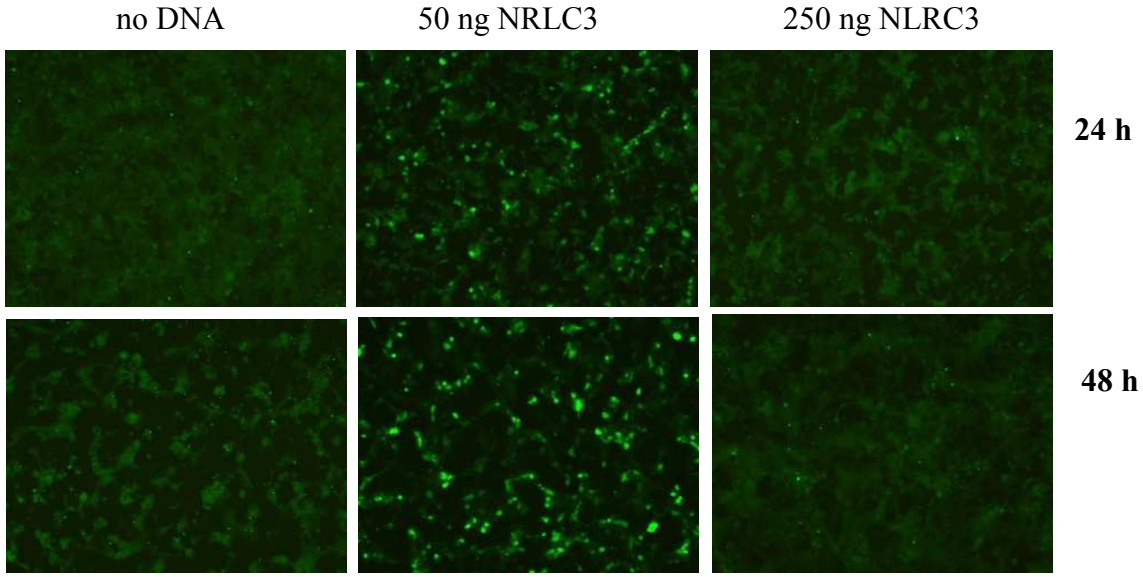

Figure 5.32. Dose and Time Dependent Increase in Speck Formation in NLRC3 Transfected Cells. $1x10^6$ cells were seeded 24 hours before transfection, performed with 50 ng, 100 ng and 250 ng NLRC3 plasmid per well.

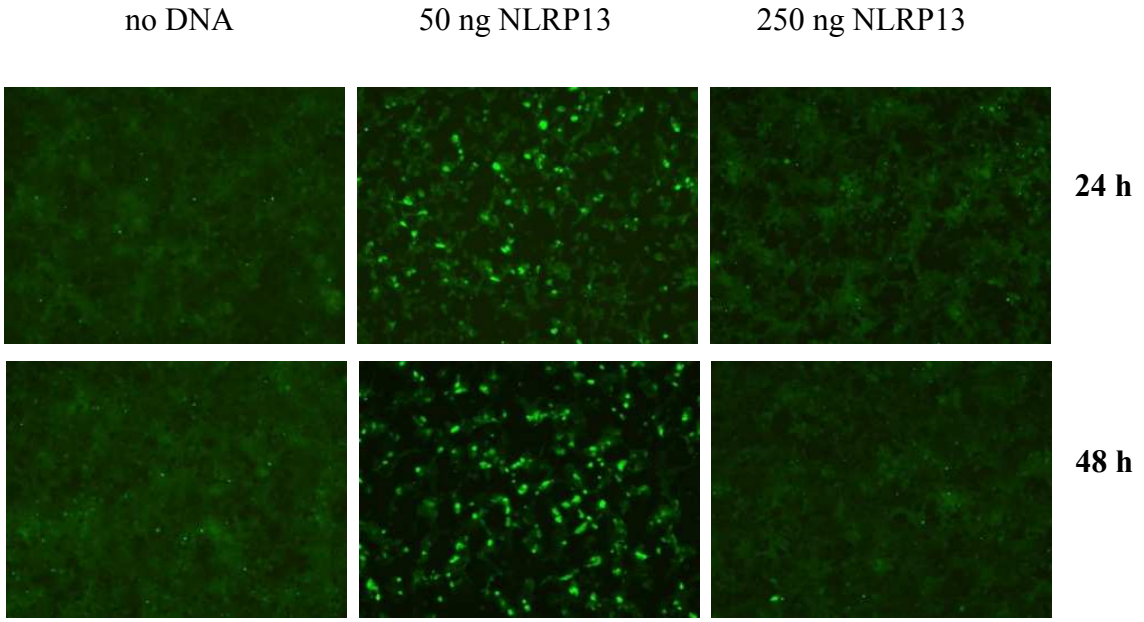

Figure 5.33. Dose and Time Dependent Increase in Speck Formation in NLRP13 Transfected Cells. $1X10^6$ cells were seeded 24 hours before transfection, performed with 50 ng, 100 ng and 250 ng NLRP13 plasmid per well.

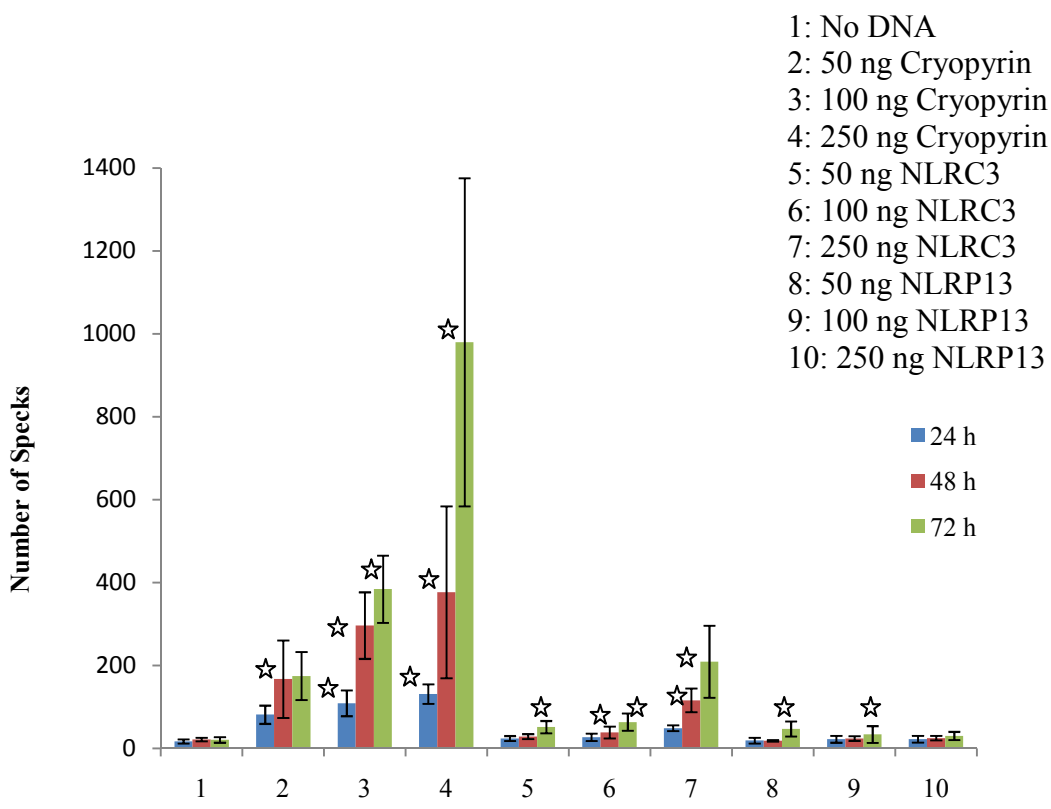

Figure 5.34. Quantification of ASC Speck Formation after FLAG pcDNA3 Cryopyrin, MYC pcDNA3 NLRC3 and FLAG pcDNA3 NLRP13 Transfections. Colourful bars indicate time after transfection (blue= 24 h, red=48 h and gren= 72 h) (n=9) (p<0.05).

As expected, Cryopyrin/NLRP3 transfection into stable EGFP ASC HEK293FT cells induced speck formation of ASC in a concentration and time dependent manner. For the case of NLRC3, it can be suggested that NLRC3 increased the number of speck formation in a time and dose dependent manner when EGFP ASC HEK293FT cells were transfected. When the numbers of speck structures of NLRC3 and NLRP13 were compared to the negative control and the student *t* test was applied, all NLRC3 outcomes were statistically significant. However, NLRP13 did not present the same patterns. The number of speck formations were quite low and only the 72 h 50 ng and 250 ng results were significant *(p<0.05)*, when the *t* test was applied (Figure 5.34). In addition to induction effect of NLRC3 and NLRP13 on speck formation, both speck and non-speck formed cells started to die after 24 hours (Figure 5.32 and 5.33). Nonetheless, we did not carry out any cell death assay. To confirm this observation, we should apply cell death assays.

5.7. Downregulation Effect of NLRC3 and NLRP13 on NF-κB Signaling

It was previously reported that several members of the *NLR* genes family such as NOD1 and NOD2 can upregulate NF-κB signaling. On the other hand, several NLRs like NLRP10 can downregulate this signaling pathway. In order to determine the effect of NLRC3 and NLRP13 on NF-κB signaling, luciferase reporter gene assay was performed. To test the effects of NLRC3 and NLRP13 on NF-κB activation, the luciferase reporter genes pBVIX, pRLTK and NLRC3 or NLRP13 were co-transfected into HEK293FT cells. All conditions were performed as triplicate and the results were repeated twice.

A

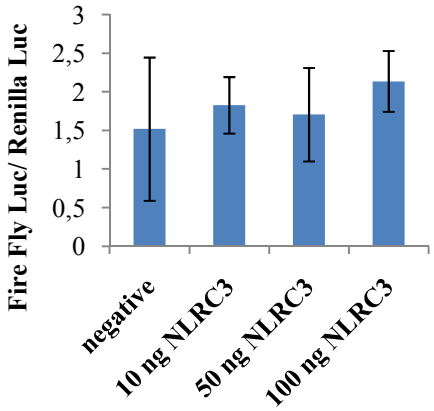

B

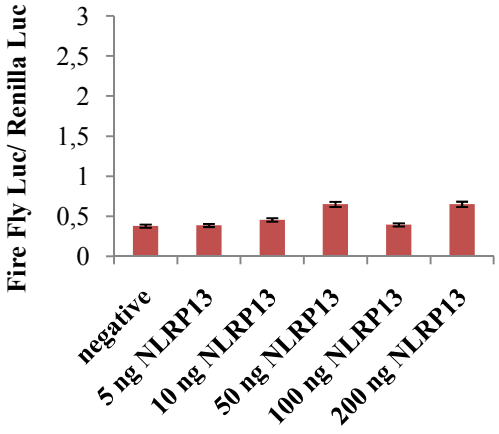

Figure 5.35. NLRC3 and NLRP13 do not Upregulate NF-κB Activity. (A) NF-κB activity for NLRC3 in a dose dependent manner. (B) Luciferase reporter assay for NF-κB activity of NLRP13 in a dose dependent manner.

In conclusion, NLRC3 and NLRP13 do not upregulate the NF-κB signaling when they are overexpressed in HEK293FT cells (Figure 5.35).

As a next experiment, to test the downregulation potential of NLRC3 and NLRP13, co-transfections of NOD1 or NOD2 with NLRC3 or NLRP13 was planned. It is known that NOD1 and NOD2 upregulate the signaling of the NF-κB pathway. In parallel with earlier reports we showed that NOD1 and NOD2 increase the levels of NF-κB regulated luciferase reporters (Figure 5.36).

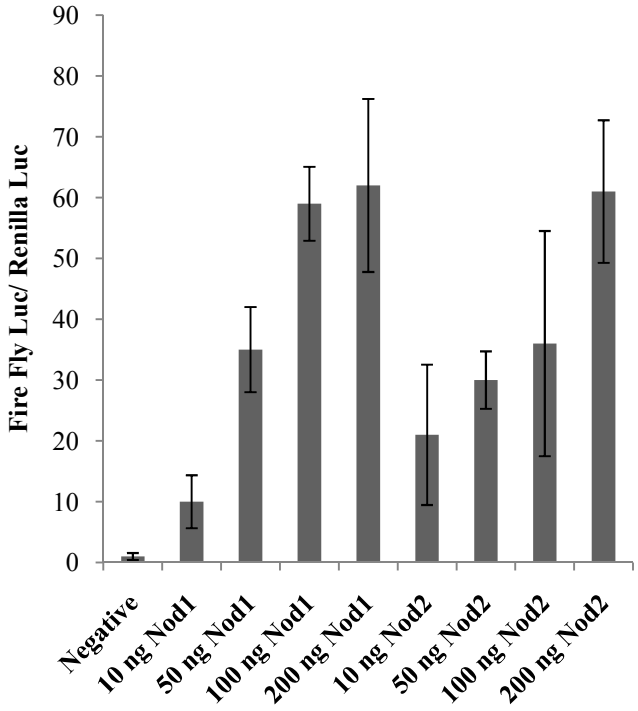

Figure 5.36. NOD1 and NOD2 Upregulate NF-κB Activity.

To determine the downregulation potential of NLRC3 and NLRP13, either of the genes were co-transfected with 100 ng NOD1 or NOD2.

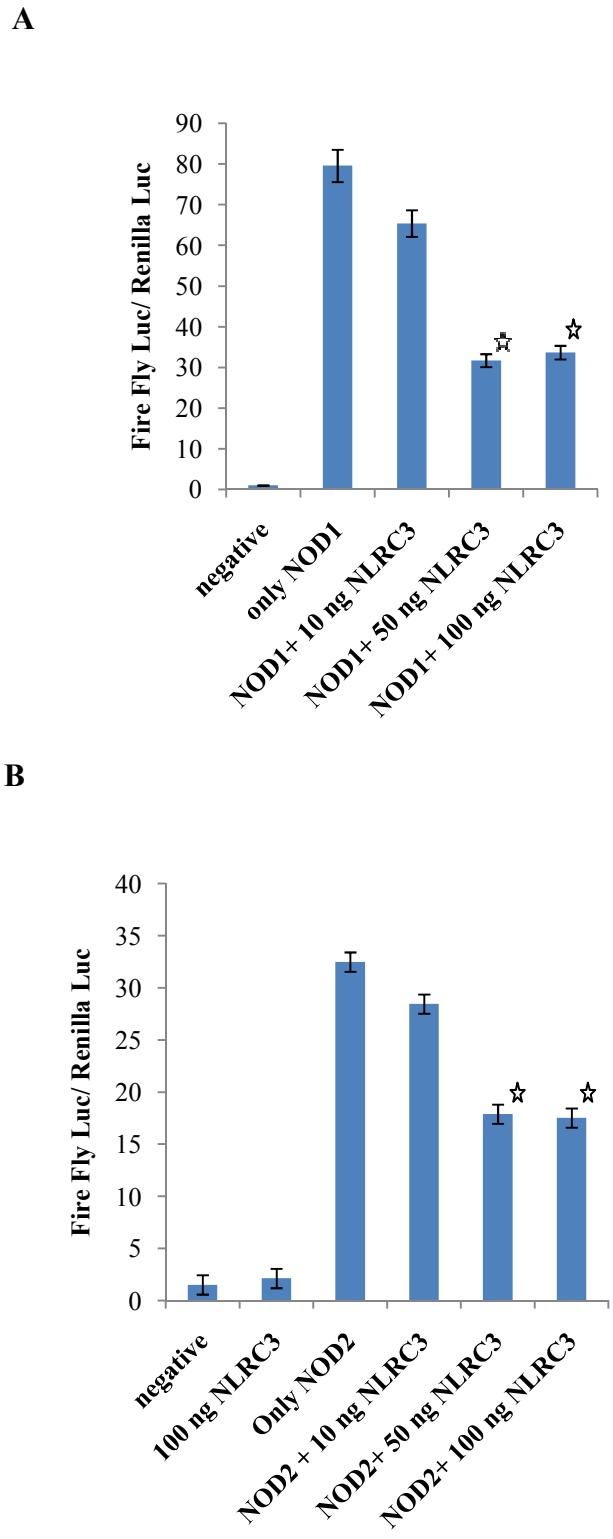

Figure 5.37. NLRC3 Suppresses NOD1 and NOD2 Induced NF-κB Activity. (A) NF-κB activity for co-transfection of NOD1 and NLRC3. (B) NF-κB activity for co-transfection of NOD2 and NLRC3 (p= 0.0001).

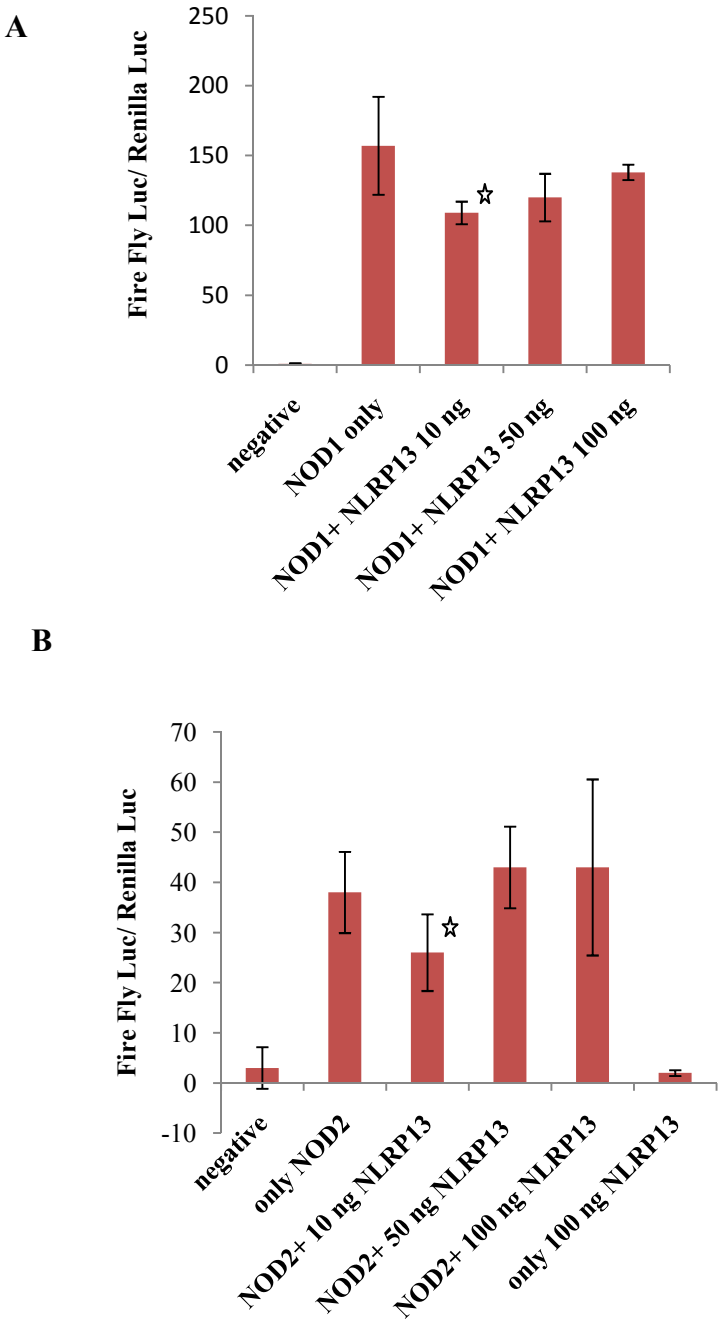

Figure 5.38. NLRP13 Suppresses NOD1 and NOD2 Induced NF-κB Activity. (A) NF-κB activity for co-transfection of NOD1 and NLRP13. (B) NF-κB activity for co-transfection of NOD1 and NLRP13 ($p < 0.05$).

In conclusion, overexpression of NLRC3 and NLRP13 proteins with NOD1 or NOD2 resulted in NF-κB downregulation (Figures 5.37 and 5.38).

6. DISCUSSION

In this thesis, we document for the first time that both NLRC3 and NLRP13 are mainly localized in cytoplasm and also they can be found in mitochondria. In addition, we document for the first time that inflammasome components can interact with NLRC3 and NLRP13. Both NLRC3 and NLRP13 weakly interacted with ASC. We indicated that the majority of the proteins were free in the cytosol and induced more than one speck formation in each cell when they were co-transfected with ASC. Furthermore, we showed for the first time that Caspase 1 can interact with NLRC3 and NLRP13 when overexpressed in HEK293FT cells. They were completely co-localized in every cell. In addition to this we have shown for the first time that Caspase 5 can interact with NLRC3 and under overexpression conditions, RFP NLRC3 perfectly co-localized with EGFP Caspase 5 in HEK293FT cells. We document for the first time that NLRC3 led to increase in the speck formation of ASC in a dose and time dependent manner. Finally, it was shown for the first time that both NLRC3 and NLRP13 suppressed NOD1 and NOD2 induced NF-κB activity when overexpressed in HEK293FT cells.

NLRC3 has CARD domain and however, it represent no sequence homology to known CARD or PYRIN domains. Nevertheless, NLRC3 is predicted to have a 6 α-helical bundle. This indicates that NLRC3 effector domain is structurally similar to CARD or PYRIN domains, whereas it may feature a different interface. On the other hand, NLRP13 has a PYRIN domain in its architecture and it shows sequence similarity to known PYRIN domain. This domain represent high homology with PYRIN domain of the Pyrin protein. Also, both NACHT domains have a sequence homology. The NACHT of NLRC3 mostly looks like Cryopyrin whereas the NACHT domain of NLRP13 is most similar to the NACHT domain of NALP1. In addition to the NACHT domain, the LRR motifs are highly conserved and present high similarity within family members (Figure 5.1). Plant resistance genes called *P* genes and TLRs also share this domain and it is suggested that this motif has a role in pathogen sensing.

NLRC3 is one of the evolutionarily conserved NLR family members. It seems to be expressed and functioned from zebrafish to humans (Figure 5.1.A). However, NLRP13 is not expressed as widely. Rat and mouse do not express NLRP13, but they express *NLRP5*. Human *NLRP5* gene presents a high homology with human, mouse or rat *NLRP5* gene. When the human, rat and mouse *NLRP5* genes are aligned with human *NLRP13* gene, it can be suggested that the NLRP5 and NLRP13 share a common ancestor (Figure 5.2.B).

Bioinformatic analysis of cellular localization of NLRC3 suggests that it can be found 48% in cytosol and 4% in mitochondria. On the other hand, NLRP13 is predicted as a 48% cytosolic and 17% mitochonrial protein (Moore et al., 2008). Both EGFP NLRC3 and EGFP NLRP13 were overexpressed in HEK293FT cells with different organnel markers. Both of EGFP fusion proteins were largely localized in the cytoplasm (Figures 5.10 to 5.22). However, it was observed for the first time that NLRP13 was pre-dominantly localized with mitochondria (Figures 5.17 and 5.18). Generally, NLRs are located into cytoplasm. However, there are several members with different features. To illustrate, CIITA behaves as a transcription factor. When it is stimulated, it translocates into the nucleus and induces the expression of MHC class II genes. On the other hand, NLRC5 is a transcriptional regulator of MHC class I genes. It can also translocate into the nucleus. In addition, NLRX1 functions as a mitochondrial protein. It interacts with the mitochondrial adaptor MAVS to inhibit the RIG-I-mediated signaling pathway and triggers the generation of reactive oxygen species (Tattoli et al., 2008). NLRX1 was identified as a regulator of mitochondrial antiviral responses and represents an intersection of three ancient cellular processes: NLR signalling, intracellular virus detection and the use of mitochondria as a platform for anti-pathogen signalling (Moore et al., 2008). Moreover, it is indicated that under resting situations, NLRP3 is localized in endoplasmic reticulum structures. On the contrary, when the inflammasome was activated, both NLRP3 and its adaptor ASC redistrubited to the perinuclear region where they co-localized with endoplasmic reticulum and mitochondria. When mitochondrial activation was dysregulated by inhibition of the voltage-dependent anion channel, not only ROS generation but also inflammasome activation were supressed (Zhou et al., 2010). Like Cryopyrin, NLRs can have a role in apoptosis because there is a significant crosstalk between innate immunity and apoptosis. Recently, it has been suggested that BID can interact with NOD1 or NOD2 and have a role in triggering inflammation and immune responses (Yeretssian et al.,

2011). Mitochondria are organelles that enhance the process of cell death by releasing cytochrome-c. In this thesis, we document for the first time NLRP13 was pre-dominantly localized with mitochondria. This may link between NLRC3 or NLRP13 and mitochondrial cell death. Therefore, the decision to induce innate immune responses and survive or commit suicide by apoptosis can be dependent on the crosstalk between NLRs and apoptotic proteins. To confirm our sub-cellular localization data, immunocytochemistry or immunohistochemistry experiments should be performed in the cells or tissues which endogeneously express NLRC3 and NLRP13. In addition to immunocytochemistry experiment, the interaction of NLRC3 or NLRP13 with apoptosis related proteins should be tested via Co-IP and co-localization studies with confocal microscopy.

Our Co-IP experiments document for the first time that both NLRC3 and NLRP13 can interact with inflammasome components, ASC and Caspase 1 (Figures 5.20 and 5.23). EGFP NLRC3 and EGFP NLRP13 co-localized with RFP ASC and ECFP Caspase 1 when they are overexpressed in HEK293FT cells (Figure 5.21, 5.22, 5.24 and 5.25). This interaction suggests that NRLC3 and NLRP13 can assemble inflammasome like structures. This suggestion was tested with co-expression of EGFP NLRC3 or EGFP NLRP13 with RFP ASC and ECFP Caspase 1. Under confocal microscopy, it was determined that both EGFP NLRC3 and EGFP NLRP13 form inflammasome like structures (Figure 5.27 and 5.28). These results suggest that several NLRs can be found in the inflammasome assembly. To illustrate the point, NLRC5 was found in Cryopyrin inflammasome to augment its activity (Davis et al., 2011). APAF1 can assemble multiple protein platforms with its eight or seven NOD domains to generate the structure of the apoptosome (Yuan S. et al., 2010). What is more, in our experiments, we determined speck formation was induced when stable EGFP ASC HEK293FT cells were transfected with Cryopyrin, NLRP13 or NLRC3. The effect of NLRC3 was not as dramatic as Cryopyrin but its induction of ASC speck formation was statistically important in all cases. However, NLRP13 did not produce the same outcome (Figure 5.34).

Moreover, stable EGFP ASC HEK293 FT cells underwent death when they were transfected with NLR members judged by their appearance under the microscope. However, we did not measure the death rates; thus, this observation should be verified with

cell death assays (Figures 5.31, 5.32 and 5.33). Furthermore, Caspase 1 also leads to cell death known as pyroptosis. It is possible that NLRC3 or NLRP13 can form death assembly platforms in the multiprotein complexes with ASC and Caspase 1. To test the effect of NLRC3 and NLRP13 with or without ASC or Caspase 1 on cell death, annexin V apoptosis assay should be applied.

What is more, we have shown for the first time that Caspase 5 can interact with NLRC3 (Figure 5.29). Under overexpression conditions, RFP NLRC3 completely co-localized with EGFP Caspase 5 in HEK293FT cells (Figure 5.30). Caspase 5 can be found in NALP1 inflammasome. Therefore, it can be suggested that NLRC3 and NLRP13 can form multiprotein platforms.

The effects of NLRC3 and NLRP13 on Caspase 1 cleavage, IL-1β expression and secretion are not known yet. However, it can be suggested that NLRC3 and NLRP13 can be anti-inflammatory NLRs when their effects on NF-κB signaling can be taken into consideration. It was shown that both NLRC3 and NLRP13 suppressed *NOD1* and *NOD2* induced NF-κB activity when overexpressed in HEK293FT cells (Figure 5.37 and 5.38). When they were transfected into HEK293FT cells alone, they did not have upregulation effects on NF-κB (Figure 5.35). Thus, it can be concluded that NLRC3 and NLRP13 can be members of the anti-inflammatory NLR subgroup.

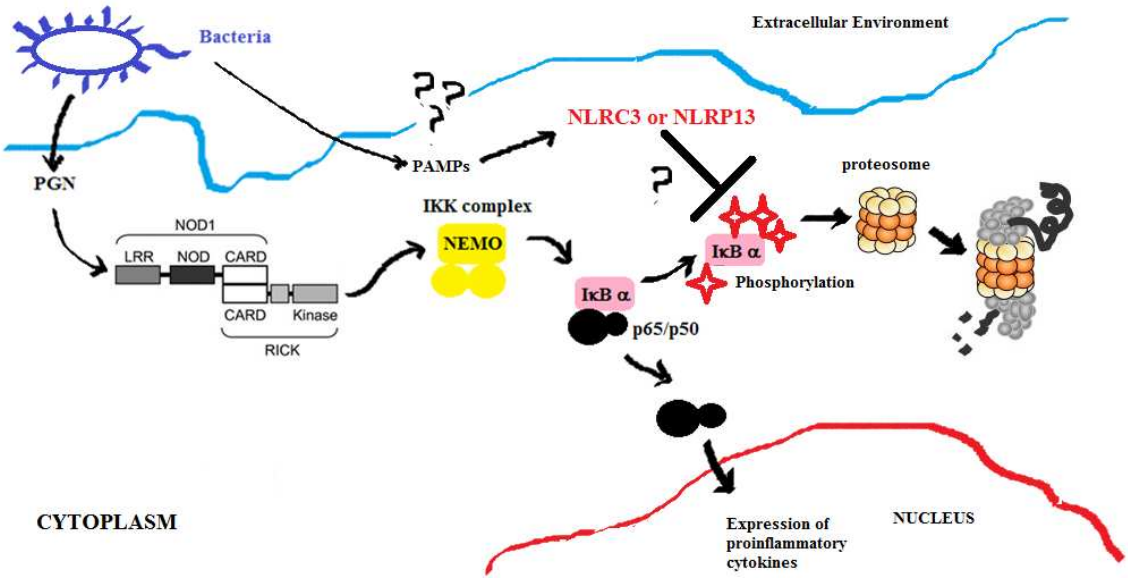

Figure 6.1. Hypothetical Signaling Pathway of NLRC3 and NLRP13.

Our preliminary results suggest that both NLRC3 and NLRP13 have anti-inflammatory effects. They probably interact with the inflammasome components and may negatively regulate the inflammasomes. However, our experimental system is based on overexpression conditions. We should test the functions of NLRC3 and NLRP13 under endogenous levels and in mouse models. For the case of NLRP13, knock out strategy will not work because they lack this gene already. Therefore, NLRP13 knock-in mouse can be generated as an animal model to study the functions of NLRP13. In addition, NLRC3 knocked out mice models and siRNA mediated knocked down cells should be generated to investigate the NLRC3 related pathways. Finally, possible integrators of NLRC3 and NLRP13 in apoptosis pathways should be investigated since there is a significant crosstalk between NLRs and apoptosis. When these experiments are carried out, the results will indicate the possible scenario for the functions of NLRC3 and NLRP13 on the inflammasome and apoptosis.

The suppression of T cell activation is one of the mechanisms that all immune privilege areas share. NLRC3 may be important in immune tolerance to inhibit the activation of T cells. Additionaly, *NLRC3* gene expression was detected in uterus, brain and placenta which are immunologically privileged areas. What is more, placenta is the only known tissue with expression of *NLRP13* and it can be suggested that NLRP13 might be important for immune privilege in the placenta. Therefore, it can be hypothesized that both NLRC3 and NLRP13 can be anti-inflammatory NLRs and have functions in immune tolerance. Hopefully, this thesis will be a good initiator to discover any links between NLRC3 and NLRP13 signaling and immune tolerance. The possible outcomes may be helpful in improving innovative therapeutics against the immune tolerance enjoyed by cancer existing cells.

REFERENCES

Akira, S., S. Uematsu, O. Takeuchi, 2006, "Pathogen Recognition and Innate Immunity", *Cell*, Vol. 124, pp. 783-801.

Aksentijevich, I., C. D. Putnam, E. F. Remmers, J. L. Mueller, J. Le, R. D. Kolodner, Z. Moak, M. Chuang, F. Austin, R. Goldbach-Mansky, H. M. Hoffman, 2007, "The clinical continuum of cryopyrinopathies: novel CIAS1 mutations in North American patients and a new cryopyrin model", Arthritis Rheum., Vol. 56 (4), pp. 1273-85.

Allen, Irving C, E. TeKippe McElvania, T. Woodford Rita-Marie et al., 2010, "The NLRP3 inflammasome functions as a negative regulator of tumorigenesis during colitis-associated cancer", *JEM*, Vol. 207 (5), pp. 1045-1056.

Balkwill, F., K. A. Charles., A. Mantovani, 2005, "Smoldering and polarized inflammation in the initiation and promotion of malignant disease", *Cancer Cell*, Vol. 7, pp. 211-217.

Bartel, D. P., 2009, "MicroRNAs: target recognition and regulatory functions", *Cell*, Vol. 136**,** pp. 215-233.

Bryant, C., A. K. Fitzgerald, 2009, "Molecular Mechanisms involved in inflammasome activation", *Trends in Cell Biology*, Vol.19 (9).

Bo, H., E. Eran, H. Samuel, J. B. Carmen, S. Till, et al., 2010, "Inflammation-induced tumorigenesis in the colon is regulated by caspase-1 and NLRC4, *PNAS*, Vol. 107 (50), pp. 21635-21640.

Botsios, C., P. Sfriso, A. Furlan, L. Punzi, C. A. Dinarello, 2008, "Resistant Behçet disease responsive to anakinra", *Ann Intern Med.*, Vol. 149 (4), pp.284-6.

Bouchier-Hayes, L., J. S. Martin, 2002, "CARD games in apoptosis and immunity", *EMBO Reports*, Vol. 3 (7), pp. 616-621.

Calin, C., C. D. Sevignani, T. Dumitru, E. Hyslop, et al., 2004, "Human microRNA genes are frequently located at fragile sites and genomic regions involved in cancers", *Proc. Natl. Acad. Sci.*, Vol. 101, pp. 2999-3004.

Chaofeng, H., S. Liping, H. Yiling, L. Daxiang, W. Huadong, T. Suisheng, 2010, "Functional characterization of the NF-κB binding site in the human NOD2 promoter", *Cellular & Molecular Immunology*, Vol. 7, pp. 288- 295.

Chen, G. Y., M. H. Shaw, G. Redondo, G. Nunez, 2008, "The innate immune receptor NOD1 protects the intestine from inflammation-induced tumorigenesis", *Cancer Res*., Vol. 68, pp. 10060-10067.

Conti, B. J., B. K. Davis, J. Zhang,. Jr. W. O'connor, K. L. Williams, J. P. Ting, 2005, "CATERPILLER 16.2 (CLR16.2), a novel NBD/LRR family member that negatively regulates T cell function", *J Biol Chem*., Vol. 280 (18), pp. 18375-85.

Cui, J., Zhu L., X. Xia, Y. H. Wang, X. Legras, J. Hong, J. Ji, P. Shen, S. Zheng, J. Z. Chen, R-F. Wang, 2010, "NLRC5 negatively regulates the NF-κB and type I interferon signaling pathways", *Cell*, Vol. 141, pp. 483-496.

Davis, B. K., R. A. Roberts, M. T. Huang, S. B. Willingham, B. J. Conti, W. J. Brickey, B. R. Barker, M. Kwan, D. J. Taxman, M. A. Accavitti-Loper, J. A. Duncan, J. P. Ting, 2011, "Cutting edge: NLRC5-dependent activation of the inflammasome", *J Immunol*., Vol. 186 (3), pp. 1333-7.

Deveault, C., J. H. Qian, W. Chebaro, A. Ao, L. Gilbert, A. Mehio, R. Khan, S. L. Tan, A. Wischmeijer, P. Coullin, X. Xie, R. Slim, 2009, "NLRP7 mutations in women with diploid androgenetic and triploid moles: a proposed mechanism for mole formation", *Hum Mol Genet*., Vol. 18(5), pp. 888-97.

Dinarello, C. A., 1998, "Interleukin-1 beta, interleukin-18, and the interleukin-1 beta converting enzyme", *Ann N Y Acad Sci*, Vol. 856, pp. 1-11.

Dostert, C., V. Pétrilli, 2008, "Asbestos triggers inflammation by activating the Nalp3 inflammasome", *Med Sci (Paris)*. Vol. 24 (11), pp. 916-8.

Dowds, A. T., J. Maumoto, L. Zhu, N. Inohara, G. Nunez, 2004, "Cryopyrin-induced interleukin 1 β in Monocytic cells", *The Journal of Biological Chemistry*, Vol. 279 (21), pp: 21924-21928.

Eisenbarth, S. C., O. R. Colegio, W. O'Connor, F. S. Sutterwala, R. A. Flavell, 2008, "Crucial role for the Nalp3 inflammasome in the immunostimulatory properties of aluminium adjuvants", *Nature,* Vol. 453, pp. 1122-1126.

Fernandes- Alnemri, T., J. Wu, J. W. Yu, P. Datta, B. Miller, W. Jankowski, S. Rosenberg, J. Zhang, E. S. Alnemri, 2007, "The pyroptosome: a supramolecular assembly of ASC dimers mediating inflammatory cell death via Caspase 1 activation", *Cell Death Differ.*, Vol. 14 (9), pp. 1590-604.

Ferrari, D. *et al.,* 2006 "The P2X7 receptor: a key player in IL-1 processing and release", *J. Immunol.,* Vol. 176, pp. 3877–3883.

Franchi, L., N. Warner, K. Viani, G. Nuñez, 2009, "Function of Nod-like receptors in microbial recognition and host defense", *Immunol Rev.*, Vol. 227 (1), pp. 106-28.

Fleischmann, R. M., J. Tesser, M. H. Schiff, et al., 2006, "Safety of extended treatment with anakinra in patients with rheumatoid arthritis", *Annals of the rheumatic diseases*, Vol. 65 (8), pp. 1006-12.

Ghiringhelli, F., L. Apetoh, A. Tesniere, L. Aymeric, Y. Ma, C. Ortiz, 2009, "Activation of the NLRP3 inflammasome in dendritic cells induces IL-1β-dependent adaptive immunity against tumors", *Nat. Med.*, Vol. 15 (10), pp. 1170-8.

Gomes, A. Q., D. V. Correia, B. Silva-Santos, 2007, "Non-classical major histocompatibility complex proteins as determinants of tumour immunosurveillance", *EMBO Rep*., Vol. 8 (11), pp. 1024-30.

Green, D. R., T. A. Ferguson, 2001, "The role of Fas ligand in immune privilege", *Nat. Rev. Mol Cell Biol.*, Vol. 2(12), pp. 917-24.

Green, D. R., T. Ferguson, L. Zitvogel, G. Kroemer, 2009, "Immunogenic and tolerogenic cell death", *Nat. Rev. Immunol*., Vol. (5), pp. 353-63.

Grenier, J. M., L. Wang, G. A. Manji, W. J. Huang, A. Al-Garawi, R. Kelly, A. Carlson, S. Merriam, J. M. Lora, M. Briskin, P. S. DiStefano, J. Bertin, 2002, "Functional screening of five PYPAF family members identifies PYPAF5 as a novel regulator of NF-κB and Caspase 1", *FEBS Lett*., Vol. 530(1-3), pp. 73-8.

Gregory, M. S., K. B. Davis, A. J. West, J. D. Taxman, S. Matsuzawa, C. J. Reed, Y.P. J. Ting, D. Blossom, 2011, "Discovery of a Viral NLR Homolog that Inhibits the Inflammasome", *Science*, Vol. 331.

Gül, A., 2005, "Behçet's Disease as an Autoinflammatory Disorder", *Current Drug Targets - Inflammation & Allergy*, Vol. 4, pp. 81-83.

Hashimoto, C., K. L. Hudson, K. V. Anderson, 1988, "The Toll gene of *Drosophila,* required for dorsal-ventral embryonic polarity, appears to encode a transmembrane protein", *Cell*, Vol. 52, pp. 269-79.

Hawkins, P. N., et al., 2004, "Spectrum of clinical features in Muckle–Wells syndrome and response to anakinra", *Arthritis Rheum*, Vol. 50, pp. 607–612.

Hoffman, H. M., et al., 2004, "Prevention of coldassociated acute inflammation in familial cold autoinflammatory syndrome by interleukin-1 receptor antagonist", *Lancet*, Vol. 364, pp. 1779-1785.

Illiopoulos, D., A. H. Hirsch, K. Struhl, 2009, "An epigenetic switch involving NF-κB, Lin28, Let7 microRNA and IL6 links inflammation to cell transformation", *Cell*, pp. 693-706.

Imamura, R., Y. Wang, T. Kinoshita, M. Suzuki, T. Noda, J. Sagara, S. Taniguchi, H. Okamoto, T. Suda, 2010, "Anti-inflammatory activity of PYNOD and its mechanism in humans and mice", *J Immunol*., Vol. 184 (10), pp. 5874-84.

Inohara, N., G. Nunez, 2003, "NODs: Intracellular proteins involved in inflammation and apoptosis", *Nature Rev*., Vol. 3.

Ishii, J. K., S. Akira, 2005, "Innate immune recognition of nucleic acids: Beyond toll-like receptors", *Int. J. Cancer*, Vol. 117, pp. 517-523.

Jarry, A., 1999, "Interleukin 1 and interleukin 1 beta converting enzyme (Caspase 1) expression in the human colonic epithelial barrier and Caspase 1 downregulation in colon cancer", *Gut*, Vol. 45, pp. 246-251.

Je´ru, I., P. Duquesnoy, T. Fernandes-Alnemri, E. Cochet, W. J. Yu, M. Lackmy-Port-Lis, E. Grimprel, J. Landman-Parker, V. Hentgen, S. Marlin, K. McElreavey, T. Sarkisian, G. Grateau, E. S. Alnemri, and S. Amselem, 2008, "Mutations in NALP12 cause hereditary periodic fever syndromes", *PNAS*, Vol. 105 (5), pp. 1614-1619.

Jin, Y., C. M. Mailloux, K. Gowan, S. L. Riccardi, G. LaBerge, D. C. Bennett, P. R. Fain, R. A. Spritz, 2007, "NALP1 in vitiligo-associated multiple autoimmune disease", *N Engl J Med.*, Vol. 356 (12), pp. 1216-25.

Jun, C., Z. Liang, X. Xiaojun, Y. W. Helen, L. Xavier, H. Jun, J. Jiabing, S. Pingping, Z. Shu, J. C. Zhijian, and W. Rong-Fu, 2010, "NLRC5 Negatively Regulates the NF-κB and Type I Interferon Signaling Pathways", *Cell*, Vol. 141, pp. 483-496.

Kanneganti, T. D., et al., 2006, "Critical role for Cryopyrin/Nalp3 in activation of Caspase 1 in response to viral infection and double-stranded RNA", *J. Biol. Chem.,* Vol. 281, pp. 36560-36568.

Kanneganti, T. D., et al., 2006, "Bacterial RNA and small antiviral compounds activate Caspase 1 through Cryopyrin/Nalp3", *Nature,* Vol. 440, pp. 233-236.

Kou, Y. C., L. Shao, H. H. Peng, R. Rosetta, D. del Gaudio, A. F. Wagner, T. K. Al-Hussaini, I. B. Van den Veyver, 2008, "A recurrent intragenic genomic duplication, other novel mutations in NLRP7 and imprinting defects in recurrent biparental hydatidiform moles", *Mol Hum Reprod*., Vol. 14 (1), pp. 33-40.

Kepp, O., L. Galluzzi, L. Zitvogel, and G. Kroemer, 2010, "Pyroptosis – a cell death modality of its kind? ", *Eur. J. Immunol*., Vol. 40, pp. 595-653.

Kim, Y. S., S. B. Ho, 2010, "Intestinal goblet cells and mucins in health and disease: recent insights and progress", *Curr Gastroenterol Rep*., Vol. 12 (5), pp. 319-30.

Kinoshita, T., Y. Wang, M. Hasegawa, R. Imamura, T. Suda, 2005, "PYPAF3, a PYRIN-containing APAF-1-like protein, is a feedback regulator of Caspase 1 dependent interleukin-1beta secretion", *J Biol Chem.,* Vol. 280 (23), pp. 21720-5.

Krelin, Y., E. Voronov, S. Dotan, M. Elkabets, E. Reich, M. Fogel, M. Huszar, Y. Iwakura, S. Segal, C. A. Dinarello, R. N. Apte, 2007, "Interleukin-1β driven

inflammation promotes the development and invasiveness of chemical carcinogen-induced tumors", *Cancer Res*., Vol. 67, pp. 1062-1071.

Lemaitre, B., E. Nicolas, L. Michaut, J. M. Reichhart, J. A. Hoffmann, 1996, "The dorsoventral regulatory gene cassette spatzle/Toll/cactus controls the potent antifungal response in *Drosophila* adults", *Cell*, Vol. 86, pp. 973-83.

Lich, D. J., L. K. Williams B. C. , Moore, C. J. Arthur, K. B. Davis, J. D. Taxman, and P.Y. J. Ting, 2007, "Cutting Edge: Monarch-1 Suppresses Non-Canonical NF-κB Activation and p52-Dependent Chemokine Expression in Monocytes", *J Immunol.*, Vol. 178, pp. 1256-1260.

Lich, J. D., J. P. Ting, 2007, "Monarch-1/PYPAF7 and other CATERPILLER (CLR, NOD, NLR) proteins with negative regulatory functions", *Microbes Infect.*, Vol. 9 (5), pp. 672-6.

Lu, B., O. J. Finn, 2008, "T-cell death and cancer immune tolerance", *Cell Death Differ.*, Vol. 15 (1), pp. 70-9.

Luedde, T., N. Beraza, V. Kotsikoris, G. van Loo, A. Nenci, R. De Vos, T. Roskams, C. Trautwein and M. Pasparakis, 2007, "Deletion of NEMO/IKKgamma in liver parenchymal cells causes steatohepatitis and hepatocellular carcinoma", *Cancer Cell*, Vol. 11, pp. 119-132.

Martinon, F., V. Petrilli, A. Mayor, A. Tardivel & J. Tschopp , 2007, "Gout-associated uric acid crystals activate the NALP3 inflammasome", *Nature*, Vol. 440 (9).

Medzhitov, R., P. Preston-Hurlburt, Jr. C. A. Janeway, 1997, "A human homologue of the Drosophila Toll protein signals activation of adaptive immunity", *Nature*, Vol. 388, pp. 394-7.

Meissner, T. B., A. Li, A. Biswas, K. H. Lee, Y. J. Liu, E. Bayir, D. Iliopoulosc, J. van den P. Elsen, and S. K. Kobayashi, 2010, "NLR family member NLRC5 is a

transcriptional regulator of MHC class I genes", *PNAS*, Vol. 107 (31), pp. 13794-13799.

Meyer, E., D. Lim, S. Pasha, L. J. Tee, F. Rahman, J. R. Yates, C. G. Woods, W. Reik, E. R. Maher, 2009, "Germline mutation in NLRP2 (NALP2) in a familial imprinting disorder (Beckwith-Wiedemann Syndrome) ", *PLoS Genet*., Vol. 3.

Miao, E. A., E. Andersen-Nissen, S. E. Warren, A. Aderem, 2007, "TLR5 and Ipaf: dual sensors of bacterial flagellin in the innate immune system", *Semin Immunopathol.*, Vol. (3), pp. 275.

Moore, C. B., T. D. Bergstralh, A. J. Duncan, L. Yu, E. M. Thomas, G. Z. Albert, et al., 2008, "NLRX1 is a regulator of mitochondrial antiviral immunity", *Nature*, Vol 451. (31).

Neerincx, A., K. Lautz, M. Menning, E. Kremmer, P. Zigrino, M. Hösel, H. Büning, R. Schwarzenbacher, T. A. Kufer, 2010, "A role for the human NLR family member NLRC5 in antiviral response", *JBC*.

Ogura, Y., D. K. Bonen, N. Inohara, D. L. Nicolae, F. F. Chen, R. Ramos, H. Britton, T. Moran, R. Karaliuskas, R. H. Duerr, et. al., 2001, "A frameshift mutation in NOD2 associated with susceptibility to Crohn's disease", *Nature*, Vol. 411 (6837), pp. 603-6.

Olkkonen, V. and H. Stenmark, 1997, "Role of Rab GTPases in membrane traffic", *Int. Rev. Cytol.*, Vol. 176, pp. 1-85.

Ouellette, A. J., 2010, "Paneth cells and innate mucosal immunity", *Curr Opin Gastroenterol.*, Vol. 26 (6), pp. 547-53.

O'Connell, S. M., et al., 2007, "Response to IL-1- receptor antagonist in a child with familial cold autoinflammatory syndrome", *Pediatr Dermatol*., Vol. 24, pp. 85-89.

Niederkorn, J. Y., 2006, "See no evil, hear no evil, do no evil: the lessons of immune privilege", *Nat Immunol*., Vol. 4, pp. 354-9.

Neven, B., M. P. Anne and dit Q. P. Maire, 2008, "Cryopyrinopathies: update on pathogenesis and treatment", *Nature Clinical Practice Rheumatology*, Vol. 4 (9).

Takeda, K., S. Akira, 2004, "TLR signaling pathways", *Seminars in Immunology*, Vol. 16.

Takeuchi, O., S. Akira, 2010, "Pattern Recognition Receptors and Inflammation", *Cell*, Vol. 140, pp. 805-820.

Tattoli, I., L. A. Carneiro, M. Jehanno, J. G. Magalhaes, Y. Shu, D. J. Philpott, D. Arnoult and S. E. Girardin, 2008, "NLRX1 is a mitochondrial NOD-like receptor that amplifies NF-kappaB and JNK pathways by inducing reactive oxygen species production", *EMBO Rep*., Vol. 9, pp. 293-300.

Ting, J. P., J. Trowsdale, 2002, "Genetic control of MHC class II expression", *Cell,* Vol. 109.

Qian, J., C. Deveault, R. Bagga, X. Xie, R. Slim, 2007, "Women heterozygous for NALP7/NLRP7 mutations are at risk for reproductive wastage: report of two novel mutations", *Hum Mutat*., Vol. 28(7), pp. 741.

Pålsson-McDermott, E. M., J. A. L. O'Neill, 2007, "Building an immune system from nine domains", *Biochemical Society Transactions,* Vol. 35**,** pp. 1437-1444.

Remmers, F. E., F. Cosan, Y. Kirino, J. M. Ombrello, N. Abaci, C. Satorius, M. J. Le, et al., 2010, "Genome-wide association study identifies variants in the MHC class I, *IL10*, and *IL23R-IL12RB2* regions associated with Behçet's disease", *Nature Genetics*, Vol. 42 (8).

Rhee, S. H., E. Im, and C. Pothoulakis, 2008, "Toll-like receptor 5 engagement modulates tumor development and growth in a mouse xenograft model of human colon cancer", *Gastroenterology,* Vol. 135: 518-528.

Riteau, B., N. Rouas-Freiss, C. Menier, P. Paul, J. Dausset, E. D. Carosella, 2001, "HLA-G2, -G3, and -G4 isoforms expressed as nonmature cell surface glycoproteins inhibit NK and antigen-specific CTL cytolysis", *J Immunol*., Vol. 166 (8), pp. 5018-26.

Sánchez, B., M. C. Urdaci, A. Margolles, 2010, "Extracellular proteins secreted by probiotic bacteria as mediators of effects that promote mucosa-bacteria interactions", *Microbiology*, Vol. 156 (Pt 11), pp. 3232-42.

Sasser, A. K., N. J. Sullivan, A.W. Studebaker, L.F. Hendey, A.E. Axel and B. M. Hall, 2007, "Interleukin-6 is a potent growth factor for ER-alpha-positive human breast cancer", *FASEB J.*, Vol. 21, pp. 3763-3770.

Schroder, K., J. Tschopp, 2010, "The Inflammasomes", *Cell*, Vol. 140, pp. 821-832

So, A., T. De Smedt, S. Revaz, J. Tschopp, 2007, "A pilot study of IL-1 inhibition by anakinra in acute gout", *Arthritis research & therapy*, Vol. 9 (2).

Steimle, V., L. A. Otten, M. Zufferey, B. Mach, 1993, "Complementation cloning of an MHC class II transactivator mutated in hereditary MHC class II deficiency (or bare lymphocyte syndrome) ", *Cell*. Vol. 75 (1), pp. 135-46.

Villani, A. C., M. Lemire, G. Fortin, E. Louis, M. S. Silverberg, C. Collette, N. Baba, C. Libioulle, J. Belaiche, A. Bitton, et al., 2009, "Common variants in the NLRP3 region contribute to Crohn's disease susceptibility", *Nat. Genet*., Vol. 41, pp. 71-76.

Wang, C. M., P. H. Dixon, S. Decordova, M. D. Hodges, N. J. Sebire, S. Ozalp, M. Fallahian, A. Sensi, F. Ashrafi, V. Repiska, J. Zhao, Y. Xiang, P. M. Savage, M. J. Seckl, R. A. Fisher, 2009, "Identification of 13 novel NLRP7 mutations in 20

families with recurrent hydatidiform mole; missense mutations cluster in the leucine-rich region", *J Med Genet.,* Vol. 46 (8), pp. 569-75.

Wegiel, A., B. Bjartell, Z. Culig, and J. L. Persson, 2008, "Interleukin-6 activates PI3K/Akt pathway and regulates cyclin A1 to promote prostate cancer cell survival", *Int. J. Cancer*, Vol. 122, pp. 1521-1529.

West, A. P, S. Gerald, S. S. Ghosh, 2011, "Mitochondria in innate immune responses", *Nature*, Vol. 11, pp. 389-402.

Wilcke, M., L. Johannes, T. Galli, V. Mayau, B. Goud, J. Salamero, 2000, "Rab11 regulates the compartmentalization of early endosomes required for efficient transport from early endosomes to the trans-golgi network", *J Cell Biol*., Vol. 151 (6), pp. 1207-20.

Wilmanski, M. J., T. Petnicki-Ocwieja, S. K. Kobayashi, 2008, "NLR proteins: integral members of innate immunity and mediators of inflammatory diseases", *Journal of Leukocyte Biology*, Vol: 83.

Yaneyama, M., and T. Fujita, 2007, "RIG-I family RNA helicases: cytoplasmic sensor for antiviral innate immunity", *Cytokine Growth Factor Rev*., Vol. 18, pp. 545-551.

Yeretssian, G., R. G. Correa, K. Doiron, P. Fitzgerald, C. P. Dillon, D. R. Green, J.C. Reed & M. Saleh, 2011, "Non-apoptotic role of BID in inflammation and innate immunity", *Nature*, Vol. 000.

Ye, Z., D. J. Lich, B. C. Moore, A. J. Duncan, L. K. Williams, and P. Y. J. Ting, 2008, "ATP Binding by Monarch-1/NLRP12 Is Critical for Its Inhibitory Function", *Molecular and Cellular Biology*, Vol. 28 (5), pp. 1841-1850.

Yu, W-J., J. Wu, Z. Zhang, P. Datta, I. Ibrahini, S. Taniguchi, J. Sagara, T. Fernandes-Alnemri, E.S. Alnemri, , 2006, "Cryopyrin and pyrin activate caspase-1, but not

NF-κB, via ASC oligomerization", *Cell Death and Differentiation*, Vol. 13, pp. 236-249.

Yuan, S., X. Yu, M. Topf, S. J. Ludtke, X. Wang, C. W. Akey, 2010, "Structure of an apoptosome-procaspase-9 CARD complex", *Structure*, Vol. 18 (5), pp. 571-83.

Yuksel, S., E. Eren, A. Sahillioglu, Y. Gultekin, D. Demiroz, G. Hatemi, İ. Fresko, H. Yazıcı and N. Özören, 2011, "Inflammasome Components in Behçet's Disease", (manuscript in preparation for J of Rheumatology).

Zhang, P., D. Morag, M. Zucchelli, F. Hambiliki, L. Levkov, O. Hovatta, J. Kere, 2008, "Expression Analysis of the NLRP Gene Family Suggests a Role in Human Preimplantation Development", *PLoS ONE*, Vol. 3 (7).

Zaki, H. M., P. Vogel, M. Body-Malapel, M. Lamkanfi, T. D. Kanneganti, 2010, "IL-18 production downstream of the NLRP3 Inflammasome confers protection aganist colorectal tumor formation", *The Journal of Immunology*, Vol. 185.

Zaki, M. H., K. L. Boyd, P. Vogel, M. B. Kastan, M. Lamkanfi, and T. D. Kanneganti, 2010, "The NLRP3 inflammasome protects against loss of epithelial integrity and mortality during experimental colitis", *Immunity*, Vol. 32, pp. 379-391.

Zhou, R., A. S. Yazdi, P. Menu, J. Tschopp, 2011, "A role for mitochondria in NLRP3 inflammasome activation", *Nature*, Vol. 469 (7329), pp. 221-5.